STUDIES ON ENANTIOMER SELECTIVE COMPLEXATION OF OPTICALLY ACTIVE, PHENOLIC CROWN ETHERS AND PODANDS WITH CHIRAL SECONDARY AMINES

光学活性フェノール性クラウンエーテルとポダンドのキラル第二級アミンとの鏡像体選択的錯形成に関する研究

Akihito FUJIWARA

藤　原　明　比　等

Division of Chemistry
Department of Chemical Science and Engineering
Graduate School of Engineering Science
Osaka University

2003

Contents

Chapter 1: **General Introduction** **1**

1.1: Background of this thesis 1

1.1.1: History of crown ethers 1

1.1.2: Chiral recognition ability of crown ethers 1

1.1.3: Application of optically active crown ethers to chiral stationary phase for liquid chromatography 4

1.2: Chiral recognition of secondary amines 5

1.3: References and notes 8

Chapter 2: **Synthesis of optically active crown ethers and podands** **10**

2.1: Introduction 10

2.1.1: Design of host molecules 10

2.1.2: Synthesis of phenolic podand possessing a 2,4-dinitrophenylazo group 13

2.1.3: Strategies for synthesizing host molecules 16

2.2: Synthesis of optically active crown ethers 17

2.3: Synthesis of optically active podands 21

2.4: Experimental section 22

2.5: References and notes 38

Chapter 3: **Enantiomer selectivities in complexation of phenolic crown ethers and podands with amines** **39**

3.1: Determination of association constants for the complexation of crown ethers and podands with amines 39

3.1.1: ^{1}H NMR titration method 39

3.1.2: UV-vis titration method 42

3.2: Binding ability of phenolic crown ethers and podands toward achiral amines 43
3.3: Enantiomer recognition ability of phenolic crown ethers and podand 46
3.4: Interpretation of enantioselectivities in complexation of phenolic crown ether and podand with secondary amines 48
3.5: Conclusion 52
3.6: Experimental section 53
3.6.1: Synthesis of chiral secondary amines 53
3.6.2: Determination of association constants by ^{1}H NMR titration method 54
3.6.3: Determination of association constants by UV-vis titration method 55
3.6.4: ^{1}H NMR titration and UV-vis titration data for determining binding constants 55
3.7: References and notes 93

Appendix: **List of Host and Guest Compounds** **94**

Publication list **98**

Acknowledgement **99**

Chapter 1

General Introduction

1.1 Back ground of this thesis

1.1.1 History of crown ethers

Since the first synthetic crown ethers **1** and **2**, which have been simply called 18-crown-6 (18C6) and dibenzo-18-crown-6 (DB18C6), respectively, were described by Pedersen in 1967,[1] the specific abilities of crown ethers and their derivatives, namely, bicyclic type cryptands and open chain type podands, have been extensively studied. A

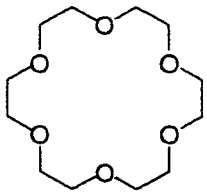

1

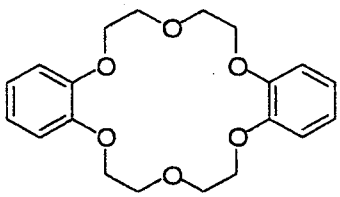

2

representative ability of crown ethers, cryptands, and podands is inclusion of alkali and alkaline earth metal ions. They stabilize the guest cations mainly by ion-dipole interactions. Regarding nonmetal ions, it is well known that crown ethers as simple as 18C6 form stable complexes with organic cations, such as primary ammonium ions (RNH_3^+).[2] 18C6 binds primary ammonium cations through three-point hydrogen bonds, as illustrated in Figure 1.1.

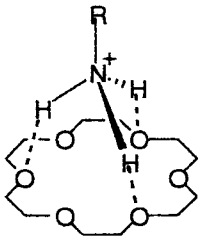

Figure 1.1 Complexatoin of 18-crown-6 with primary ammonium ion.

1.1.2 Chiral recognition ability of crown ethers

The study of enantiomeric recognition of amine and protonated amine compounds is of significance since these compounds are basic building blocks of biological molecules.

Moreover, chiral recognition is a fundamental property of biological molecules and a better understanding of the interactions operating in chiral recognition is essential to developing new methods of asymmetric synthesis and chromatographic resolution of enantiomers.

Useful applications of chiral macrocyclic compounds in enantiomeric separations have been demonstrated by chiral gas and liquid chromatographies, capillary zone eledctrophoresis, and other approaches.[3] Among several types of compounds studied as chiral stationary phases, chiral crown ethers have been recognized as one of the successful selectors for the resolution for amine-containing compounds.[4]

The first example of molecular recognition by chiral crown ethers was published in 1973.[5] Compounds **3** and **4** having 1,1'-binaphthyl as the chiral moiety were prepared by

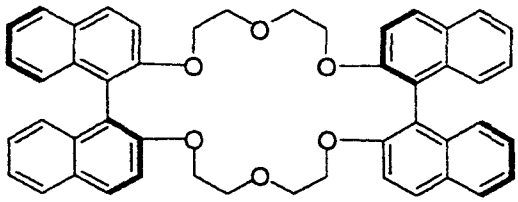

3

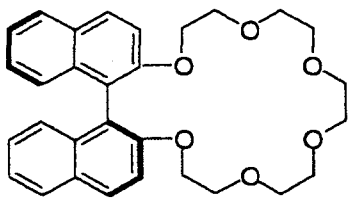

4

Cram and co-workers.[6] Since Cram's report appeared, a variety of chiral macrocycles have been synthesized and their enantiomeric recognition abilities were studied in detail. Representative examples **5** and **6** are shown below. Bradshaw and Izatt prepared **5** containing a pyridine ring which formed stable complexes with (*R*)- and (*S*)-1-(1-naphthyl)ethylamine with high degree of enantiomer selectivity.[7] Chiral aza-crown ether **6** was reported to form more stable complex with (*R*)-1-phenylethylammonium salt than with the (*S*)-enantiomer.[8]

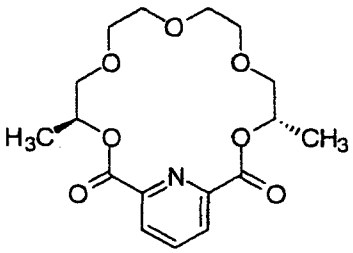

5

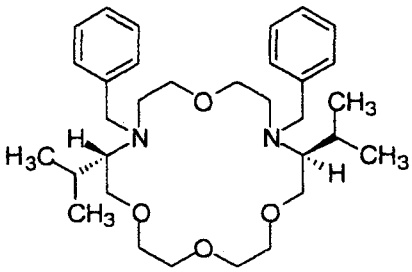

6

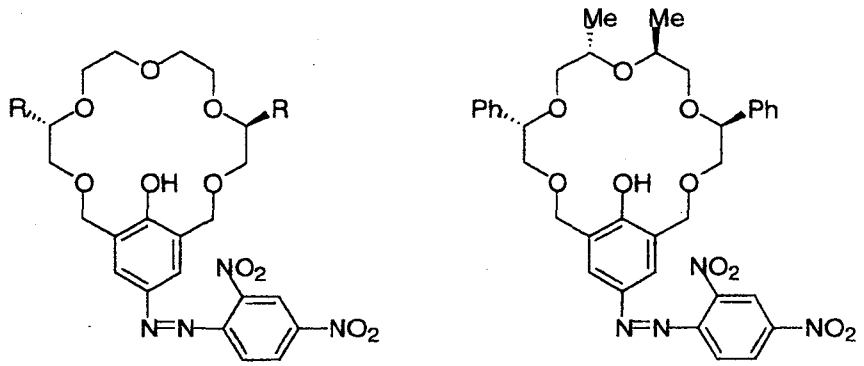

7 (R=Ph) **8**

R = adamantyl, phenyl, *t*-butyl, and methyl

Scheme 1.1 The basic structures of pseudo-18-crown-6 type hosts.

Naemura, Hirose, and Tobe prepared a number of chiral phenolic crown ethers which have a pseudo-18-crown-6 type framework and investigated their complexation ability and enantiomer selectivity toward chiral amines.[9] Two representative basic structures are shown in Scheme 1.1. These crown ethers have following characteristic features. First, since the phenol group of these crown ethers are relatively acidic ($pKa \approx 7.3$) owing to the strongly electron-withdrawing 2,4-dinitrophenylazo group,[10] they can bind neutral amines to form salt complexes, called saltex.[11] Second, these molecules have two or four chiral centers in the macrocyclic framework, keeping C_2 symmetry of the molecule. Therefore, they bind each enantiomer of amines to form diastereomeric complexes, whose stability difference leads enantiomer selectivity. Third, various substituents R, ranging from small methyl group to bulky adamantyl group, can be introduced to the macrocyclic framework as a chiral barrier. The phenolic crown ethers like **7** and **8** showed high binding ability and chiral recognition ability toward primary ethanolamine derivatives.[9b,9d] For example, **7** binds 2-amino-2-phenylethanol with $K_R=(4.6\pm0.4)\times10^3$ and $K_S=(4.1\pm0.1)\times10^2$ leading to $K_R/K_S=11$. In addition, because of the high enantiomer selectivity of **8** toward 2-amino-2-phenylethanol, the chirality of 2-amino-2-phenylethanol can be identified from the dramatic color difference of the solutions.[12]

The author expected that the excellent properties of these hosts could be exploited to develop host molecules for different purpose by modifying the basic structure of **7** and **8**.

1.1.3 Application of optically active crown ethers to chiral stationary phase for liquid chromatograpy

The liquid chromatographic separation of enantiomers based on chiral stationary phases (CSPs) has emerged as an effective and convenient method for determining the enantiomeric composition of many chiral compounds. This method has also been applied to the preparative-scale separation of enantiomers in an industrial scale. CSPs based on chiral crown ethers have been shown to be effective in resolving the enantiomers of chiral compounds that contain a primary amine functional group. In the pioneering work during the late 1970s, Cram and co-workers reported bis(1,1'-binaphthyl)-22-crown-6 immobilized on polystyrene or silica gel showed reasonable resolution of the enantiomers of α-amino acids and their derivatives.[3f,13] In 1987, Shinbo and co-workers reported the separation of chiral amines and amino acids by using CSP in which a hydrophobic chiral crown ether was dynamically coated on a reversed stationary phase.[14] This type of CSP was commercialized as CROWNPAK CR® and until a few years ago, this had been the only commercially available chiral column containing a chiral crown ether as CSP.[15] The CSP showed excellent enantiomer selectivity toward amino acids and amines. However, it has a serious disadvantage due to the fact that only reversed mobile phase can be used.

Recently, since the demand on chiral columns that can be used under a variety of conditions, i.e., normal and reversed mobile phases, has been increasing, chiral columns containing covalently bound chiral crown ethers have been developed. Namely, Machida et al.[16] and Hyun et al.[17] reported about CSPs prepared by covalently binding (+)-(18-crown-6)-2,3,11,12-tetracarboxylic acid to silica gel. Hyun also reported a covalently bound binaphthyl-based chiral selector.[18] Hirose, Tobe, and Nishioka developed CSPs based on chiral pseudo-18-crown-6 type hosts having a OMe or OH group in the crown

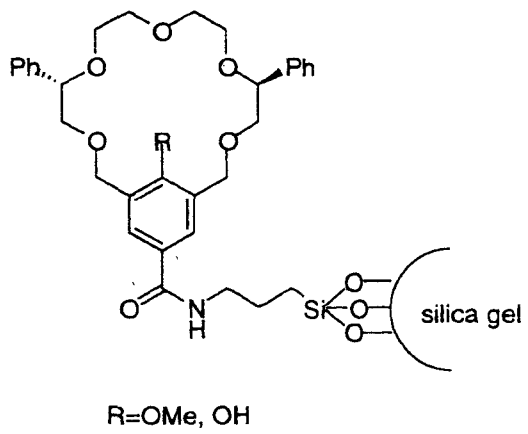

Scheme 1.2 Chiral stationary phase consisting of a silica gel covalently bound with chiral pseudo-18-crown-6 type host.

cavity which are covalently bound to silica gel by an amide linkage (Scheme 1.2).[19] These CSPs exhibit good enantiomer separation of lipophilic ammonium salts and amines and one of them is produced on a commercial basis as SUMICHIRAL OA-8000®. Because of the versatility of the basic framework of pseudo-18-crown-6s, this type of chiral selector should be applied to the related CSPs.

1.2 Chiral recognition of secondary amines

There exist many biologically active secondary amines as with primary amines for which many biologically active compounds are known. Biologically active secondary amines having sympathomimetic property are illustrated in Figure 1.2 and those having β-blocking property are illustrated in Figure 1.3.[20] Ephedrine and epinephrine, which are famous for their property as pressor agents, are representative sympathomimetic amines and propranolol, which possesses arrhythmias property, is representative of β-adrenergic blocking agent. As can be seen from Figures 1.1 and 1.2, many biologically active secondary amines have a phenylglycinol structure.

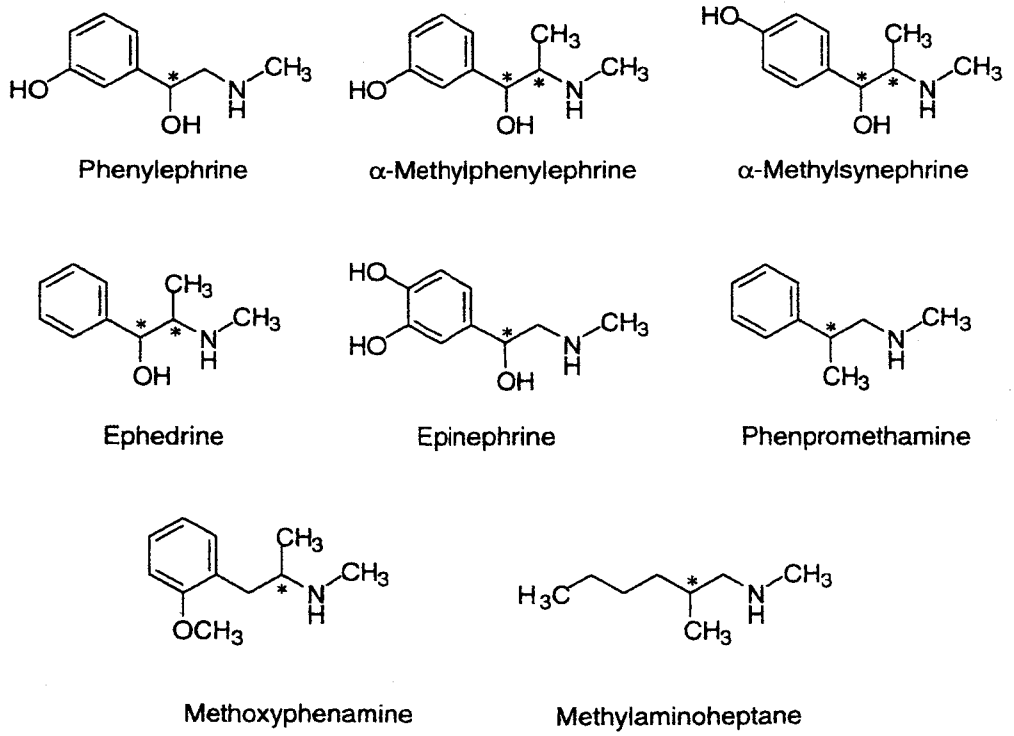

Figure 1.2 List of chiral secondary amines possessing sympathomimetics property.

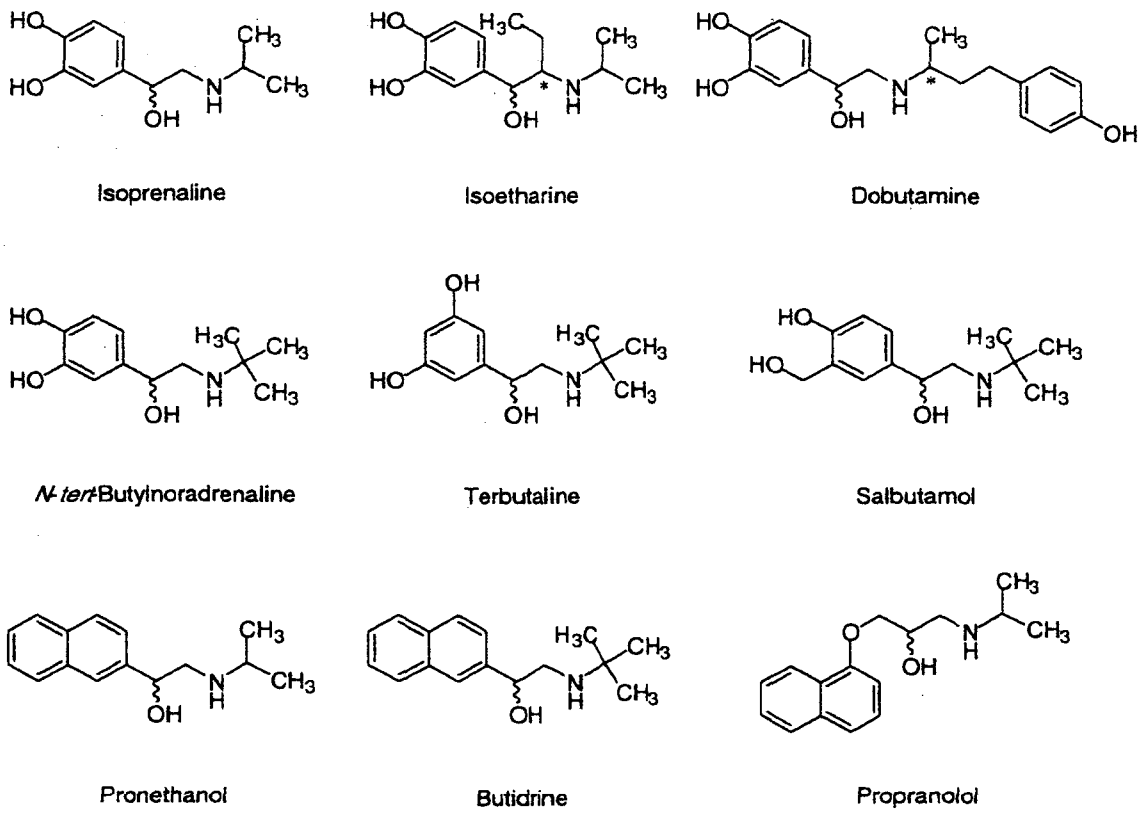

Figure 1.3 List of chiral secondary amines possessing β-receptor antagonists activity.

It has been reported that the biological activities of secondary amines are frequently different from the corresponding enantiomers.[21] For example, in the case of β-adrenergic blocking agents (Figure 1.3), (–)-type compounds always possess stronger activity than the corresponding (+)-isomers.[20] In the case of propranolol, the (–)- isomer was reported to exhibit different activity from that of the (+)-enantiomer; namely, (–)-enantiomer is a β-blocker and an arrhythmias while (+)-enantiomer is a contraceptive.

Because of these differences between the biological activities of secondary amines, the separation of their enantiomers is a critical issue in pharmaceutical and analytical chemistry. Chiral HPLC is one of important methods to obtain enantiomerically pure compounds besides asymmetric synthesis, kinetic resolution, and recrystallization. In addition, among the methods for determination of optical purity of chiral compounds, HPLC performed by chiral columns has been widely used because of its convenience and quantitativeness. As described in Section 1.1.2, chiral discrimination of primary amines has been well studied, and excellent host molecules for primary amines have been prepared. Moreover, they are applied to selectors of chiral stationary phases for HPLC as described in Section 1.1.3. By contrast, little has been reported for chiral recognition of secondary amines. To the best knowledge, there are only two reports regarding chiral

recognition of secondary amine derivatives, one with chiral binaphthyl derivatives[22] and the other with a liquid chromatography stationary phase based on a chiral 18-crown-6.[23] Accordingly, the development of host molecules with chiral recognition ability toward secondary amines has been keenly desired.

On the basis of these background, the author embarked a project to prepare host molecules capable of not only binding secondary amines but also recognizing their chirality by modifying the structures of **7** and **8** which have been shown to exhibit excellent binding ability and chiral recognition ability toward primary amines. In Chapter 2, the design of host molecules for chiral recognition of secondary amines and their synthesis are described. In Chapter 3, the binding and chiral recognition abilities of the host molecules described in Chapter 2 toward secondary amines are described.

1.3 References and notes

1. (a) Pedersen, C. J.; *J. Am. Chem. Soc.* **1967**, *89*, 2495–2496; (b) Pedersen, C. J.; *J. Am. Chem. Soc.* **1967**, *89*, 7017–7036.
2. Cram, D. J.; Trueblood, K. N. *Top. Curr. Chem.* **1981**, *98*.
3. (a) Gasparrini, F.; Misiti, D.; Villani, C.; Borchardt, A.; Burger, M. T.; Still, W. C. *J. Org. Chem.* **1995**, *60*, 4314– 4315; (b) Joly, J. P.; Moll, N. *J. Chromatogr.* **1990**, *521*, 134–140; (c) Kuhn, R.; Erni, F.; Bereuter, T.; Häusler, *J. Anal. Chem.* **1992**, *64*, 2815–2820; (d) Kuhn, R.; Riester, D.; Fleckenstein, B.; Wiesmüller, K. H. *J. Chromatogr. A* **1995**, *716*, 371–379; (e) Castelnovo, P.; Albanesi, C. *J. Chromatogr. A* **1995**, *715*, 143–149; (f) Sousa, L. R.; Sogah, G. D. Y.; Hoffman, D. H.; Cram, D. J. *J. Am. Chem. Soc.* **1978**, *100*, 4569–4576.
4. Krstulovic, A. M. "*Chiral Separation by HPLC*", Ellis Horwood, Chichster, 1989.
5. Kyba, E. B.; Koga, K. ;Sousa, L. R.; Siegel, M. G.; Cram, D. J. *J. Am. Chem. Soc.* **1973**, *95*, 2692–2693.
6. Kyba, E. B.; Gokel, G. W.; Jong, F. de; Koga, K.; Sousa, L. R.; Siegel, M. G.; Kaplan, L.; Sogah, G. D. Y.; Cram, D. J. *J. Org. Chem.* **1977**, *42*, 4173–4184.
7. Izatt, R. M.; Wang, T.; Hathaway, J. K.; Zhang, X. X.; Curtis, J. C.; Bradshaw, J. S.; Zhu, C. Y. *J. Inclusion Phenom. Mol. Recognit. Chem.* **1994**, *17*, 157–175.
8. Chadwick, D. J.; Cliffe, I. A.; Sutherland, I. O. *J. Chem. Soc., Perkin Trans. 1* **1984**, 1707–1717.
9. (a) Naemura, K.; Fuji, J.; Ogasahara, K.; Hirose, K.; Tobe, Y. *Chem. Commun.* **1996**, 2749–2750; (b) Ogasahara, K.; Hirose, K.; Tobe, Y.; Naemura, K. *J. Chem. Soc., Perkin Trans. 1* **1997**, 3227–3236; (c) Naemura, K.; Nishioka, K.; Ogasahara, K.; Nishikawa, Y.; Hirose, K.; Tobe, Y. *Tetrahedron: Asymmetry* **1998**, *9*, 563–574; (d) Hirose, K.; Ogasahara, K.; Nishioka, K.; Tobe, Y.; Naemura, K. *J. Chem. Soc., Perkin Trans. 2* **2000**, 1984–1993.
10. Naemura, K.; Nishikawa, Y.; Fuji, J.; Hirose, K.; Tobe, Y. *Tetrahedron: Asymmetry* **1997**, *8*, 873–882.
11. The word "saltex" is used in place of "salt complex": Kaneda, T.; Ishizaki, Y.; Misumi, S. *J. Am. Chem. Soc.* **1988**, *110*, 2970–2972.
12. Hirose, K. *J. Incl. Phenom. Macrocyclic Chem.* **2001**, *39*, 193–209.
13. Sogah, G. D. Y.; Cram, D. J. *J. Am. Chem. Soc.* **1979**, *101*, 3035–3042.
14. Shinbo, T.; Yamaguchi, T.; Nishimura, K.; Sugiura, M. *J. Chromatogr.* **1987**, *45*, 145–153.
15. Shinbo, T.; Yamaguchi, Yanagishita, H.; Kitamoto, D.; Sasaki, M.; K.; Sugiura, M. *J. Chromatogr.* **1992**, *625*, 101–108.
16. Machida, Y.; Nishi, H.; Nakamura, K.; Nakai, H.; Sato, T. *J. Chromatogr. A* **1998**, *805*, 85–92.

17. (a) Hyun, M. H.; Jin, J. S.; Lee, W. *J. Chromatogr. A* **1998**, *822*, 155–161; (b) Hyun, M. H.; Jin, J. S.; Koo, H. J.; Lee, W. *J. Chromatogr. A* **1999**, *837*, 75–82; (c) The chiral column based on (+)-(18-crown-6)-2,3,11,12-tetracarboxylic acid reported in references 17a, b is now commercially available as OPTICROWN®.
18. Hyun, M. H.; Han, S. C.; Lipshutz, B. H.; Shin, Y. J.; Welch, C. J. *J. Chromatogr. A* **2001**, *910*, 359–365.
19. Hirose, K.; Nakamura, T.; Nishioka, R.; Ueshige, T.; Tobe, Y. *Tetrahedron Lett.* in press.
20. (a) Bowman, W. C.; Rand, M. J. in "*Textbook of Pharmacology*", 2nd Eds. Blackwell Scientific Publications: London, 1980; (b) Main, B. G.; Tucker, H. in "*Medicinal Chemistry*", 2nd Eds. Genellin, C. R.; Roberts, S. M. Eds. Academic Press: London, 1993; pp 187–208.
21. (a) Patil, P. N.; LaPidius, J. B.; Tye, A. *J. Pharm. Sci.* **1970**, *59*, 1205–1234; (b) Brittain, R. T.; Farmer, J. B.; Marshall, R. J. *Br. J. Pharmac.* **1973**, *48*, 144–147.
22. Kawabata, T.; Kuroda, A.; Nakata, E.; Takasu, K.; Fuji, K. *Tetrahedron Lett.* **1996**, *37*, 4153–4156.
23. Steffeck, R. J.; Zelechonok, Y.; Gahm, K. H. *J. Chromatogr. A* **2002**, *947*, 301–305.

Chapter 2

Synthesis of Optically Active Crown Ethers and Podands

2.1 Introduction

2.1.1 Design of host molecules

As described in Section 1.2, the author planned to synthesize hosts capable of binding secondary amines and recognize their chirality. The design for the hosts is based on pseudo-18-crown-6 derivatives such as (*S*,*S*)-**7** which have been shown to exhibit not only excellent enantiomer selectivity toward primary ethanolamine derivatives but also distinct difference between the color developed by complexation with each guest enantiomer,[1] as described in Section 1.1. The salient features of the basic structure of the hosts (Figure 2.1) involve (i) a phenolic hydroxy group which binds neutral amines to form a

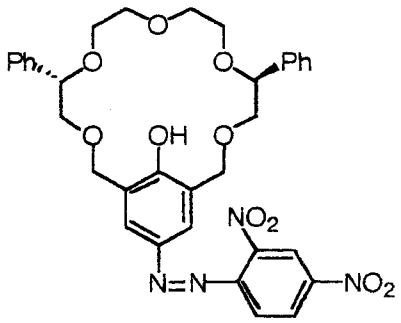

(*S*,*S*)-**7**

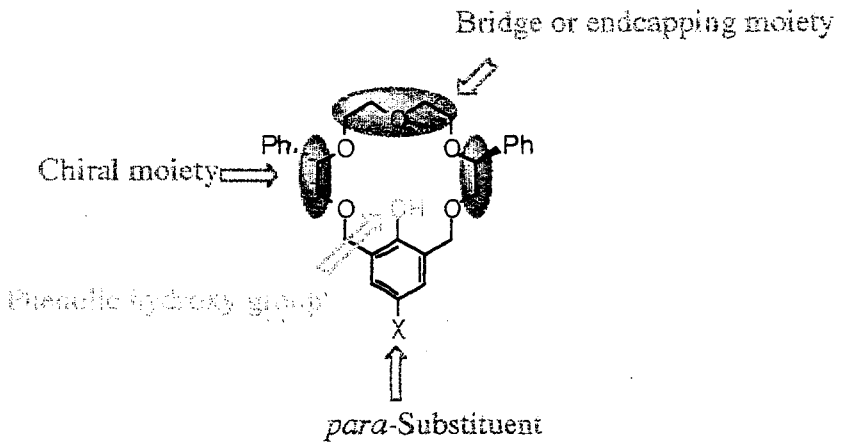

Figure 2.1 Design for our host molecules.

salt complex, (ii) para-substituent X which not only can control the acidity of the phenol group thereby changing the binding ability toward neutral amines but also can be transformed into a covalent linkage between the chiral crown ether and a stationary phase for chiral chromatography, (iii) various chiral barrier groups that can be introduced to appropriate positions of the macrocyclic framework, and (iv) the ring size of crown ether that can be in principle adjusted by changing the length of bridge or endcapping moiety.

With these features in mind, the author designed host molecules for chiral recognition of secondary amines as follows: (i) The hosts should possess a phenolic hydroxy group. (ii) As the para substituent X, they possess a strong electron-withdrawing nitro group or a carboxy group. Nitro group was selected because of the complexity observed in a podand having a dinitrophenylazo group as described in the subsequent section. The carboxy group can be covalently bound to aminopropyl silica commonly used for chiral stationary phase (CSP) for liquid chromatography. (iii) Phenyl groups are introduced as chiral barriers because their building block can readily be prepared from commercially available mandelic acid. In addition, among chiral pseudo-18-crown-6 derivatives, those having phenyl groups exhibit relatively high enantiomer selectivities toward primary amines.[1] (iv) The design of the endcapping group suitable for secondary amines is most critical, as described below.

Although the ring size of the 18-crown-6-ether is suitable for binding primary alkylammonium ions (RNH_3^+), secondary dialkyl- ($R_2NH_2^+$) and tertiary trialkyl- (R_3NH^+) ammonium ions do not bind to 18-crown-6-ether.[2] Concerning the binding ability of crown ethers with secondary ammonium salts, Stoddart et al. reported that 24-crown-8 derivatives formed stable complexes with secondary ammonium ions.[3] The two different solid state structures of the complex of dibenzo-24-crown-8 (DB24C8) with dibenzylammonium hexafluorophosphate are shown in Figure 2.2.[4]

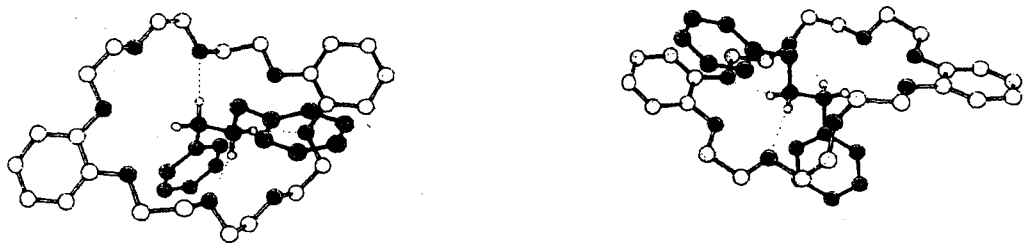

Figure 2.2 The different crystal structures of complex of dibenzo-24-crown-8 and dibenzylammonium ion. The anion is not shown for clarity.

Taking the facts described above into account, the macrocyclic framework should have almost the same size as that of DB24C8 to achieve sufficient binding with secondary amines. Accordingly, as a first candidate, the author designed (*S,S*)-**10** having a pseudo-24-crown-8 framework. Since the binding site of (*S,S*)-**10** is supposed to be smaller than that of dibenzo-24-crown-8, the author also planned to prepare pseudo-27-crown-9 (*S,S*)-**11** possessing a larger binding site. The author considered that open chain type podands possessing more flexible structure than those of pseudo-24-crown-8 (*S,S*)-**10** and pseudo-27-crown-9 (*S,S*)-**11** can also be possible candidates, although the binding ability may be smaller than the crown ethers because of the absence of the additional donor atom. As open chain hosts, the author designed (*R,R*)-**12** and its methyl ether (*R,R*)-**13**. In order to compare the binding abilities of these hosts with that of a standard primary amine binder, nitro-substituted pseudo-18-crown-6 (*S,S*)-**9** possessing the same ring size as that of (*S,S*)-**7** was also prepared. Moreover, in order to apply to the chiral stationary phase for secondary amines, (*S,S*)-**14** having a carboxyl group at the para position of the methoxy group was prepared.

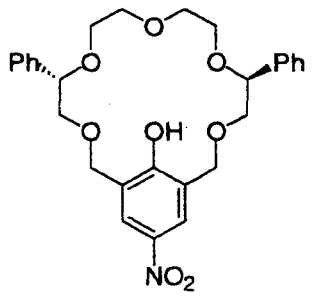

(*S,S*)-**9**

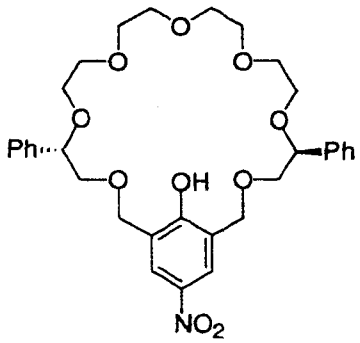

(*S,S*)-**10**

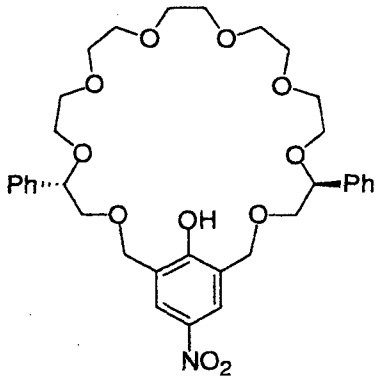

(*S,S*)-**11**

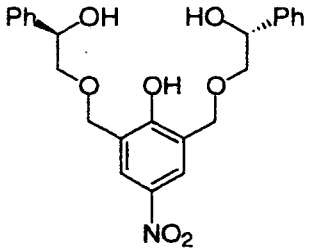

(*R*,*R*)-**12**

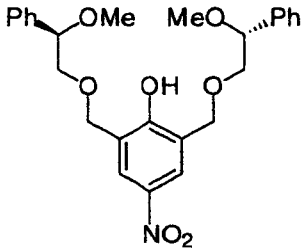

(*R*,*R*)-**13**

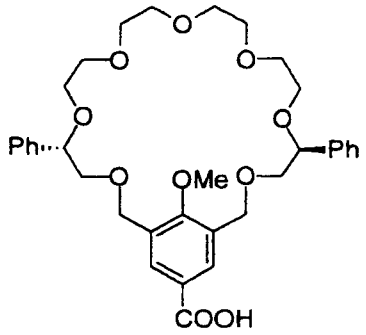

(*S*,*S*)-**14**

2.1.2 Synthesis of phenolic podand possessing a 2,4-dinitrophenylazo group

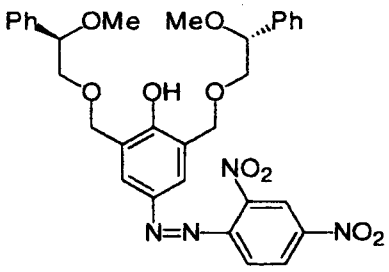

(*R*,*R*)-**15**

Before the author fixed the para substituent of the phenol ring to the nitro group, podand (*R*,*R*)-**15** possessing a 2,4-dinitrophenylazo group was prepared. Since this compound, however, turned out to exist in both azophenol and hydrazone forms in solution, its complexation behavior was not investigated. Moreover, because of this possible complexity due to tautomerization, nitro group was chosen as the para substituent, which has similar electron-withdrawing property as that of dinitrophenylazo group.[5] Podand (*R*,*R*)-**15** was prepared by combining the chiral ethylene glycol unit (*R*)-**16** derived from (*R*)-mandelic acid and *m*-xylylene dibromide **17**.

The chiral subunits (*R*)-**16** was prepared from (*R*)-mandelic acid according to the published route[6] depicted in Scheme 2.1. Thus, (*R*)-mandelic acid was converted to the methyl ester and the hydroxy group was protected as a THP ether. $LiAlH_4$ reduction of the ester gave

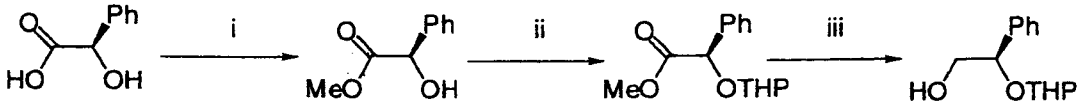

(*R*) - mandelic acid

(*R*)-**16**

Scheme 2.1 *Reagents*: (i) $SOCl_2$, MeOH; (ii) DHP, pyridinium *p*-toluenesulfonate; (iii) $LiAlH_4$, 94% for three steps.

(*R*)-**16** in 94% overall yield.

The *m*-xylylene subunit **17** was prepared from *p*-methoxyphenol according to the published method (Scheme 2.2).[5] Thus hydroxymethylation of *p*-methoxyphenol gave triol **18**. The phenolic hydroxy group of **18** was methylated and the remaining hydroxy groups were transformed into bromo to give **17**.

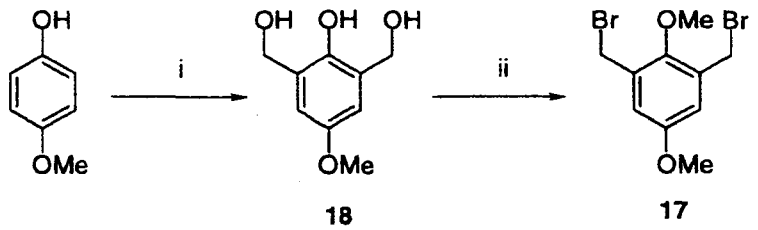

Scheme 2.2 *Reagents*: (i) HCHO, NaOH, 93%; (ii) 1. $(MeO)_2SO_2$, K_2CO_3, 86% 2. PBr_3, 73%.

Preparation of podand (R,R)-15

As shown in Scheme 2.3, for the synthesis of (*R*,*R*)-**15**, condensation of 2 equiv. of (*R*)-**16** with **17** in the presence of NaH followed by deprotection with pyridinium *p*-toluenesulfonate in methanol gave (*R*,*R*)-**19** in 51% overall yield. Methylation of the hydroxy groups of (*R*,*R*)-**19** with iodomethane in the presence of NaH was first carried out to furnish (*R*,*R*)-**20** in 71% yield. In order to facilitate the transformation of the dimethoxybenzene moiety to the *p*-benzoquinone moiety, the inner methoxy group of (*R*,*R*)-**20** was selectively cleaved by treatment with sodium ethanethiolate in DMF,[7] giving phenol (*R*,*R*)-**21**. Oxidation of (*R*,*R*)-**21** with ceric (IV) ammonium nitrate in acetonitrile followed by treatment with 2,4-dinitrophenylhydrazine furnished (*R*,*R*)-**15** in 22% overall yield *via* quinone (*R*,*R*)-**22**.

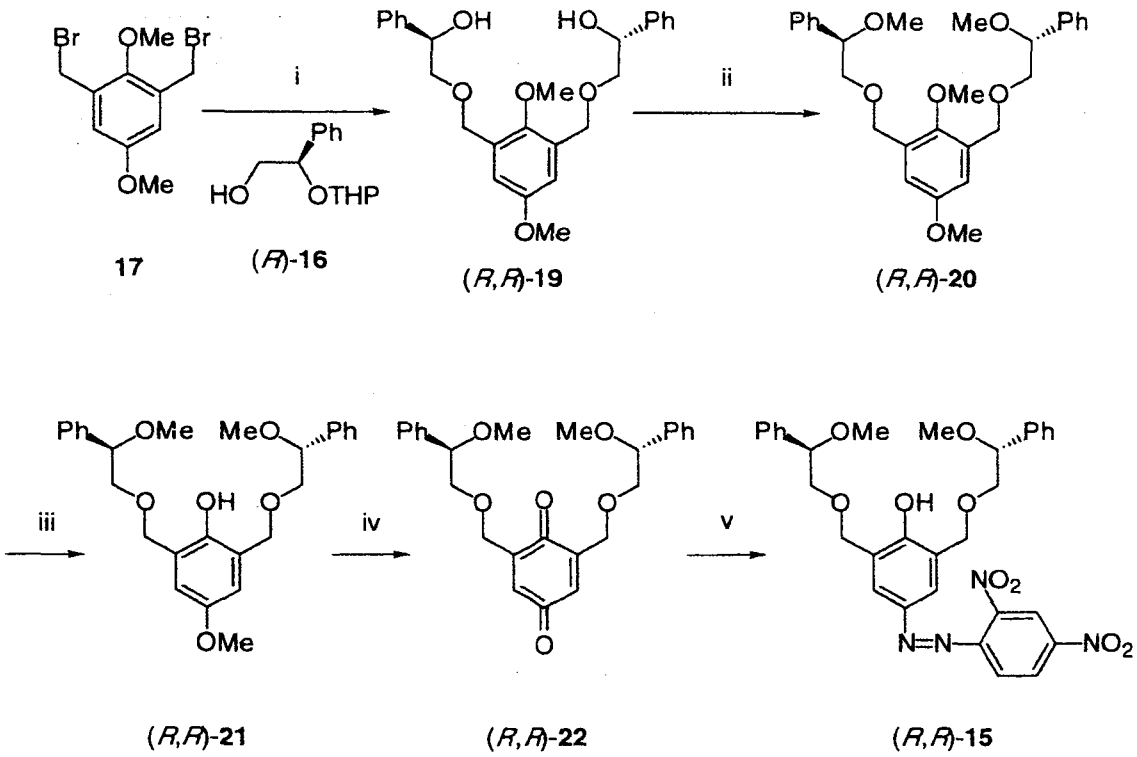

Scheme 2.3 *Reagents*: (i) 1. NaH, 2. pyridinium *p*-toluenesulfonate, methanol, 51% for two steps; (ii) CH_3I, NaH, 71%; (iii) EtSNa; (iv) ceric (IV) ammonium nitrate; (v) 2,4-dinitrophenylhydrazine, H_2SO_4, 22% for three steps from (*R*,*R*)-**20**.

Tautomerization of *(R,R)*-**15**

It was found that podand type host (*R*,*R*)-**15** having 2,4-dinitrophenylazo group existed as both azophenol ((*R*,*R*)-**15**) and its tautomeric hydrazone form ((*R*,*R*)-**23**). As shown in Figure 2.3, ^{1}H NMR spectrum of (*R*,*R*)-**15** in $CDCl_3$ at 30 °C exhibits signals due to (*R*,*R*)-**23** in addition to those of (*R*,*R*)-**15** which are exchanging slowly on the NMR time scale. The low field resonance (12.2 ppm) for Hf' presents a strong support for the structure of (*R*,*R*)-**23**. The ratio of (*R*,*R*)-**15** and (*R*,*R*)-**23** estimated from the intensity of Ha and Ha' is 5:1.

In the case of pseudo-crown ethers having 2,4-dinitrophenylazo group such as (*S*,*S*)-**7**, the hydrazone form is not observed, presumably because the orientation of the oxygen atoms are restricted inside of the macrocycle, thereby stabilizing phenolic hydroxy group by hydrogen bonding. On the other hand, in the case of podand (*R*,*R*)-**15**, since the orientation of the oxygen atoms is not restricted, hydrogen bonding with the phenolic hydroxyl group is weaker

than that of pseudo-crown ether (*S*,*S*)-**7**. For this reason, (*R*,*R*)-**15** exists as both azophenol and hydrazone forms.

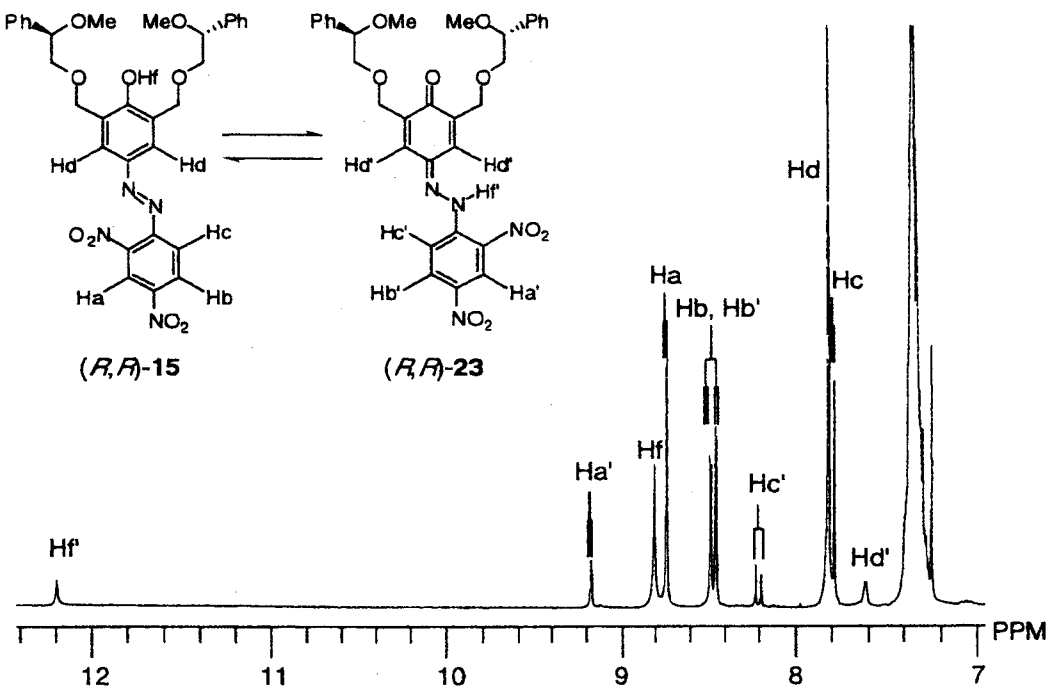

Figure 2.3 ^{1}H NMR spectrum (270 MHz) of (*R*,*R*)-**15** and its tautmeric form (*R*,*R*)-**23** in $CDCl_3$ at 30 °C.

2.1.3 Strategies for synthesizing host molecules

A retrosynthetic analysis for the basic structure of the crown ethers and podands is shown in Scheme 2.4. Crown ethers of 18-crown-6 type (*S*,*S*)-**29**, 24-crown-8 type (*S*,*S*)-**30**, and 27-crown-9 type (*S*,*S*)-**31** would be obtained by cyclization of (*S*,*S*)-**25**, which would be prepared by coupling of (*S*)-**16** and **24**, with the corresponding oligoethylene glycol ditosylates, **26**, **27**, and **28**, respectively. The bromo group of these crown ethers can be transformed into various functional groups, such as a nitro group of (*S*,*S*)-**9**, (*S*,*S*)-**10**, and (*S*,*S*)-**11** and a carboxy group of (*S*,*S*)-**14**, which can be used as a covalent link to silica gel to produce CSP for liquid chromatography. The podands (*R*,*R*)-**12** and (*R*,*R*)-**13** would be obtained by way of (*R*,*R*)-**25** which can be prepared by employing (*R*)-**16**, the enantiomer of (*S*)-**16**. (*R*)-**16** was employed simply by chance.

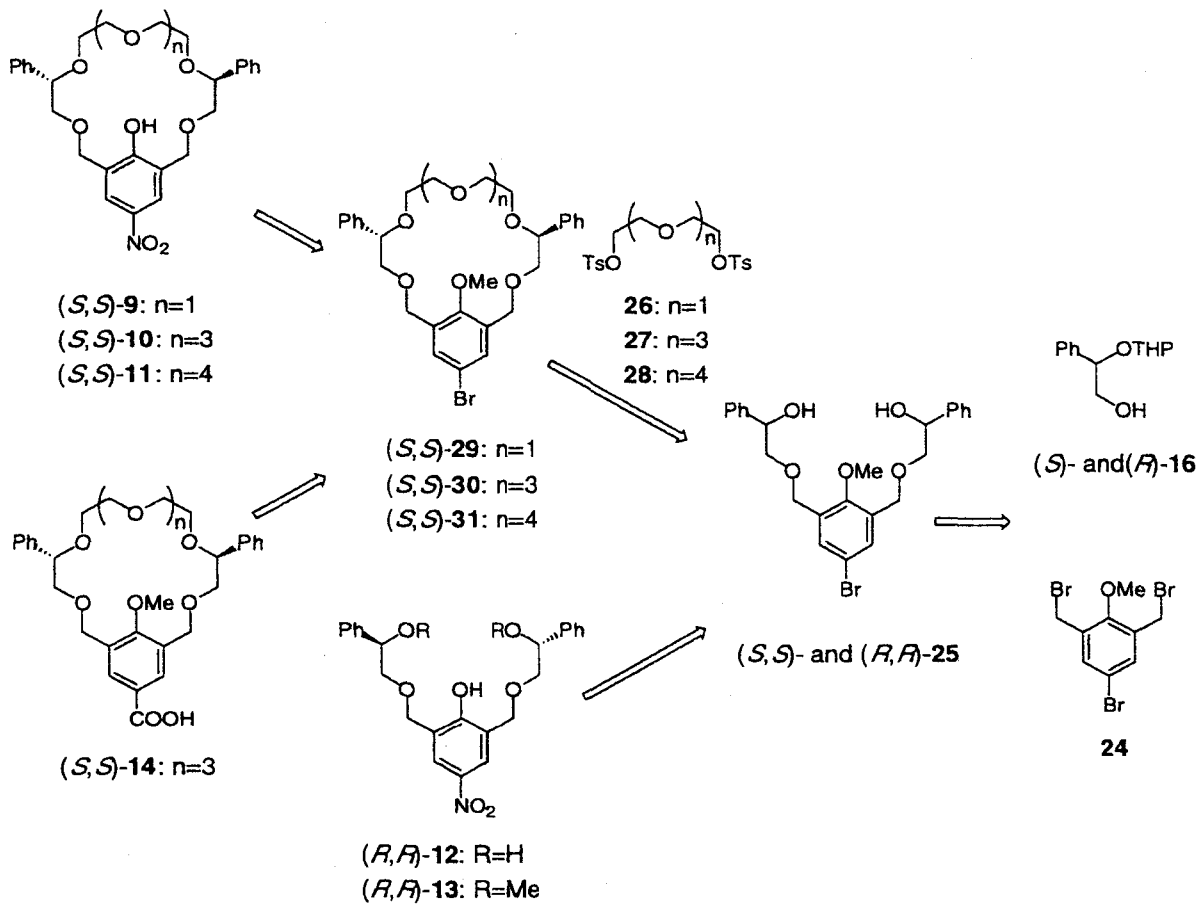

Scheme 2.4 Retrosynthetic analysis for synthesis of crown ethers and podands.

2.2 Synthesis of optically active crown ethers

The crown ethers (*S*,*S*)-**9**–(*S*,*S*)-**11** were prepared by combining the oligoethylene glycol units **26**, **27**, and **28**, monoprotected chiral ethylene glycol unit (*S*)-**16** derived from (*S*)-mandelic acid, and *m*-xylylene dibromide **24**.

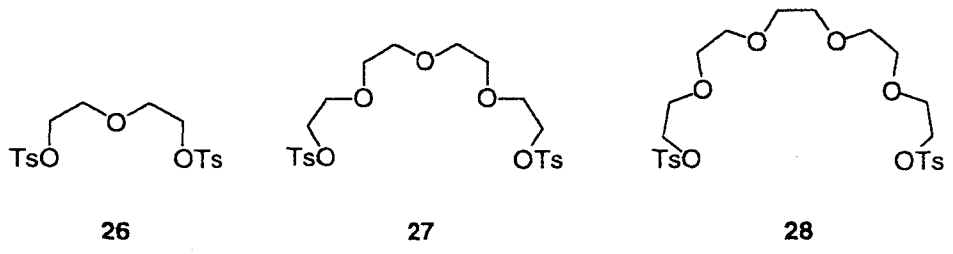

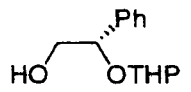

(*S*)-**16**

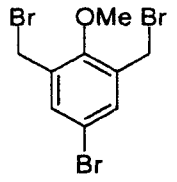

24

Di-, tetra-, and pentaethylene glycol ditosylates **26**, **27**, and **28** were prepared by tosylation of the commercially available corresponding diols. Chiral subunit (*S*)-**16** was prepared by essentially the same procedure[6] as that of (*R*)-**16** except for using (*S*)-mandelic acid as starting material in 95% overall yield. The aromatic subunit **24** was prepared from *p*-bromophenol according to the published method (Scheme 2.5).[5] Hydroxymethylation of *p*-bromophenol gave the triol **32**. The phenolic hydroxy group of **32** was methylated and the remaining hydroxy groups were transformed into bromo to give **24**.

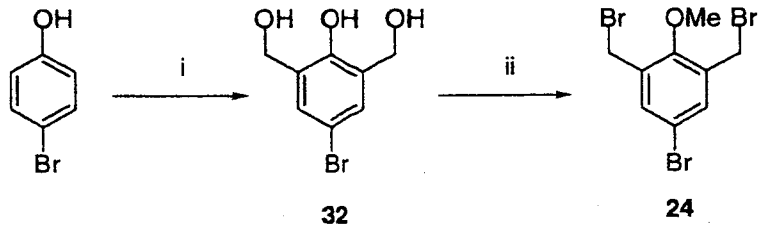

32 **24**

Scheme 2.5 *Reagents*: (i) HCHO, NaOH; (ii) 1. $(MeO)_2SO_2$, K_2CO_3, 2. HBr, 73% for three steps.

Preparation of crown ethers (S,S)-9, (S,S)-10, and (S,S)-11

The synthesis of pseudo-crown ethers (*S,S*)-**9**, (*S,S*)-**10**, and (*S,S*)-**11** was carried out as outlined in Scheme 2.6. Condensation of 2 equiv. of monoprotected chiral ethylene glycol unit (*S*)-**16** with *m*-xylylene dibromide **24** in the presence of NaH followed by deprotection with pyridinium *p*-toluenesulfonate in ethanol gave (*S,S*)-**25** in 95% overall yield, which was used as a common precursor for preparation of phenolic crown ethers (*S,S*)-**9**, (*S,S*)-**10**, and (*S,S*)-**11**. Synthesis of (*S,S*)-**9** was initiated from ring closure of (*S,S*)-**25** with **26** in the presence of NaH in THF under high dilution conditions to give (*S,S*)-**29** in 44% yield. Reaction of (*S,S*)-**29** with *n*-BuLi followed by quenching with water at –78 °C afforded (*S,S*)-

33 in 62% yield. The intra-annular methyl ether of (*S,S*)-**33** was selectively cleaved with sodium ethanetiolate in DMF[7] to furnish (*S,S*)-**34** in 91% yield. By reaction with HNO_3 and $NaNO_2$,[8] the para position of the hydroxy group of (*S,S*)-**34** was selectively nitrated to give (*S,S*)-**9** in 58% yield. Pseudo-24-crown-8 (*S,S*)-**10** and pseudo-27-crown-9 (*S,S*)-**11** were prepared by essentially the same procedure as that for the preparation of (*S,S*)-**9**. In the case of (*S,S*)-**10**, ring closure of (*S,S*)-**25** with **27** gave (*S,S*)-**30** in 36% yield, which was transformed to (*S,S*)-**10** in 18% yield (for three steps) *via* (*S,S*)-**35** and (*S,S*)-**36**. Pseudo-27-crown-9 (*S,S*)-**11** (through (*S,S*)-**31**, (*S,S*)-**37**, and (*S,S*)-**38**) was prepared from (*S,S*)-**25** and **28** in 2.1% overall yield.

The yields for each step of the synthesis of (*S,S*)-**9**, (*S,S*)-**10**, and (*S,S*)-**11** are summarized in Table 2.1. As can be seen from Table 2.1, the yields of the cyclization step (ii) drop with increasing the ring size of the resulting macrocycles. The low overall yield of (*S,S*)-**11** is mainly due to the low yield of the demethylation step (iv). The reason for this is not understood.

Table 2.1 Products and yields for each step of preparation of crown ethers (*S,S*)-**9**, (*S,S*)-**10**, and (*S,S*)-**11**.

Ring size	Synthetic step in Scheme 2.6			
	ii	iii	iv	v
n=1	**29**: 44%	**33**: 62%	**34**: 91%	**9**: 58%
n=3	**30**: 36%	**35**: 62%	**36**: 86%	**10**: 34%
n=4	**31**: 25%	**37**: 68%	**38**: 30%	**11**: 42%

Preparation of crown ether (S,S)-14

The pseudo-crown ether (*S,S*)-**14** was obtained by lithiation of the para position of the inner methoxy group of (*S,S*)-**30**, followed by the treatment with gaseous CO_2 then with aqueous HCl in 32% yield (Scheme 2.7).

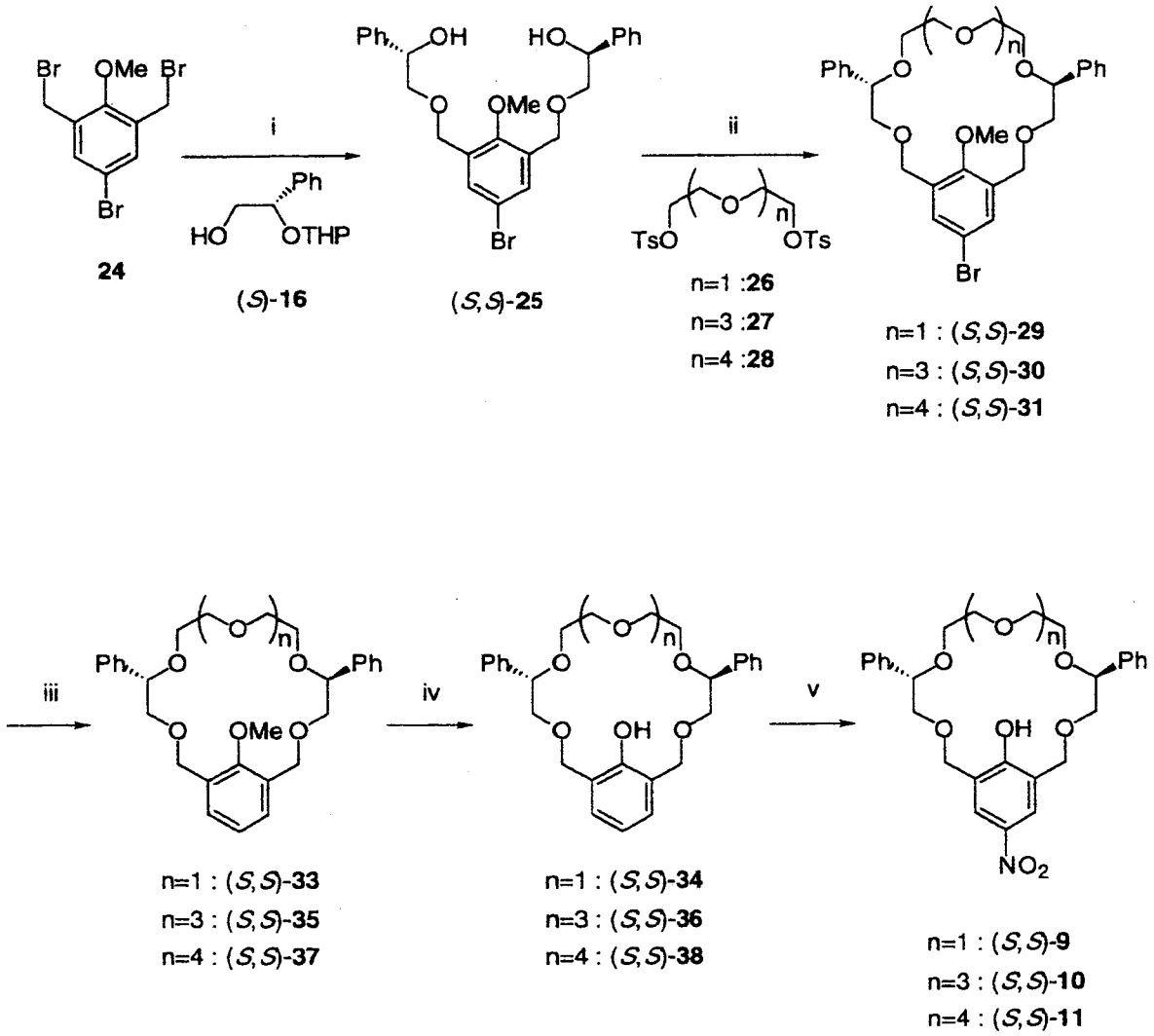

Scheme 2.6 *Reagents and conditions*: (i) 1. NaH, 2. pyridinium *p*-toluenesulfonate, ethanol, 95% for two steps; (ii) **26**, NaH, 44% (n=1), **27**, NaH, 36% (n=3), **28**, NaH, 25% (n=4); (iii) *n*-BuLi, then H_2O, 62% (n=1), 62% (n=3), 68% (n=4); (iv) EtSNa, 91% (n=1), 86% (n=3), 30% (n=4); (v) HNO_3, $NaNO_2$, 58% (n=1), 34% (n=3), 42% (n=4).

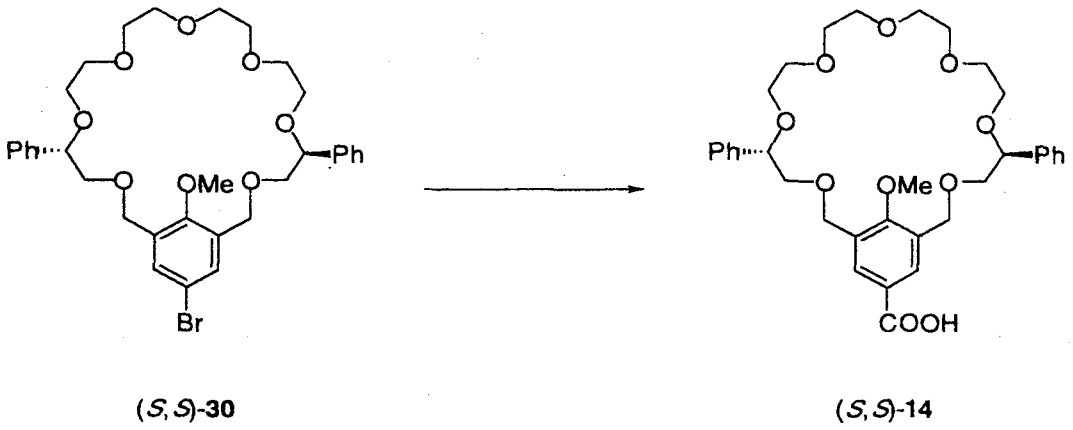

Scheme 2.7 *Reagents*: 1. *n*-BuLi, 2. gaseous CO_2, 3. aqueous HCl, 32%.

2.3 Synthesis of optically active podands

The podands (*R,R*)-**12** and (*R,R*)-**13** were prepared by combining monoprotected chiral ethylene glycol unit (*R*)-**16** derived from (*R*)-mandelic acid and *m*-xylylene dibromide **24**.

The synthesis of podands (*R,R*)-**12** and (*R,R*)-**13** was carried out as outlined in Scheme 2.8. Condensation of 2 equiv. of (*R*)-**16** with **24** in the presence of NaH followed by deprotection with pyridinium *p*-toluenesulfonate in ethanol gave (*R,R*)-**25** in 94% overall yield, which was used as a common precursor for preparation of phenolic podands (*R,R*)-**12** and (*R,R*)-**13**. For the synthesis of (*R,R*)-**12** the hydroxy groups of (*R,R*)-**25** were protected. Treatment of (*R,R*)-**25** with LiBr, TsOH and formaldehyde dimethyl acetal gave MOM ether (*R,R*)-**39** in 50% yield. Debromination of (*R,R*)-**39** afforded (*R,R*)-**40** in 71% yield and subsequent deprotection with hydrochloric acid gave (*R,R*)-**41** in 72% yield. Demethylation[7] of (*R,R*)-**41** followed by nitration at the para position of the hydroxy group[8] of the resulting (*R,R*)-**42** furnished (*R,R*)-**12** in 19% yield for two steps. For the preparation of (*R,R*)-**13**, methylation of the hydroxy groups of (*R,R*)-**25** was first carried out to give (*R,R*)-**43** in 86% yield. Subsequent reduction, demethylation[7] and nitration[8] *via* (*R,R*)-**44** and (*R,R*)-**45** afforded (*R,R*)-**13** in 32% yield for three steps.

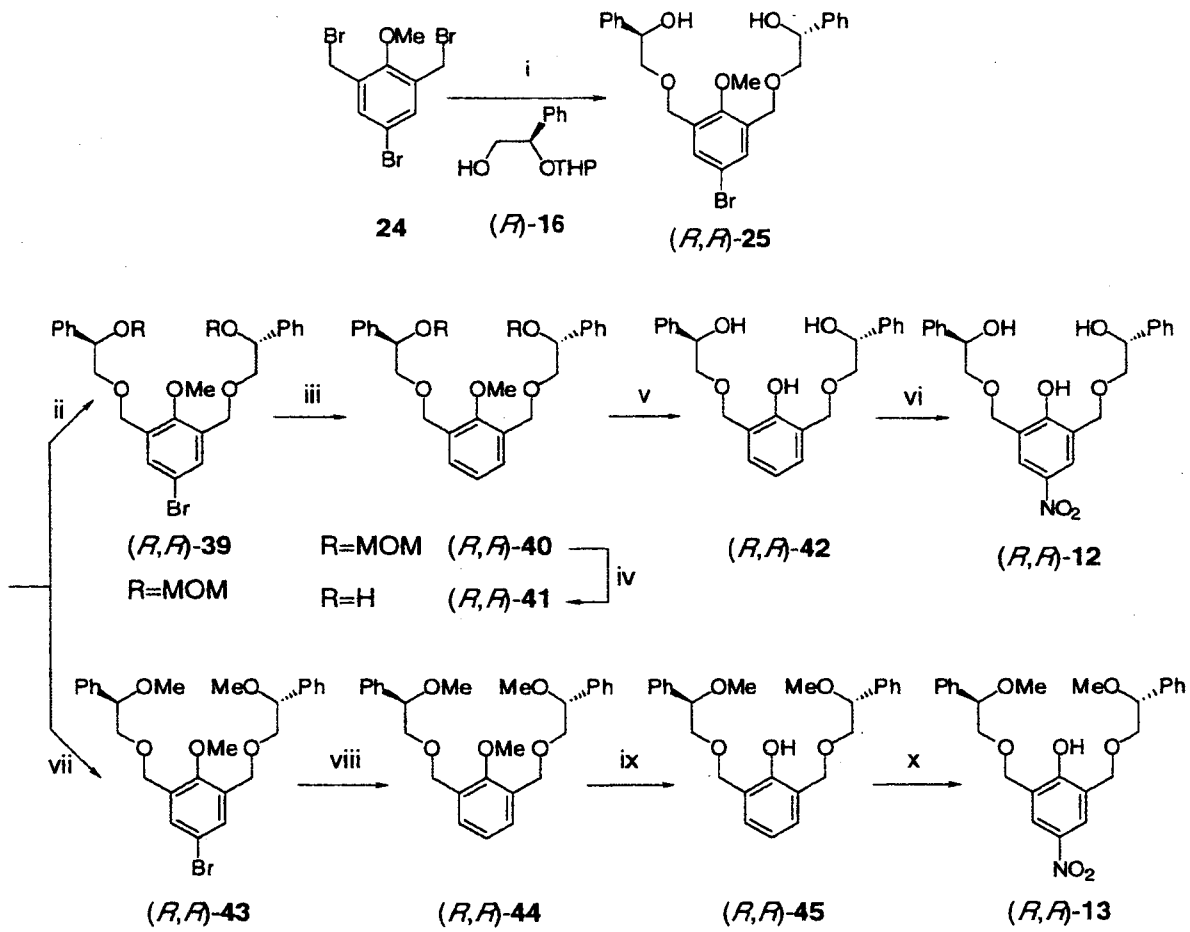

Scheme 2.8 *Reagents and conditions*: (i) 1. NaH, 2. pyridinium *p*-toluenesulfonate, ethanol, 94% for two steps; (ii) $(CH_3O)_2CH_2$, LiBr, TsOH, 50%; (iii) *n*-BuLi, then H_2O, 71%; (iv) 6 N HCl, 72%; (v) EtSNa, 76%; (vi) HNO_3, $NaNO_2$, 25%; (vii) CH_3I, NaH, 86%; (viii) *n*-BuLi, then H_2O, 75%; (ix) EtSNa, 74%; (x) HNO_3, $NaNO_2$, 58%.

2.4 Experimental section

General procedure

^{1}H NMR spectra were recorded at 270, 300 or 400 MHz and ^{13}C NMR spectra at 67.8 MHz on a JEOL JNM-GSX-270, a Varian Mercury 300 or a JMN-AL-400 in $CDCl_3$ and with Me_4Si or residual solvent as an internal standard at 30 °C unless otherwise stated. IR spectra were recorded as a KBr disk or a neat film with a JASCO FTIR-410 spectrometer. UV spectra were recorded on a Hitachi 220A or a U-3310 spectrometer. Mass spectral analyses were performed on a JEOL JMS-DX303HF spectrometer or a JEOL JMS-700 spectrometer by EI

and FAB ionization. Elemental analyses were performed on a Perkin-Elmer 2400II analyzer. Melting points were measured with a hot-stage apparatus and are uncorrected. Optical rotations were measured using a JASCO DIP-40 polarimeter at ambient temperature and $[\alpha]_D$ values are given in units of 10^{-1} deg cm^2 g^{-1}. Column chromatography and TLC were performed with Merck silica gel 60 (70–230 mesh ASTM) and Merck silica gel 60 F_{254}, respectively. Preparative HPLC separation was undertaken with a JAI LC-908 chromatograph using 600-mm × 20-mm JAIGEL-1H and 2H GPC columns with $CHCl_3$ as an eluent. All reagents were obtained from commercial suppliers and used as received. Solvents were dried (drying agent in parentheses) and distilled prior to use: $CDCl_3$ (P_4O_{10}), DMF (CaH_2) and THF (CaH_2 followed by sodium benzophenone ketyl).

1,3-Bis[(4*R*)-hydroxy-4-phenyl-2-oxabutyl]-2,5-dimethoxybenzene (*R*,*R*)-19

A solution of (*R*)-(–)-**16** (9.10 g, 410 mmol) in dry THF (100 mL) was slowly added to a suspension of sodium hydride (60% in mineral oil, 4.69 g, 117 mmol) in dry THF (100 mL) at room temperature. After being refluxed for 2 h, a solution of **17** (6.00 g, 185 mmol) in dry THF (150 mL) was added slowly. After additional reflux for 6 h, 20 mL of water was carefully added to the reaction mixture with ice-cooling. Then the solvent was removed under reduced pressure. The residue was extracted with a mixed solvent containing hexane and ethyl acetate, the combined extracts were washed with water and dried over anhydrous $MgSO_4$, and then the solvent was removed under reduced pressure. The residue was stirred with pyridinium *p*-toluenesulfonate (0.462 g, 1.8 mmol) in methanol (200 mL) for 3 h at 50 °C. After the solvent was removed under reduced pressure, the residue was dissolved in $CHCl_3$, washed with water, and dried over anhydrous $MgSO_4$. The solvent was removed under reduced pressure and the residue was chromatographed on silica gel (hexane:ethyl acetate) to give (*R*,*R*)-**19** (4.1 g, 51%) as a yellow oil: $[\alpha]_D^{25}$=–37.3 (*c* 0.35, $CHCl_3$); IR (neat) 3450, 2900, 1480, 1250, 1110, 1069, 760, 705 cm^{-1}; δ 2.87 (2H, d, *J* = 2.3 Hz, O*H*), 3.56 (2H, dd, *J* = 9.8, 8.9 Hz, OCH(Ph)CH_2), 3.70 (2H, dd, *J* = 9.8, 3.1 Hz, OCH(Ph)CH_2), 3.71 (3H, s, ArOCH_3), 3.78 (3H, s, ArOCH_3), 4.63 (4H, s, benzylic CH_2), 4.94 (2H, ddd, *J* = 8.9, 3.1, 2.3 Hz, OC*H*(Ph)CH_2), 6.89 (2H, s, $(MeO)_2$Ar*H*), 7.27-7.40 (10H, m, C_6H_5); MS (FAB) *m/z* 438 (M^+). Anal. Calcd for $C_{22}H_{30}O_6$: C, 71.21; H, 6.90. Found: C, 70.88; H, 7.09.

2,5-dimethoxy-1,3-bis[(4*R*)-methoxy-4-phenyl-2-oxabutyl]benzene (*R*,*R*)-20

A solution of (*R*,*R*)-**19** (2.50 g, 5.70 mmol) in dry THF (20 mL) was added dropwise to a suspension of sodium hydride (60% in mineral oil, 700 mg, 17 mmol) in dry THF (40 mL) over a 2 h period at 60 °C. After the mixture was cooled to room temperature, iodomethane (2.80 ml, 46.0 mmol) was added dropwise to the reaction mixture. After all the starting material (*R*,*R*)-**19** had been vanished as indicated by TLC, the reaction mixture was neutralized with water and 6 N HCl with ice cooling. After excess iodomethane and the solvent were removed under reduced pressure, the residue was extracted with ethyl acetate. The extract was dried over anhydrous $MgSO_4$ and the solvent was removed under reduced pressure. Chromatography on silica gel (hexane:ethyl acetate) of the residue gave (*R*,*R*)-**20** (1.9 g, 71% yield) as a yellow oil: IR (neat) 2950, 1460, 1360, 1220, 1105, 1005, 870, 760, 701 cm^{-1}; ^1H NMR ($CDCl_3$, 270 MHz) δ 3.29 (s, 6H, OCH_3), 3.55 (dd, *J*=7.5, 10.3 Hz, 2H, $OCH(Ph)CH_2$), 3.61 (3H, s, $ArOCH_3$), 3.70 (dd, *J*=3.8, 10.3 Hz, 2H, $OCH(Ph)CH_2$), 3.73 (3H, s, $ArOCH_3$), 4.41 (dd, *J*=3.8, 7.5 Hz, 2H,$OCH(Ph)CH_2$), 4.58 (s, 4H, benzylic CH_2), 6.86 (s, 2H, $(MeO)_2ArH$), 7.25–7.40 (m, 10H, C_6H_5); MS (FAB) *m/z* 515 $(M+H)^+$.

2-Hydroxy-5-(2,4-dinitrophenylazo)-1,3-bis[(4*R*)-methoxy-4-phenyl-2-oxabutyl]benzene (*R*,*R*)-15

To a suspension of sodium hydride (60% in mineral oil, 860 mg, 21 mmol) in dry DMF (30 mL) was added slowly ethanethiol (1.9mL, 10 mmol) with ice-cooling. After hydrogen evolution ceased, a solution of (*R*,*R*)-**20** (500 mg, 1.1 mmol) in dry DMF (10 mL) was added to the resulting clear solution. The reaction mixture was stirred for 1.5 h at 80 °C, cooled to 5 °C, neutralized with hydrochloric acid and extracted with $CHCl_3$. The combined extract was washed with aqueous solution of sodium hypochorite, washed with water, and dried over anhydrous $MgSO_4$. The solvent was removed under reduced pressure, and the residue was chromatographed on silica gel (hexane:ethyl acetate) to give crude (*R*,*R*)-**21** (150 mg) as a yellow oil.

A solution of crude (*R*,*R*)-**21** in CH_3CN (15 mL) was added to a solution of ceric (IV) ammonium nitrate (363 mg, 660 mmol) in CH_3CN (10 mL). The mixture was stirred for 1.5 h at room temperature and then cooled to 0–5 °C, when it was diluted with water and extracted with diethylether. The combined extracts were washed with water then, dried over anhydrous $MgSO_4$. The solvent was evaporated under reduced pressure to give crude (*R*,*R*)-**22** (124 mg)

as a yellow oil.

To a solution of crude (*R*,*R*)-**22** (112 mg) in a mixture of CH_2Cl_2 (4.5 mL) and EtOH (3 mL) was added a solution of 2,4-dinitrophenylhydrazine (415 mg, 1.00 mmol) dissolved in a mixture of ethanol (2 mL) and concentrated H_2SO_4 (2 mL). The mixture was stirred for 1.5 h at room temperature, after which it was diluted with water and extracted with $CHCl_3$. The combined extracts were washed with aqueous sodium hydrogen carbonate, then with water, dried over anhydrous $MgSO_4$. The solvent of extracts was evaporated under reduced pressure. The residue was chromatographed on silica gel (hexane:ethyl acetate) to give a solid followed by preparative recycling HPLC to give (*R*,*R*)-**15** (145 mg, 22%) as a red solid: ^{1}H NMR ($CDCl_3$, 300 MH) δ 3.34 (s, 6H, OC*H*$_3$), 3.69 (dd, *J*=7.9, 10.7 Hz, 2H, OCH(Ph)C*H*$_2$), 3.76 (dd, *J*=4.0, 10.7 Hz, 2H, OCH(Ph)C*H*$_2$), 4.49 (dd, *J*=4.0, 7.9 Hz, 2H,OC*H*(Ph)CH$_2$), 4.78 (s, 4H, benzylic C*H*$_2$), 7.20–7.40 (m, 10H, C$_6$*H*$_5$), 7.82 (d, *J* = 8.9 Hz, 1H, (NO$_2$)$_2$Ar*H*),7.83 (s, 2H, phenol ring C*H*), 8.49 (dd, *J* = 2.5, 8.9 Hz, 1H, (NO$_2$)$_2$Ar*H*), 8.76 (d, *J* = 2.5 Hz, 1H, (NO$_2$)$_2$Ar*H*), 8.81 (s, 1H, phenolic O*H*).

5-Bromo-1,3-bis[(4*S*)-hydroxy-4-phenyl-2-oxabutyl]-2-methoxybenzene (*S*,*S*)-**25**

A solution of (*S*)-(+)-**16** (18.6 g, 83.7 mmol) in dry THF (150 mL) was slowly added to a suspension of sodium hydride (60% in mineral oil, 4.69 g, 117 mmol) in dry THF (300 mL) at room temperature. After being refluxed for 1.5 h, a solution of **24** (12.0 g, 32.2 mmol) in dry THF (150 mL) was added slowly. After additional reflux for 6 h, 35 mL of water was carefully added to the reaction mixture with ice-cooling. Then the solvent was removed under reduced pressure. The residue was extracted with a mixed solvent containing hexane and ethyl acetate, the combined extracts were washed with water and dried over anhydrous $MgSO_4$, and then the solvent was removed under reduced pressure. The residue was stirred with pyridinium *p*-toluenesulfonate (0.966 g, 3.84 mmol) in ethanol (125 mL) for 12 h at 50 °C. After the solvent was removed under reduced pressure, the residue was dissolved in $CHCl_3$, and washed with water, and dried over anhydrous $MgSO_4$. The solvent was removed under reduced pressure and the residue was chromatographed on silica gel (hexane:ethyl acetate) to give (*S*,*S*)-**25** (14.9 g, 95%) as a yellow oil: $[\alpha]_D^{25}$=+25.1 (*c* 1.03, $CHCl_3$); IR (neat) 3431, 2871, 1454, 1211, 1105, 757, 701 cm^{-1}; ^{1}H NMR ($CDCl_3$, 300 MHz): δ 2.78 (2H, br s, O*H*), 3.53–3.71 (m, 4H, C*H*$_2$), 3.73 (3H, s, OC*H*$_3$), 4.60 (s, 4H, benzylic C*H*$_2$), 4.94 (dd, *J*=2.9, 8.7 Hz, 2H, OC*H*(Ph)CH$_2$), 7.27–7.41 (m, 10H, C$_6$*H*$_5$), 7.48 (s, 2H, MeOAr*H*). MS (FAB) *m/z*

487 $(M+H)^+$. Anal. Calcd for $C_{25}H_{27}O_5Br$: C, 61.61; H, 5.58; Br, 16.39. Found: C, 61.44; H, 5.51; Br, 16.12.

(5*S*,13*S*)-19-Bromo-21-methoxy-5,13-diphenyl-3,6,9,12,15-pentaoxabicyclo-[15.3.1]henicosa-1(20),17(21),18-triene (*S*,*S*)-**29**

A solution of (*S*,*S*)-**25** (1.01 g, 2.06 mmol) and **26** (0.858 g, 2.07 mmol) in dry THF (125 mL) was added dropwise to a suspension of sodium hydride (60% in mineral oil, 0.349 g, 8.73 mmol) in dry THF (85 mL) over a 9 h period at 60 °C. After being stirred for 18 h, 20 mL of water was added carefully with ice-cooling and then the solvent was removed under reduced pressure. The residue was extracted with a solvent containing hexane and ethyl acetate, the combined extracts were washed with water and dried over anhydrous $MgSO_4$. The solvent was removed under reduced pressure and the residue was chromatographed on silica gel (hexane:ethyl acetate) to give (*S*,*S*)-**29** (0.500 g, 44% yield) as colorless powder: mp 99–100 °C; $[\alpha]_D^{28}$=+92.3 (*c* 1.24, $CHCl_3$); IR (KBr) 2864, 1470, 1430, 1359, 1227, 1096, 1003, 761, 703 cm^{-1}; ^1H NMR ($CDCl_3$, 300 MHz) δ 3.39–3.71 (m, 12H, CH_2), 4.25 (3H, s, OCH_3), 4.52 (dd, *J*=2.5, 8.3 Hz, 2H, OCH(Ph)CH_2), 4.45, 4.69 (AB, *J*=7.4 Hz, Δν=65.6 Hz, 4H, benzylic CH_2), 7.28–7.37 (m, 10H, C_6H_5), 7.42 (s, 2H, MeOAr*H*); MS (FAB) *m/z* 558 $(M+H)^+$. Anal. Calcd for $C_{29}H_{33}O_6Br$: C, 62.48; H, 5.97. Found: C, 62.69; H, 6.12.

(5*S*,13*S*)-21-Methoxy-5,13-diphenyl-3,6,9,12,15-pentaoxabicyclo[15.3.1]henicosa-1(20),17(21),18-triene (*S*,*S*)-**33**

A 1.6 M solution of *n*-BuLi (3.7 mL, 6.1 mmol) in hexanes was added to a solution of (*S*,*S*)-**29** (2.85 g, 5.11 mmol) in dry THF (40 mL) over a 15 min period at –78 °C under nitrogen. After being stirred for 1.5 h at the same temperature, 3 mL of water was added dropwise to the reaction mixture at –78 °C and the mixture was stirred for an additional 1 h at the same temperature. The reaction mixture was warmed to room temperature and extracted with a solvent containing hexane and ethyl acetate. The combined extracts were washed with water and dried over anhydrous $MgSO_4$. The solvent was removed under reduced pressure and the residue was chromatographed on silica gel (hexane:ethyl acetate) to give (*S*,*S*)-**33** (1.52 g, 62% yield) as colorless powder: mp 129–130 °C; $[\alpha]_D^{24}$ +147.1 (*c* 0.54, $CHCl_3$); IR (KBr) 2859, 1596, 1453, 1360, 1232, 1095, 995, 955, 790, 762, 703 cm^{-1}; ^1H NMR ($CDCl_3$, 400 MHz) δ 3.39–3.72 (m, 12H, CH_2), 4.29 (3H, s, OCH_3), 4.52 (dd, *J*=2.4, 8.2 Hz, 2H,

OC*H*(Ph)CH_2), 4.51, 4.74 (AB, *J*=7.1 Hz, Δv=61.6 Hz, 4H, benzylic CH_2), 7.06 (t, *J*=7.4 Hz, 1H, MeOAr*H*), 7.25–7.36 (m, 12H, MeOAr*H* and C_6H_5); MS (FAB) *m/z* 479 $(M+H)^+$.

(5*S*,13*S*)-21-Hydroxy-5,13-diphenyl-3,6,9,12,15-pentaoxabicyclo[15.3.1]henicosa-1(20),17(21),18-triene (*S*,*S*)-34

To a suspension of sodium hydride (60% in mineral oil, 2.79 g, 69.8 mmol) in dry DMF (70 mL) was added slowly ethanethiol (6.4 mL, 84 mmol) with ice-cooling. After hydrogen evolution ceased, a solution of (*S*,*S*)-**33** (1.66 g, 3.46 mmol) in dry DMF (150 mL) was added to the resulting clear solution. The reaction mixture was stirred for 2 h at 80 °C, cooled to 5 °C, neutralized with hydrochloric acid and extracted with $CHCl_3$. The combined extract was washed with aqueous solution of sodium hypochorite, washed with water, and dried over anhydrous $MgSO_4$. The solvent was removed under reduced pressure, and the residue was chromatographed on silica gel (hexane:ethyl acetate) followed by recrystallization from hexane to give (*S*,*S*)-**34** (1.47 g, 91% yield) as colorless powder: mp 92–94 °C; $[\alpha]_D^{21}$=+117.1 (*c* 0.34, $CHCl_3$); IR (KBr) 3366, 2867, 1600, 1467, 1360, 1244, 1097, 754, 703 cm^{-1}; ^1H NMR ($CDCl_3$, 400 MHz) δ 3.60–3.80 (m, 12H, CH_2), 4.67 (dd, *J*=2.8, 8.3 Hz, 2H, OC*H*(Ph)CH_2), 4.76 (s, 4H, benzylic CH_2), 6.81 (t, *J*=7.4 Hz, 1H, phenol ring C*H*), 7.13 (d, *J*=7.4 Hz, 2H, phenol ring C*H*), 7.27–7.35 (m, 10H, C_6H_5), 8.14 (s, 1H, phenolic O*H*); MS (FAB) *m/z* 465 $(M+H)^+$. Anal. Calcd for $C_{29}H_{33}O_6Br$: C, 72.39; H, 6.94. Found: C, 72.15; H, 7.01.

(5*S*,13*S*)-21-Hydroxy-19-nitro-5,13-diphenyl-3,6,9,12,15-pentaoxabicyclo[15.3.1]-henicosa-1(20),17(21),18-triene (*S*,*S*)-9

A solution of sodium nitrite (0.590 g, 8.55 mmol) in water (120 mL) and 0.3 N nitric acid (34 mL) was added to a solution of (*S*,*S*)-**34** (1.00 g, 2.15 mmol) in $CHCl_3$ (80 mL) successively. The mixture was then stirred vigorously for 4 h at room temperature. The reaction mixture was neutralized with saturated aqueous solution of sodium hydrogencarbonate and the $CHCl_3$ layer was separated. The organic phase was washed with water and dried over anhydrous $MgSO_4$. After the solvent was removed under reduced pressure, the residue was purified by chromatography on alumina (hexane:ethyl acetate then ethanol) to give (*S*,*S*)-**9** (0.636 g, 58% yield) as yellow powder: mp 52–54 °C; $[\alpha]_D^{21}$=+97.2 (*c* 0.61, $CHCl_3$); IR (KBr) 3319, 2871, 1600, 1520, 1452, 1339, 1091, 749, 703 cm^{-1}; ^1H NMR ($CDCl_3$, 400 MHz) δ 3.54–3.78 (m, 12H, CH_2), 4.66 (dd, *J*=3.7, 7.2 Hz, 2H, OC*H*(Ph)CH_2),

4.83 (s, 4H, benzylic CH_2), 7.30–7.38 (m, 10H, C_6H_5), 8.10 (s, 2H, phenol ring CH), 9.20 (s, 1H, OH); ^{13}C NMR ($CDCl_3$, 67.8 Hz) δ 69.0, 70.0, 70.6, 75.2, 76.5, 125.1, 125.2, 126.8, 128.1, 128.5, 138.0, 139.9, 161.2; MS (FAB) *m/z* 510 $(M+H)^+$; HRMS (FAB) calcd for $C_{28}H_{32}NO_8$ $(M+H)^+$ 510.2128; found 510.2102.

(5*S*,19*S*)-25-Bromo-27-methoxy-5,19-diphenyl-3,6,9,12,15,18,21-heptaoxabicyclo-[21.3.1]heptacosa-1(26),23(27),24-triene (*S*,*S*)-**30**

A solution of (*S*,*S*)-**25** (6.56 g, 13.5 mmol) and **27** (8.12 g, 16.1 mmol) in dry THF (125 mL) was added dropwise to a suspension of sodium hydride (60% in mineral oil, 4.93 g, 123 mmol) in dry THF (600 mL) over a 10 h period at 60 °C. After being stirred for 5 h, 50 mL of water was added carefully with ice-cooling and then the solvent was removed under reduced pressure. The residue was extracted with a solvent containing hexane and ethyl acetate, the combined extracts were washed with water and dried over anhydrous $MgSO_4$. The solvent was removed under reduced pressure and the residue was chromatographed on silica gel (hexane:ethyl acetate) followed by alumina ($CHCl_3$) to give (*S*,*S*)-**30** (3.14 g, 36% yield) as a colorless oil: $[\alpha]_D^{29}$=+56.9 (*c* 1.00, $CHCl_3$); IR (neat) 2867, 1453, 1346, 1216, 1107, 1004, 757, 702 cm^{-1}; ^1H NMR ($CDCl_3$, 270 MHz) δ 3.46–3.77 (m, 20H, CH_2), 3.93 (3H, s, OCH_3), 4.63 (dd, *J*=3.3, 8.0 Hz, 2H, $OCH(Ph)CH_2$), 4.65, 4.70 (AB, *J*=11.6 Hz, Δν=13.2 Hz, 4H, benzylic CH_2), 7.27–7.36 (m, 10H, C_6H_5), 7.51 (s, 2H, MeOArH); ^{13}C NMR ($CDCl_3$, 67.8 MHz) δ 63.13, 67.95, 68.84, 70.60, 70.67, 70.70, 75.33, 82.31, 116.71, 126.75, 127.82, 128.35, 132.25, 133.91, 138.90, 155.66; MS (FAB) *m/z* 645 $(M+H)^+$, 667 $(M+Na)^+$; HRMS (FAB) calcd for $C_{33}H_{42}O_8Br$ $(M+H)^+$ 642.2043; found 642.2032.

(5*S*,19*S*)-27-Methoxy-5,19-diphenyl-3,6,9,12,15,18,21-heptaoxabicyclo[21.3.1]heptacosa-1(26),23(27),24-triene (*S*,*S*)-**35**

A 1.6 M solution of *n*-BuLi (1.2 mL, 1.84 mmol) in hexanes was added to a solution of (*S*,*S*)-**30** (541 mg, 0.838 mmol) in dry THF (7 mL) over a 15 min period at –78 °C under nitrogen. After being stirred for 1.5 h at the same temperature, 2 mL of water was added dropwise to the reaction mixture at –78 °C and the mixture was stirred for an additional 2 h at the same temperature. The reaction mixture was warmed to room temperature and extracted with a solvent containing hexane and ethyl acetate. The combined extracts were washed with water and dried over anhydrous $MgSO_4$. The solvent was removed under reduced pressure

and the residue was chromatographed on silica gel (hexane:ethyl acetate) to give (*S*,*S*)-**35** (294 mg, 0.519 mmol, 62% yield) as a colorless oil: $[\alpha]_D^{30}$=+70.7 (*c* 0.43, $CHCl_3$); IR (neat) 2866, 1452, 1346, 1215, 1100, 1007, 760, 702 cm^{-1}; ^1H NMR ($CDCl_3$, 270 MHz) δ 3.45–3.79 (m, 20H, CH_2), 3.97 (3H, s, OCH_3), 4.62 (dd, *J*=3.0, 8.2 Hz, 2H, OC*H*(Ph)CH_2), 4.68, 4.72 (AB, *J*=11.4 Hz, Δν=10.7 Hz, 4H, benzylic CH_2), 7.10 (t, *J*=7.5 Hz, 1H, MeOAr*H*), 7.27–7.39 (m, 12H, MeOAr*H* and C_6H_5); ^{13}C NMR ($CDCl_3$, 67.8 MHz) δ 63.32, 68.61, 68.93, 70.67, 70.75, 70.76, 75.28, 82.27, 123.82, 126.80, 127.75, 128.32, 130.13, 131.57, 139.19, 157.10; MS (FAB) *m/z* 567 $(M+H)^+$, 589 $(M+Na)^+$; HRMS (FAB) calcd for $C_{33}H_{42}O_8Na$ $(M+Na)^+$ 589.2778; found 589.2786.

(5*S*,19*S*)-27-Hydroxy-5,19-diphenyl-3,6,9,12,15,18,21-heptaoxabicyclo[21.3.1]heptacosa-1(26),23(27),24-triene (*S*,*S*)-**36**

To a suspension of sodium hydride (60% in mineral oil, 1.41 g, 35.3 mmol) in dry DMF (50 mL) was added slowly ethanethiol (3.3 mL, 44 mmol) with ice-cooling. After hydrogen evolution ceased, a solution of (*S*,*S*)-**35** (1.00 g, 1.77 mmol) in dry DMF (30 mL) was added to the resulting clear solution. The reaction mixture was stirred for 2 h at 80 °C, cooled to 5 °C, neutralized with hydrochloric acid and extracted with $CHCl_3$. The combined extract was washed with aqueous solution of sodium hypochorite, washed with water, and dried over anhydrous $MgSO_4$. The solvent was removed under reduced pressure, and the residue was chromatographed on silica gel (hexane:ethyl acetate) to give (*S*,*S*)-**36** (0.838 g, 86% yield) as a colorless oil: $[\alpha]_D^{26}$=+72.1 (*c* 0.839, $CHCl_3$); IR (neat) 3361, 2866, 1598, 1453, 1347, 1225, 1100, 758, 703 cm^{-1}; ^1H NMR ($CDCl_3$, 270 MHz) δ 3.51–3.78 (m, 20H, OCH_2), 4.69 (dd, *J*=3.7, 8.6 Hz, 2H, OC*H*(Ph)CH_2), 4.74, 4.81 (AB, *J*=11.9 Hz, Δν=17.7 Hz, 4H, benzylic CH_2), 6.80 (t, *J*=7.7 Hz, 1H, phenol ring C*H*), 7.12 (d, *J*=7.7 Hz, 2H, phenol ring C*H*), 7.27–7.36 (m, 10H, C_6H_5), 8.05 (s, 1H, phenolic O*H*); ^{13}C NMR ($CDCl_3$, 67.8 Hz) δ 68.75, 70.52, 70.74, 70.76, 70.98, 75.21, 81.64, 119.25, 124.33, 126.89, 127.90, 128.23, 128.38, 138.76, 154.15; MS (FAB) *m/z* 553 $(M+H)^+$, 575 $(M+Na)^+$, HRMS (FAB) calcd for $C_{32}H_{40}O_8Na$ $(M+Na)^+$ 575.2621; found 575.2623.

(5*S*,19*S*)-27-Hydroxy-25-nitro-5,19-diphenyl-3,6,9,12,15,18,21-heptaoxabicyclo-[21.3.1]heptacosa-1(26),23(27),24-triene (*S*,*S*)-**10**

A solution of sodium nitrite (338 mg, 4.90 mmol) in water (100 mL) and 1.0 N nitric acid

(10 mL) was added to a solution of (*S*,*S*)-**36** (660 mg, 1.19 mmol) in $CHCl_3$ (180 mL) successively. The mixture was then stirred vigorously for 2 h at room temperature. The reaction mixture was neutralized with saturated aqueous solution of sodium hydrogencarbonate and the $CHCl_3$ layer was separated. The organic phase was washed with water and dried over anhydrous $MgSO_4$. After the solvent was removed under reduced pressure, the residue was purified by on silica gel (hexane:ethyl acetate) followed by alumina ($CHCl_3$) to give (*S*,*S*)-**10** (240 mg, 34% yield) as a yellow oil: $[\alpha]_D^{25}$=+53.3 (*c* 1.06, $CHCl_3$); IR (neat) 3277, 2867, 1596, 1521, 1452, 1339, 1097, 751, 702 cm^{-1}; ^1H NMR ($CDCl_3$, 270 MHz) δ 3.45–3.87 (m, 20H, CH_2), 4.70 (dd, *J*=5.8, 5.8 Hz, 2H, OC*H*(Ph)CH_2), 4.81, 4.85 (AB, *J*=12.9 Hz, Δν=17.9 Hz, 4H, benzylic CH_2), 7.26–7.40 (m, 10H, C_6H_5), 8.08 (s, 2H, phenol ring C*H*), 9.13 (1H, s, O*H*); ^{13}C NMR ($CDCl_3$, 67.8 MHz) δ 68.76, 69.86, 69.87, 70.73, 70.90, 75.50, 81.67, 123.63, 125.26, 126.82, 128.11, 128.49, 138.17, 140.22, 159.56; MS (FAB) *m/z* 598 $(M+H)^+$, 620 $(M+Na)^+$; HRMS (FAB) calcd for $C_{32}H_{40}NO_{10}$ $(M+H)^+$ 598.2652; found 598.2671.

(5*S*,22*S*)-8-Bromo-30-methoxy-5,22-diphenyl-3,6,9,12,15,18,21,24-octaoxabicyclo[24.3.1]triaconta-1(29),26(30),27-triene (*S*,*S*)-**31**

A solution of (*S*,*S*)-**25** (9.30 g, 19.1 mmol) and **28** (10.4 g, 19.1 mmol) in dry THF (500 mL) was added dropwise to a suspension of sodium hydride (60% in mineral oil, 6.42 g, 96.0 mmol) in dry THF (750 mL) over a 17 h period at 60 °C. After being stirred for 30 h, 100 mL of water was added carefully with ice-cooling and then the solvent was removed under reduced pressure. The residue was extracted with a solvent containing hexane and ethyl acetate, the combined extracts were washed with water and dried over anhydrous $MgSO_4$. The solvent was removed under reduced pressure and the residue was chromatographed on silica gel (hexane:ethyl acetate) followed by alumina ($CHCl_3$) to give (*S*,*S*)-**31** (3.32 g, 25% yield) as a colorless oil: $[\alpha]_D^{26}$=+56.9 (*c* 1.10, $CHCl_3$); IR (neat) 2867, 1453, 1347, 1246, 1105, 1003, 857, 759, 703 cm^{-1}; ^1H NMR ($CDCl_3$, 270 MHz) δ 3.46–3.76 (m, 24H, CH_2), 3.82 (s, 3H, OCH_3), 4.61–4.71 (m, 6H, OC*H*(Ph)CH_2 and benzylic CH_2), 7.27–7.37 (m, 10H, C_6H_5), 7.51 (s, 2H, MeOAr*H*); ^{13}C NMR ($CDCl_3$, 67.8 MHz) δ 62.71, 67.75, 68.79, 70.56, 70.58, 70.69, 70.71, 75.29, 82.14, 116.90, 126.83, 127.84, 128.36, 131.94, 133.87, 139.00, 155.26; MS (FAB) *m/z* 689 $(M+H)^+$, 711 $(M+Na)^+$; HRMS (FAB) calcd for $C_{35}H_{45}O_9BrNa$ $(M+Na)^+$ 711.2145; found 711.2158.

(5*S*,22*S*)-30-Methoxy-5,22-diphenyl-3,6,9,12,15,18,21,24-octaoxabicyclo[24.3.1]-triaconta-1(29),26(30),27-triene (*S*,*S*)-37

A 1.6 M solution of *n*-BuLi (3.4 mL, 5.57 mmol) in hexanes was added to a solution of (*S*,*S*)-**31** (2.40 g, 3.48 mmol) in dry THF (100 mL) over a 25 min period at –78 °C under nitrogen. After being stirred for 2 h at the same temperature, 10 mL of water was added dropwise to the reaction mixture at –78 °C and the mixture was stirred for an additional 1 h at the same temperature. The reaction mixture was warmed to room temperature and extracted with a solvent containing hexane and ethyl acetate. The combined extracts were washed with water and dried over anhydrous $MgSO_4$. The solvent was removed under reduced pressure and the residue was chromatographed on silica gel (hexane:ethyl acetate) to give (*S*,*S*)-**37** (1.44 g, 68% yield) as a colorless oil: $[\alpha]_D^{26}$=+60.0 (*c* 1.03, $CHCl_3$); IR (neat) 2866, 1594, 1453, 1347, 1249, 1105, 1006, 950, 788, 760, 703 cm^{-1}; ^1H NMR ($CDCl_3$, 270 MH) δ 3.49–3.78 (m, 24H, CH_2), 3.85 (s, 3H, OCH_3), 4.63 (dd, *J*=3.2, 8.2 Hz, 2H, $OCH(Ph)CH_2$), 4.68 (s, 4H, benzylic CH_2), 7.10 (t, *J*=7.2 Hz, 1H, MeOAr*H*), 7.28–7.41 (m, 12H, C_6H_5 and MeOAr*H*); ^{13}C NMR ($CDCl_3$, 67.8 MHz) δ 62.79, 68.31, 68.88, 70.62, 70.63, 70.74, 70.75, 75.22, 82.12, 123.98, 126.85, 127.75, 128.31, 129.65, 131.47, 139.23, 156.53; MS (FAB) *m/z* 611 $(M+H)^+$, 633 $(M+Na)^+$; HRMS (FAB) calcd for $C_{35}H_{46}O_9Na$ $(M+Na)^+$ 633.3040; found 633.3021.

(5*S*,22*S*)-30-Hydroxy-5,22-diphenyl-3,6,9,12,15,18,21,24-octaoxabicyclo[24.3.1]-triaconta-1(29),26(30),27-triene (*S*,*S*)-38

To a suspension of sodium hydride (60% in mineral oil, 3.05 g, 35.3 mmol) in dry DMF (100 mL) was added slowly ethanethiol (4.2 mL, 57 mmol) with ice-cooling. After hydrogen evolution ceased, a solution of (*S*,*S*)-**37** (1.40 g, 2.29 mmol) in dry DMF (50 mL) was added to the resulting clear solution. The reaction mixture was stirred for 2 h at 80 °C, cooled to 5 °C, neutralized with hydrochloric acid and extracted with $CHCl_3$. The combined extract was washed with aqueous solution of sodium hypochorite, washed with water, and dried over anhydrous $MgSO_4$. The solvent was removed under reduced pressure, and the residue was chromatographed on silica gel (hexane:ethyl acetate) to give (*S*,*S*)-**38** (0.409 g, 30% yield) as a colorless oil: $[\alpha]_D^{26}$=+55.8 (*c* 1.06, $CHCl_3$); IR (neat) 3361, 2866, 1598, 1453, 1348, 1223, 1104, 758, 703 cm^{-1}; ^1H NMR ($CDCl_3$, 270 MHz) δ 3.50–3.77 (m, 24H, CH_2), 4.65 (dd, *J*=4.0,

8.2 Hz, 2H, OC*H*(Ph)CH_2), 4.72, 4.76 (AB, *J*=12.1 Hz, Δν=12.4 Hz, 2H, benzylic C*H*$_2$), 6.80 (t, *J*=7.7 Hz, 1H, phenol ring C*H*), 7.10 (d, *J*=7.7 Hz, 2H, phenol ring C*H*), 7.28–7.35 (m, 10H, C_6H_5), 8.00 (s, 1H, phenolic O*H*); ^{13}C NMR (CDCl3, 67.8 MHz) δ 68.67, 70.39, 70.59, 70.66, 70.75, 70.81, 75.08, 81.57, 119.25, 124.23, 126.91, 127.88, 128.33, 128.36, 138.83, 154.17; MS (FAB) *m/z* 597 $(M+H)^+$, 619 $(M+Na)^+$; HRMS (FAB) calcd for $C_{34}H_{45}O_9$ $(M+1)^+$ 597.3064; found 597.3047.

(5*S*,22*S*)-30-Hydroxy-8-nitro-5,22-diphenyl-3,6,9,12,15,18,21,24-octaoxabicyclo-[24.3.1]triaconta-1(29),26(30),27-triene (*S*,*S*)-**11**

A solution of sodium nitrite (160 mg, 2.27 mmol) in water (100 mL) and 1.0 N nitric acid (5 mL) was added to a solution of (*S*,*S*)-**38** (330 mg, 0.553 mmol) in $CHCl_3$ (80 mL) successively. The mixture was then stirred vigorously for 1 h at room temperature. The reaction mixture was neutralized with saturated aqueous solution of sodium hydrogencarbonate and the $CHCl_3$ layer was separated. The organic phase was washed with water and dried over anhydrous $MgSO_4$. After the solvent was removed under reduced pressure, the residue was purified by on silica gel (hexane:ethyl acetate) followed by alumina ($CHCl_3$) to give (*S*,*S*)-**11** (149 mg, 42% yield) as a yellow oil: $[\alpha]_D^{27}$=+50.5 (*c* 0.84, $CHCl_3$); IR (neat) 3282, 2868, 1595, 1520, 1453, 1338, 1100, 751, 703 cm^{-1}; ^{1}H NMR ($CDCl_3$, 270 MHz) δ 3.49–3.79 (m, 24H, C*H*$_2$), 4.67 (dd, *J*=4.7, 6.7 Hz, 2H, OC*H*(Ph)CH_2), 4.75, 4.82 (AB, *J*=12.7 Hz, Δν=19.3 Hz, 4H, benzylic C*H*$_2$), 7.27–7.41 (m, 10H, C_6H_5), 8.08 (s, 2H, phenol ring C*H*), 9.24 (1H, s, O*H*); ^{13}C NMR ($CDCl_3$, 67.8 MHz) δ 68.52, 69.60, 70.55, 70.61, 70.68, 75.36, 81.67, 123.91, 125.29, 126.83, 128.08, 128.46, 138.25, 140.18, 159.56; MS (FAB) m/z 642 $(M+H)^+$, 664 $(M+Na)^+$; HRMS (FAB) calcd for $C_{34}H_{44}NO_{11}$ $(M+H)^+$ 642.2914; found 642.2908.

(5*S*,19*S*)-27-Methoxy-5,19-diphenyl-3,6,9,12,15,18,21-heptaoxabicyclo-[21.3.1]heptacosa-1(26),23(27),24-triene-25-carboxylic acid (*S*,*S*)-**14**

A 1.6 M solution of *n*-BuLi (4.7 mL, 7.56 mmol) in hexanes was added to a solution of (*S*,*S*)-**30** (1.28 g, 1.99 mmol) in dry THF (80 mL) over a 20 min period at –86 °C under nitrogen. After being stirred for 1.5 h at the same temperature, gaseous CO_2 was introduced to the reaction vessel by bubbling through a glass tube. After an additional 5 h stirring, 5 mL of 1N HCl was added dropwise to the reaction mixture at –86 °C and the mixture was stirred for

an additional 2 h at the same temperature. The reaction mixture was warmed to room temperature and extracted with $CHCl_3$. The combined extracts were washed with water and dried over anhydrous $MgSO_4$. The solvent was removed under reduced pressure and the residue was chromatographed on silica gel (hexane:ethyl acetate) to give (*S,S*)-**14** (0.384 g, 32% yield) as a colorless oil: $[\alpha]_D^{23}$=+48.5 (*c* 1.02, $CHCl_3$); IR (neat) 2856, 1714, 1461, 1376, 1203, 1116, 1002, 760, 703 cm^{-1}; ^1H NMR ($CDCl_3$, 270 MHz) δ 3.45–3.80 (m, 20H, CH_2), 4.05 (3H, s, OCH_3), 4.65 (dd, *J*=3.0, 8.2 Hz, 2H, $OCH(Ph)CH_2$), 4.71, 4.77 (AB, *J*=11.5 Hz, Δν=17.2 Hz, 4H, benzylic CH_2), 7.27–7.39 (m, 10H, C_6H_5), 8.13 (s, 2H, MeOAr*H*); ^{13}C NMR ($CDCl_3$, 67.8 MHz) δ 63.45, 68.45, 68.74, 70.60, 70.62, 70.70, 75.33, 82.33, 124.94, 126.73, 127.76, 128.31, 131.99 132.31, 138.86, 161.64, 170.29; MS (FAB) *m/z* 611 $(M+H)^+$, 633 $(M+Na)^+$.

5-Bromo-1,3-bis[(4*R*)-hydroxy-4-phenyl-2-oxabutyl]-2-methoxybenzene (*R,R*)-**25**

In a manner similar to that described for the preparation of (*S,S*)-**25**, treatment of (*R*)-(–)-**16** (18.3 g, 91.5 mmol) with **24** (14.0 g, 41.6 mmol) and sodium hydride (60% in mineral oil, 4.87 g, 0.122 mol) followed by deprotection gave (*R,R*)-**25** (17.2 g, 94%) as a yellow oil after chromatography on silica gel (hexane:ethyl acetate): $[\alpha]_D^{26}$=–26.3 (*c* 1.01, $CHCl_3$); IR (neat) 3437, 2903, 1454, 1358, 1212, 1119, 1004, 760, 701 cm^{-1}; ^1H NMR ($CDCl_3$, 270 MHz) δ 2.91 (bs, 2H, O*H*), 3.53–3.71 (m, 4H, CH_2), 3.70 (3H, s, OCH_3), 4.58 (s, 4H, benzylic CH_2), 4.92 (dd, *J*=3.2, 8.5 Hz, 2H, $OCH(Ph)CH_2$), 7.24–7.38(m, C_6H_5), 7.47 (s, 2H, OMeAr*H*); MS (FAB) *m/z* 487 $(M+H)^+$.

5-Bromo-2-methoxy-1,3-bis[(4*R*)-(methoxymethoxy)-4-phenyl-2-oxabutyl]benzene (*R,R*)-**39**

$LiBr{\cdot}H_2O$ (4.40 g, 24.6 mmol) and $TsOH{\cdot}H_2O$ (3.10 g, 30.7 mmol) were added successively to a solution of (*R,R*)-**25** in formaldehyde dimethyl acetal (70 mL). After stirring for 2 days at room temperature, the reaction mixture was extracted with ethyl acetate, and combined extracts were washed with water and dried over anhydrous $MgSO_4$. After the solvent was removed under reduced pressure, the residue was chromatographed on silica gel (hexane:ethyl acetate) to give (*R,R*)-**39** (3.39 g, 50% yield) as a yellow oil: $[\alpha]_D^{26}$=–95.1 (*c* 0.98, $CHCl_3$); IR (neat) 2890, 1455, 1359, 1212, 1152, 1104, 1035, 919, 760, 702 cm^{-1}; ^1H NMR ($CDCl_3$, 300 MHz) δ 3.32 (dd, *J*=7.7, 10.4 Hz, 2H, $OCH(Ph)CH_2$), 3.37 (s, 6H,

OCH_2OCH_3), 3.61 (3H, s, OCH_3), 3.76 (dd, J=4.0, 10.4 Hz, 2H, OCH(Ph)CH_2), 4.55 (s, 4H, benzylic CH_2), 4.60, 4.65 (AB, J=6.2 Hz, $\Delta\nu$=11.7 Hz, 4H, OCH_2OCH_3), 4.86 (dd, J=4.0, 7.7 Hz, 2H, OC*H*(Ph)CH_2), 7.23–7.36 (m, 10H, C_6H_5), 7.44 (s, 2H, MeOAr*H*); MS (FAB) *m/z* 575 $(M+H)^+$.

2-Methoxy-1,3-bis[(4*R*)-(methoxymethoxy)-4-phenyl-2-oxabutyl]benzene (*R*,*R*)-40

A 1.6 M solution of *n*-BuLi (0.43 mL, 0.65 mmol) in hexanes was added to a solution of (*R*,*R*)-**39** (248 mg, 0.43 mmol) in dry THF (5 mL) over a 5 min period at –78 °C under nitrogen. After being stirred for 20 min at the same temperature, 1 mL of water was added dropwise to the reaction mixture at –78 °C and the mixture was stirred for an additional 1 h at the same temperature. The reaction mixture was warmed to room temperature and extracted with a solvent containing hexane and ethyl acetate. The combined extracts were washed with water and dried over anhydrous $MgSO_4$. The solvent was removed under reduced pressure and the residue was chromatographed on silica gel (hexane:ethyl acetate) to give (*R*,*R*)-**40** (153 mg, 71% yield) as a yellow oil: $[\alpha]_D^{26}$=–103.2 (*c* 0.64, $CHCl_3$); IR (neat) 2888, 1594, 1455, 1366, 1213, 1152, 1104, 1037, 919, 759, 701 cm^{-1}; ^1H NMR ($CDCl_3$, 270 MHz) δ 3.35 (s, 6H, OCH_2OCH_3), 3.62 (dd, J=7.8, 10.4 Hz, 2H, OCH(Ph)CH_2), 3.65 (3H, s, OCH_3), 3.77 (dd, J=4.0, 10.4 Hz, 2H, OCH(Ph)CH_2), 4.59–4.68 (m, 8H, benzylic CH_2 and OCH_2OCH_3), 4.86 (dd, J=4.0, 7.8 Hz, 2H, OC*H*(Ph)CH_2), 7.06 (t, J=7.5 Hz, 1H, MeOAr*H*), 7.24–7.34 (m, 12H, OMeAr*H* and C_6H_5); MS (FAB) *m/z* 519 $(M+Na)^+$.

1,3-Bis[(4*R*)-hydroxy-4-phenyl-2-oxabutyl]-2-methoxybenzene (*R*,*R*)-41

A 0.1 mL of 6 N HCl was added to a solution of (*R*,*R*)-**40** (898 mg, 1.80 mmol) in methanol with ice-cooling. After being stirred for 2 days at room temperature, an aqueous solution of sodium hydrogencarbonate was added to the reaction mixture. After extraction with ethyl acetate, the extract was washed with water and dried over anhydrous $MgSO_4$. The solvent was removed under reduced pressure and the residue was chromatographed on silica gel (hexane:ethyl acetate) to give (*R*,*R*)-**41** (535 mg, 72% yield) as a yellow oil: $[\alpha]_D^{26}$=–38.5 (*c* 1.08, $CHCl_3$); IR (neat) 3443, 2863, 1595, 1455, 1359, 1212, 1102, 903, 761, 701 cm^{-1}; ^1H NMR ($CDCl_3$, 300 MHz) δ 2.93 (s, 2H, O*H*), 3.55 (dd, J=8.6, 9.8 Hz, 2H, OCH(Ph)CH_2), 3.69 (dd, J=3.2, 9.8 Hz, 2H, OCH(Ph)CH_2), 3.77 (3H, s, OCH_3), 4.65 (s, 4H, benzylic CH_2), 4.92 (dd, J=3.2, 8.6 Hz, 2H, OC*H*(Ph)CH_2), 7.13 (t, J=7.4 Hz, 1H, MeOAr*H*), 7.24–7.40 (m,

12H, MeOAr*H* and C_6H_5); MS (FAB) *m/z* 409 $(M+1)^+$.

2-Hydroxy-1,3-bis[(4*R*)-hydroxy-4-phenyl-2-oxabutyl]benzene (*R*,*R*)-42

To a suspension of sodium hydride (60% in mineral oil, 546 mg, 13.7 mmol) in dry DMF (30 mL) was added slowly ethanethiol (2.0 mL, 27 mmol) with ice-cooling. After hydrogen evolution ceased, a solution of (*R*,*R*)-**41** (465 mg, 1.10 mmol) in dry DMF (50 mL) was added to the resulting clear solution. The reaction mixture was stirred for 2 h at 80 °C, cooled to 5 °C, neutralized with hydrochloric acid and extracted with $CHCl_3$. The combined extract was washed with aqueous solution of sodium hypochorite, washed with water, and dried over anhydrous $MgSO_4$. The solvent was removed under reduced pressure, and the residue was chromatographed on silica gel (hexane:ethyl acetate) to give (*R*,*R*)-**42** (341 mg, 76% yield) as a colorless oil: $[\alpha]_D^{26}$=–73.1 (*c* 1.01, $CHCl_3$); IR (neat) 3376, 2864, 1598, 1464, 1358, 1219, 1103, 901, 756, 701 cm^{-1}; ^1H NMR ($CDCl_3$, 300 MHz) δ 3.50 (dd, *J*=8.8, 10.3 Hz, 2H, OCH(Ph)C*H*$_2$), 3.56 (s, 2H, O*H*), 3.63 (dd, *J*=3.2, 10.3 Hz, 2H, OCH(Ph)C*H*$_2$), 4.62, 4.63 (AB, *J*=12.4 Hz, Δν=2.3 Hz, 4H, benzylic C*H*$_2$), 4.84 (dd, *J*=3.2, 8.8 Hz, 2H, OC*H*(Ph)CH$_2$), 7.07 (d, *J*=7.7, Hz, 2H, phenol ring C*H*), 7.40 (t, *J*=7.7 Hz, 1H, phenol ring C*H*), 7.18–7.30 (m, 10H, C_6H_5), 7.94 (s, 1H, phenolic O*H*); MS (FAB) *m/z* 395 $(M+1)^+$.

2-Hydroxy-1,3-bis[(4*R*)-hydroxy-4-phenyl-2-oxabutyl]-5-nitrobenzene (*R*,*R*)-12

A solution of sodium nitrite (538 mg, 7.80 mmol) in water (120 mL) and 0.3 N nitric acid (30 mL) was added to a solution of (*R*,*R*)-**42** (750 mg, 1.9 mmol) in $CHCl_3$ (60 mL) successively. The mixture was then stirred vigorously for 3 days at room temperature. The reaction mixture was neutralized with saturated aqueous solution of sodium hydrogencarbonate and the $CHCl_3$ layer was separated. The organic phase was washed with water and dried over anhydrous $MgSO_4$. After the solvent was removed under reduced pressure, the residue was chromatographed on silica gel (hexane:ethyl acetate) followed by preparative recycling HPLC ($CHCl_3$) to give (*R*,*R*)-**12** (212 mg, 25% yield) as yellow: mp 52–53 °C; $[\alpha]_D^{26}$=–29.3 (*c* 1.01, $CHCl_3$); IR (KBr) 3306, 2868, 1597, 1520, 1454, 1338, 1198, 1099, 909, 750, 701 cm^{-1}; ^1H NMR ($CDCl_3$, 270 MHz) δ 2.74 (s, 2H, O*H*), 3.65 (dd, *J*=8.6, 10.1 Hz, 2H, OCH(Ph)C*H*$_2$), 3.78 (dd, *J*=3.2, 10.1 Hz, 2H, OCH(Ph)C*H*$_2$), 4.77 (s, 4H, benzylic C*H*$_2$), 5.00 (dd, *J*=3.2, 8.6 Hz, 2H, OC*H*(Ph)CH$_2$), 7.25–7.40 (m, 10H, C_6H_5), 8.09 (s, 2H, phenol ring C*H*), 8.93 (s, 1H, phenolic O*H*); MS (FAB) *m/z* 440 $(M+1)^+$.

5-Bromo-2-methoxy-1,3-bis[(4*R*)-methoxy-4-phenyl-2-oxabutyl]benzene (*R*,*R*)-43

A solution of (*R*,*R*)-**25** (2.50 g, 5.10 mmol) in dry THF (50 mL) was added dropwise to a suspension of sodium hydride (60% in mineral oil, 0.620 g, 15.5 mmol) in dry THF (50 mL) over a 3 h period at 60 °C. After the mixture was cooled to room temperature, iodomethane (2.50 ml, 41.0 mmol) was added dropwise to the reaction mixture. After all the starting material (*R*,*R*)-**25** had been vanished as indicated by TLC, the reaction mixture was neutralized with water and 6 N HCl with ice cooling. After excess iodomethane and the solvent were removed under reduced pressure, the residue was extracted with ethyl acetate. The extract was dried over anhydrous $MgSO_4$ and the solvent was removed under reduced pressure. Chromatography on silica gel (hexane:ethyl acetate) of the residue gave (*R*,*R*)-**43** (2.30 g, 86% yield) as a yellow oil: $[\alpha]_D^{26}$=–34.7 (c 0.94, $CHCl_3$); IR (neat) 2930, 1455, 1357, 1210, 1106, 1004, 873, 759, 701 cm^{-1}; ^1H NMR ($CDCl_3$, 400 MHz) δ 3.30 (s, 6H, OCH_3), 3.56 (dd, *J*=7.7, 10.4 Hz, 2H, $OCH(Ph)CH_2$), 3.63 (3H, s, $ArOCH_3$), 3.70 (dd, *J*=3.8, 10.4 Hz, 2H, $OCH(Ph)CH_2$), 4.41 (dd, *J*=3.8, 7.7 Hz, 2H,$OCH(Ph)CH_2$), 4.51, 4.59 (AB, *J*=8.4 Hz, Δν=20.6 Hz, 4H, benzylic CH_2), 7.25–7.40 (m, 10H, C_6H_5), 7.43 (s, 2H, MeOAr*H*); MS (FAB) *m/z* 515 $(M+H)^+$.

2-Methoxy-1,3-bis[(4*R*)-methoxy-4-phenyl-2-oxabutyl]benzene (*R*,*R*)-44

A 1.6 M solution of *n*-BuLi (0.90 mL, 1.44 mmol) in hexanes was added to a solution of (*R*,*R*)-**43** (500 mg, 0.970 mmol) in dry THF (10 mL) over a 15 min period at –78 °C under nitrogen. After being stirred for 15 min at the same temperature, 3 mL of water was added dropwise to the reaction mixture at –78 °C and the mixture was stirred for an additional 1 h at the same temperature. The reaction mixture was warmed to room temperature and extracted with a solvent containing hexane and ethyl acetate. The combined extracts were washed with water and dried over anhydrous $MgSO_4$. The solvent was removed under reduced pressure and the residue was chromatographed on silica gel (hexane:ethyl acetate) to give (*R*,*R*)-**44** (290 mg, 75% yield) as a yellow oil: $[\alpha]_D^{26}$=–50.4 (*c* 0.52, $CHCl_3$); IR (neat) 2931, 1455, 1358, 1245, 1103, 1006, 760, 701 cm^{-1}; ^1H NMR ($CDCl_3$, 400 MHz) δ 3.29 (s, 6H, OCH_3), 3.54 (dd, *J*=7.8, 10.3 Hz, 2H, $OCH(Ph)CH_2$), 3.67 (3H, s, $ArOCH_3$), 3.70 (dd, *J*=3.9, 10.3 Hz, 2H, $OCH(Ph)CH_2$), 4.41 (dd, *J*=3.9, 7.8 Hz, 2H,$OCH(Ph)CH_2$), 4.57, 4.65 (AB, *J*=7.9 Hz, Δν=20.6 Hz, 4H, benzylic CH_2), 7.06 (t, *J*=7.6 Hz, MeOAr*H*), 7.23–7.35 (m, 12H, OMeAr*H* and C_6H_5); MS (FAB) *m/z* 435 (M^+-H).

2-Hydroxy-1,3-bis[(4*R*)-methoxy-4-phenyl-2-oxabutyl]benzene (*R*,*R*)-45

To a suspension of sodium hydride (60% in mineral oil, 367 mg, 9.10 mmol) in dry DMF (15 mL) was added slowly ethanethiol (0.8 mL, 10 mmol) with ice-cooling. After hydrogen evolution ceased, a solution of (*R*,*R*)-**44** (200 mg, 0.46 mmol) in dry DMF (5 mL) was added to the resulting clear solution. The reaction mixture was stirred for 3 h at 80 °C, cooled to 5 °C, neutralized with hydrochloric acid and extracted with $CHCl_3$. The combined extract was washed with aqueous solution of sodium hypochorite, washed with water, and dried over anhydrous $MgSO_4$. The solvent was removed under reduced pressure, and the residue was chromatographed on silica gel (hexane:ethyl acetate) to give (*R*,*R*)-**45** (144 mg, 74% yield) as a colorless oil: $[\alpha]_D^{26}$=–53.5 (*c* 0.2, $CHCl_3$); IR (neat) 3361, 2865, 2825, 1597, 1492, 1454, 1356, 1223, 1095, 869, 759, 701 cm^{-1}; ^1H NMR ($CDCl_3$, 400 MHz) δ 3.30 (s, 6H, OCH_3), 3.61 (dd, *J*=7.9, 10.6 Hz, 2H, OCH(Ph)CH_2), 3.70 (dd, *J*=3.7, 10.6 Hz, 2H, OCH(Ph)CH_2), 4.44 (dd, *J*=3.7, 7.9 Hz, 2H,OC*H*(Ph)CH_2), 4.68, 4.72 (AB, *J*=12.4 Hz, Δν=12.1 Hz, 4H, benzylic CH_2), 6.80 (t, *J*=7.4 Hz, phenol ring C*H*), 7.11 (d, *J*=7.7 Hz, 2H, phenol ring C*H*), 7.25–7.38 (m, 10H, C_6H_5), 7.76 (s, 1H, phenolic O*H*); MS (FAB) *m/z* 423 $(M+H)^+$.

2-Hydroxy-1,3-bis[(4*R*)-methoxy-4-phenyl-2-oxabutyl]-5-nitrobenzene (*R*,*R*)-13

A solution of sodium nitrite (116 mg, 1.68 mmol) in water (20 mL) and 0.3 N nitric acid (5 mL) was added to a solution of (*R*,*R*)-**45** (173 mg, 0.409 mmol) in $CHCl_3$ (20 mL) successively. The mixture was then stirred vigorously for 3 days at room temperature. The reaction mixture was neutralized with saturated aqueous solution of sodium hydrogencarbonate and the $CHCl_3$ layer was separated. The organic phase was washed with water and dried over anhydrous $MgSO_4$. After the solvent was removed under reduced pressure, the residue was chromatographed on silica gel (hexane:ethyl acetate) followed by preparative recycling HPLC ($CHCl_3$) to give (*R*,*R*)-**13** (111 mg, 58% yield) as a yellow oil: $[\alpha]_D^{28}$=–71.0 (*c* 1.07, $CHCl_3$); IR (neat) 3289, 2864, 1597, 1522, 1454, 1338, 1274, 1201, 1090, 869, 816, 760, 701 cm^{-1}; ^1H NMR ($CDCl_3$, 270 MH) δ 3.33 (s, 6H, OCH_3), 3.69 (dd, *J*=7.9, 10.7 Hz, 2H, OCH(Ph)CH_2), 3.73 (dd, *J*=3.8, 10.7 Hz, 2H, OCH(Ph)CH_2), 4.47 (dd, *J*=3.8, 7.9 Hz, 2H,OC*H*(Ph)CH_2), 4.72 (s, 4H, benzylic CH_2), 7.32–7.57 (m, 10H, C_6H_5), 8.10 (s, 2H, phenol ring C*H*), 8.86 (s, 1H, phenolic O*H*); MS (FAB) *m/z* 468 $(M+H)^+$. Anal. Calcd for $C_{26}H_{29}NO_7$: C, 66.80; H, 6.25; N, 3.00. Found: C, 66.66; H, 6.31; N, 2.78.

2.6 References and notes

1. (a) Naemura, K.; Fuji, J.; Ogasahara, K.; Hirose, K.; Tobe, Y. *Chem. Commun.* **1996**, 2749–2750; (b) Naemura, K.; Nishioka, K.; Ogasahara, K.; Nishikawa, Y.; Hirose, K.; Tobe, Y. *Tetrahedron: Asymmetry* **1998**, *9*, 563–574; (c) Hirose, K.; Ogasahara, K.; Nishioka, K.; Tobe, Y.; Naemura, K. *J. Chem. Soc., Perkin Trans. 2* **2000**, 1984–1993.
2. Pedersen, C. J. *J. Am. Chem. Soc.* **1967**, *89*, 7017–7036.
3. Ashton, P. R.; Bartsch, R. A.; Cantrill, S. J.; Hanes Jr., R. E.; Hickingbottom, S. K.; Lowe, J. N.; Preece, J. A.; Stoddart, J. F.; Talanov, V. S.; Wang, Z. H. *Tetrahedron Lett.* **1999**, *40*, 3661–3364.
4. Glink, P. T.; Schiavo, C.; Stoddart, J. F.; Williams, D. J. *Chem. Commun.* **1996**, 1483–1490.
5. Naemura, K.; Nishikawa, Y.; Fuji, J.; Hirose, K.; Tobe, Y. *Tetrahedron: Asymmetry* **1997**, *8*, 873–882.
6. (a) Huszthy, P.; Bradshaw, J. S.; Zhu, C. Y.; Izatt. R. M. *J. Org. Chem.* **1991**, *56*, 3330-3336. (b) Naemura, K.; Nishikawa, Y.; Fuji, J.; Hirose, K.; Tobe, Y. *Tetrahedron: Asymmetry* **1997**, *8*, 873-882.
7. Feutrill, G. I.; Mirrington, R. N. *Tetrahedron Lett.* **1970**, *16*, 1327–1328.
8. Browne, C. M.; Ferguson, G.; McKervey, M. A.; Mulholland, D. L.; O'Connor, T.; Parvez, M. *J. Am. Chem. Soc.* **1985**, *107*, 2703–2712.

Chapter 3

Enantiomer selectivities in complexation of phenolic crown ethers and podands with amines

3.1 Determination of association constants for complexation of crown ethers and podands with amines

In this chapter, the author describes the complexation ability and enantiomer selectivity of the crown ethers and the podands, whose preparation is described in the previous chapter, toward secondary amines and the methods for the determination of association constants. The binding constants for the complexes were determined by the ^{1}H NMR titration in $CDCl_3$ followed by the non-linear least-squares curve fitting method or by the UV-vis titration in $CHCl_3$ followed by the Rose-Drago data treatment method.[1] Both the ^{1}H NMR titration and the UV-vis titration methods can be used reliably for complexation with binding constants of the observed range (K=10–10^2 M^{-1}).[1b,2] In the case of (R,R)-**12**, however, the UV-vis titration method was employed because of its limited solubility in $CDCl_3$.

3.1.1 ^{1}H NMR titration method

The phenolic crown ethers and podands are expected to form 1:1 salt complexes with amines in solution. Accordingly, host-guest complexation is expressed by the following equilibrium.

$$\mathrm{H} + \mathrm{G} \underset{}{\overset{K}{\rightleftharpoons}} \mathrm{C}$$

The association constant (K) of a host and a guest is expressed by Eq. 1, with initial concentrations of a host and a guest, and the concentration of a complex at equilibrium.

$$K = \frac{[\mathrm{C}]}{[\mathrm{H}][\mathrm{G}]} = \frac{c}{(h-c)(g-c)} \qquad (1)$$

h, g: initial concentrations of a host and a guest
c: concentration of a complex at equilibrium

The ^{1}H NMR spectroscopic methods are classified into two cases depending on the difference between the exchange rate of the complexation equilibrium. When the rate of host-guest complexation equilibrium is comparable to the NMR time scale, since the NMR peaks broaden and/or disappear, it is not possible to determine the association constant precisely. On the other hand, when the rate of the host-guest complexation equilibrium is slow enough compared to the NMR time scale or it is faster than the time scale, it is possible to determine the binding constants.

It turned out that all the complexation described in this thesis has faster exchange rate than the NMR time scale. In this case, the signal due to the complex and the corresponding signal of the free host are fused into one signal at the weight average chemical shift of the free host and the complex as illustrated in Figure 3.1.

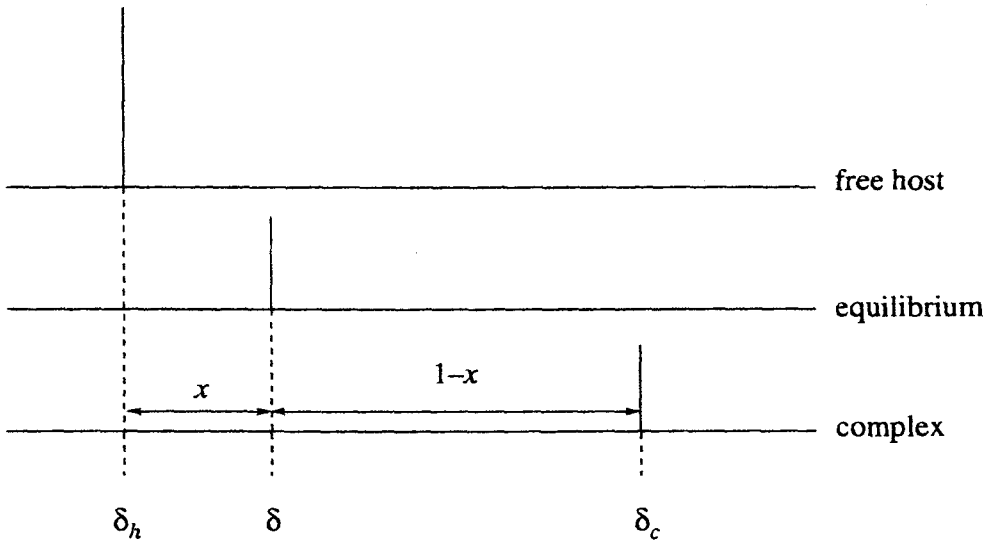

Figure 3.1 Schematic representation for NMR spectra for fast exchanging complexation. The signal at equilibrium appears at the weight average chemical shift depending on the complexation ratio x, where δ_h is chemical shift of a free host and δ_c is that of a complex.

The observed chemical shift δ is expressed by Eq. 2. Eq. 3 is derived from Eq. 1 and Eq. 2. In Eq. 3, δ, δ_h, h, and g are experimental values, while δ_c and K are unknown. The unknown δ_c and K values are obtained by titration experiments followed by the curve fitting to Eq. 3 with the non-linear least-squares curve fitting method.

As an example for the ^{1}H NMR spectroscopic method, the spectral change of host (*S*,*S*)-**10** upon addition of *N*-methylethanolamine is shown in Figure 3.2. The benzylic protons of (*S*,*S*)-**10** move upfield on addition of the guest as shown in Figure 3.2. The calculated association constant for the complex is 210 M^{-1}.

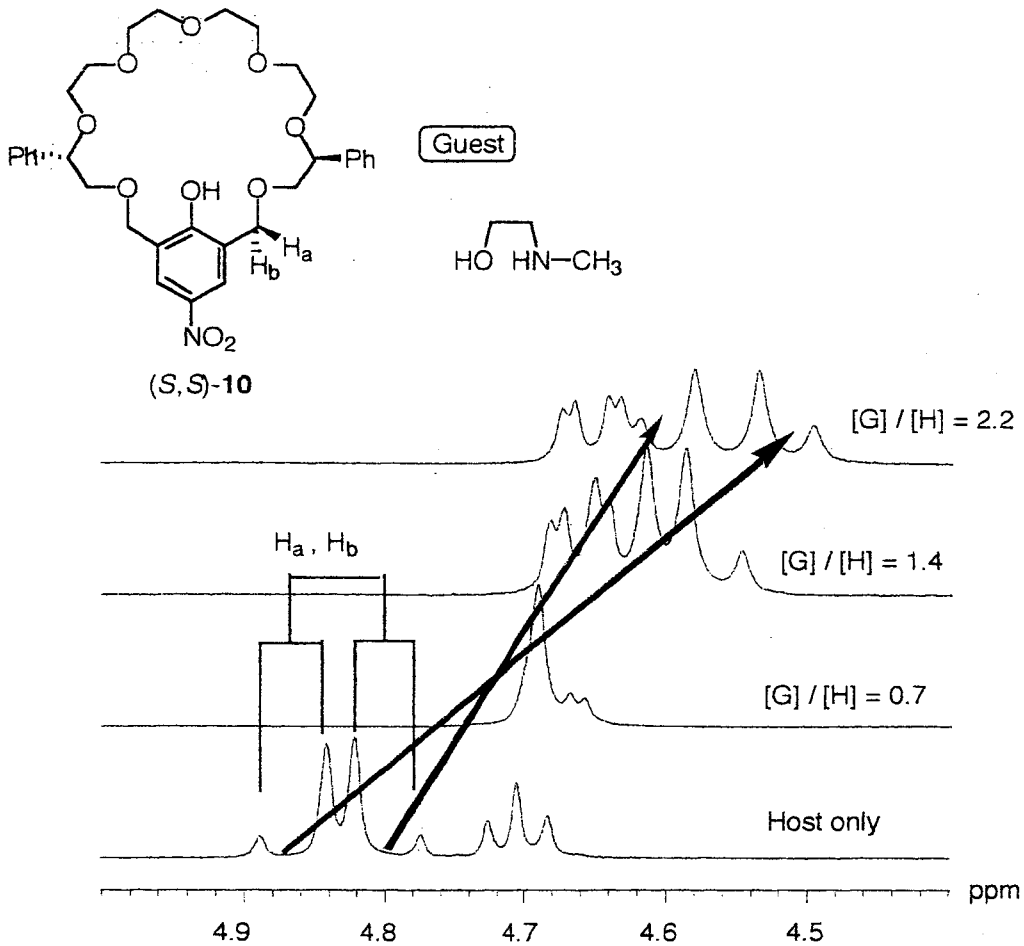

Figure 3.2 ^{1}H NMR spectral change (270 MHz) of (*S*,*S*)-**10** upon addition of different amounts of *N*-methylethanolamine in $CDCl_3$ at 30 °C.

$$\delta = \delta_h \cdot (1 - x) + \delta_c \cdot x \qquad x = \frac{c}{h} \qquad (2)$$

δ: observed chemical shift

δ_h: chemical shift of a free host

δ_c: chemical shift of a complex

x: ratio of a complexed host rerative to total host at equilibrium

$$\delta = \delta_h + (\delta_c - \delta_h) \cdot \frac{1}{h} \cdot \frac{(h + g + \frac{1}{K}) \pm \sqrt{(h + g + \frac{1}{K})^2 - 4hg}}{2} \qquad (3)$$

3.1.2 UV-vis titration method

In contrast to the NMR titration, UV-visible absorption spectra of a host and a complex are observed independently, since the rate of the complexation equilibrium is slow enough compared to photoexcitation. The absorption bands of the hosts (*S*,*S*)-**9**, (*S*,*S*)-**10**, (*S*,*S*)-**11**, (*R*,*R*)-**12**, and (*R*,*R*)-**13**, having a *p*-nitrophenol chromopohore, appeared at 311–315 nm. Upon complexation with amines, new absorption maxima due to the complexes appeared at 386–405 nm.

Eq. 1 using with initial concentrations of a host, a guest, and a complex at equilibrium is transformed to Eq. 4. Since the guests have no absorption around the 386–405 nm region, Eq. 4 can be transformed to Eq. 5 using the Beer-Lambert equation with an absorbance and the molar extinction coefficient of a complex (the Rose-Drago method).[1] Accordingly, an averaged association constant and a molar absorption coefficient of a complex are derived from the data calculated for a number of combinations of appropriate concentrations of host and guest molecules.

$$\frac{1}{K} = c - (h + g) + \frac{h \cdot g}{c} \qquad (4)$$

Beer-Lambert equation

$$\mathrm{A} = \varepsilon_c \cdot c \cdot l = \varepsilon_c \cdot c \qquad (l = 1\mathrm{cm})$$

A: absorbance of a complex

ε_c: molar extinction coefficient of a complex

$$\frac{1}{K} = \frac{\mathrm{A}}{\varepsilon_c} - (h + g) + \frac{\varepsilon_c \cdot h \cdot g}{\mathrm{A}} \qquad (5)$$

As an example, the spectral change of host (*R*,*R*)-**12** upon addition of *N*-methylethanolamine is shown in Figure 3.3. The presence of isosbestic point clearly indicates the 1:1 complex formation. In this case, the association constant was calculated from the change of absorption intensity of the complex at 386 nm to give averaged K = 220 M^{-1}.

To compare the binding constants determined by different methods, their identity should be proved. This has been done for the complexation of pseudo-18-crown-6 having a dinitrophenylazo group. In order to check if the data obtained by the different methods are identical within the experimental error, the author measured binding constants of (*S*,*S*)-**10** with (*S*)- and (*R*)-enantiomers of *N*,α-dimethylbenzylamine by the ^{1}H NMR titration and the UV-vis titration methods. The binding constants of (*S*,*S*)-**10** with (*S*)- and (*R*)-

guest amines obtained by the ^{1}H NMR titration method were (1.8±0.1)×10 M^{-1} and 8.8±0.3 M^{-1}, respectively (K_S/K_R=2.0), and those determined by the UV-vis titration were (2.1±0.3)×10 M^{-1} and (1.0±0.1)×10 M^{-1}, respectively (K_S/K_R=2.1), indicating that the comparison is valid.

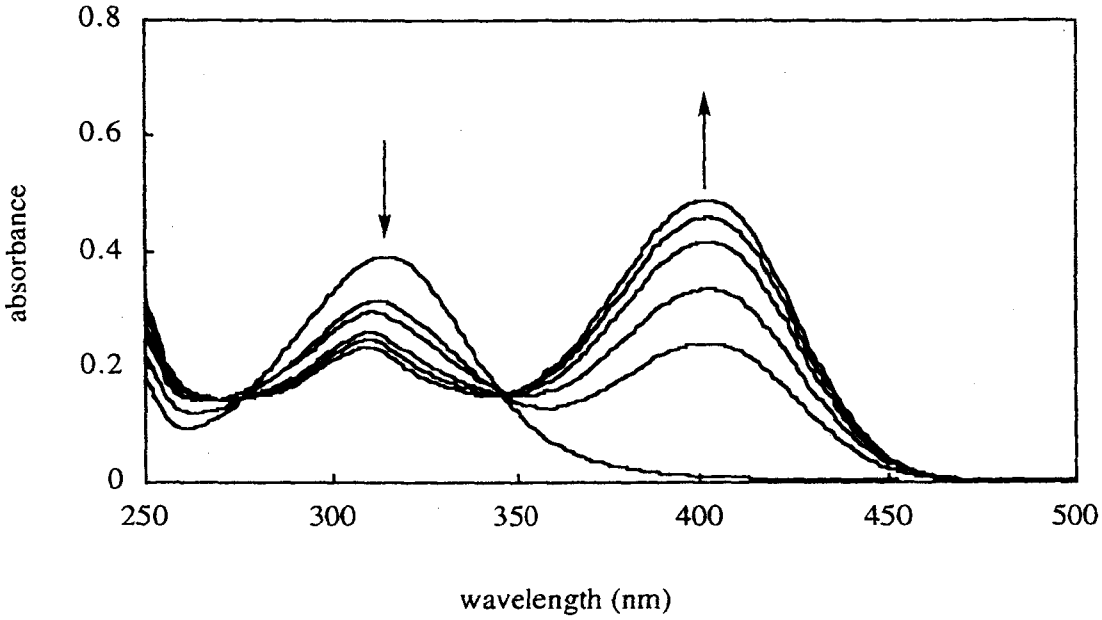

Figure 3.3 UV-visible spectral change of (*R*,*R*)-**12** ([H]=4.4×10^{-5} M) upon addition of different amounts of *N*-methylethanolamine ([G]=0–8.2×10^{-5} M) in $CHCl_3$ at 30 °C.

3.2 Binding ability of phenolic crown ethers and podands toward achiral secondary amines

In order to investigate the complexation ability of the hosts toward secondary amines, complexation of the hosts with achiral amines **46**, **47**, **48**, **49**, and **50** were examined. Compound **46** was chosen as the one without functional group other than amino. An ethanolamine derivative **48** was selected, since it has been clarified that the hydroxy group of ethanol amine derivatives participates host-guest complexation through forming hydrogen bonding with pseudo-18-crown-6 such as (*S*,*S*)-**7**.[3] In order to investigate the effect of substituents on the nitrogen atom, complexation abilities toward primary amine **47** and tertiary amine **49** were also investigated. To examine the effect of the hydroxy group of **48**, complexation with **50** with a methoxy group was also investigated.

The binding constants (*K*) of the complexes of the crown ethers (*S*,*S*)-**9**, (*S*,*S*)-**10**, and

(*S*,*S*)-**11** and podands (*R*,*R*)-**12** and (*R*,*R*)-**13** with achiral amines **46**–**50** are summarized in Table 3.1.

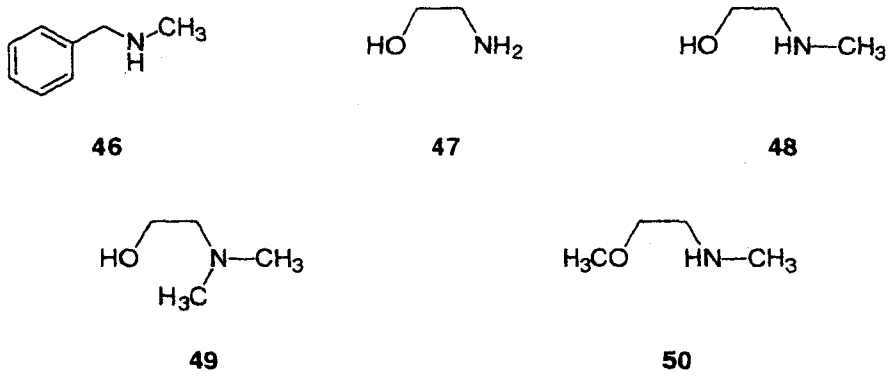

46 **47** **48** **49** **50**

Table 3.1 Binding constants for the complexes of (*S*,*S*)-**9**, (*S*,*S*)-**10**, (*S*,*S*)-**11** (*R*,*R*)-**12**, and (*R*,*R*)-**13** with **46**, **47**, **48**, **49**, and **50**.

	(*S*,*S*)-**9**	(*S*,*S*)-**10**	(*S*,*S*)-**11**	(*R*,*R*)-**12**	(*R*,*R*)-**13**
46	$(1.4\pm0.2)\times10$ [a]	$(4.6\pm0.1)\times10$ [a]	$(2.2\pm0.1)\times10$ [a]	$(1.0\pm0.1)\times10^2$ [b]	–
47	$(9.9\pm0.5)\times10^3$ [d]	$(3.7\pm0.1)\times10^2$ [d]	–	$(3.5\pm0.3)\times10$ [d]	6.2 ± 0.8 [c]
48	$(7.9\pm1.0)\times10$ [d]	$(2.5\pm0.1)\times10^2$ [d]	$(9.5\pm0.1)\times10$ [d]	$(2.2\pm0.2)\times10^2$ [d]	$(1.8\pm0.2)\times10$ [c]
49	<1 [d]	<1 [d]	–	<1 [d]	<1 [d]
50	–	$(2.1\pm0.2)\times10$ [d]	–	$(8.9\pm0.5)\times10$ [d]	–

[a] measured by ^{1}H NMR spectroscopy (270 MHz) in $CDCl_3$ at 15 °C.
[b] measured by UV-vis spectroscopy in $CHCl_3$ at 15 °C.
[c] measured by ^{1}H NMR spectroscopy (270 MHz) in $CDCl_3$ at 30 °C.
[d] measured by UV-vis spectroscopy in $CHCl_3$ at 30 °C.

With *N*-methylbenzylamine (**46**), crown ethers (*S*,*S*)-**9**, (*S*,*S*)-**10**, and (*S*,*S*)-**11** form complexes with binding constants of 14 M^{-1}, 46 M^{-1}, and 22 M^{-1}, respectively at 15 °C. Among them, pseudo-24-crown-8 (*S*,*S*)-**10** shows the largest binding constant, suggesting that the cavity of (*S*,*S*)-**10** fits nicely secondary amine **46**. This also indicates that the cavity of (*S*,*S*)-**9** is too small for **46** while that of (*S*,*S*)-**11** is too large. In addition, it should be pointed out that the binding constant of podand (*R*,*R*)-**12** with **46** is larger than those of crown ethers (*S*,*S*)-**9**, (*S*,*S*)-**10**, and (*S*,*S*)-**11** despite the absence of the cyclic structure. These results suggest that, as the author expected, receptors suitable for binding secondary amines should possess macrocyclic rings which are larger than 18C6, or they can be an

amines should possess macrocyclic rings which are larger than 18C6, or they can be an open chain podand. On the other hand, it was reported that pseudo-18-crown-6 like (*S*,*S*)-**7** showed high binding ability and enantiomer selectivity toward primary ethanolamine derivatives.[4] In order to investigate the effect of substituent on the nitrogen atom of ethanolamines, the author examined the binding ability toward primary, secondary, and tertiary ethanolamine derivatives **47**, **48** and **49**, respectively, at 30 °C. As a result, for primary amine **47**, (*S*,*S*)-**9** is the best binder. In the case of secondary amine **48**, pseudo-24-crown-8 (*S*,*S*)-**10** is the best binder among the hosts examined. However, none of the hosts bind tertiary amine **49**. Again, the binding constant of podand (*R*,*R*)-**12** toward **48** is substantially large and is similar to that of pseudo-24-crown-8 (*S*,*S*)-**10**. On the other hand, the binding constant of podand (*R*,*R*)-**13** is considerably small. In general, the binding constants with amine **48** at 30 °C are larger than those with **46** at 15 °C which does not have a hydroxy group, probably due to the steric repulsion of the phenyl group of **46** that destabilizes the complex and hydrogen bonding between the phenoxide oxygen of the hosts and the hydroxy group of **48** that stabilizes the complex.

In order to investigate the effect of the hydroxy group of guest amines, methoxyamine **50** was employed for the complexation of (*S*,*S*)-**10** and (*R*,*R*)-**12**, which showed considerable binding ability toward hydroxyamine **48**. As a result, the binding constant of (*S*,*S*)-**10** with **50** was 10 times smaller than that with **48** and that of (*R*,*R*)-**12** with **50** is less than half of that with **48**. The greater stability of the complexes with **48** than those with **50** suggests the presence of hydrogen bonding that stabilizes the former complexes.[3] With regard to the absorption maxima of the complexes, it was reported that the absorption maximum of the more favorable complex of azophenolic pseudo-crown ether such as (*S*,*S*)-**7** with one enantiomer guest appeared at shorter wavelength than that of the less stable complex with the other enantiomer.[4] Indeed, the absorption maxima of the complexes of (*S*,*S*)-**10** with **48** and **50** appear 402 and 405 nm, respectively, while those of (*R*,*R*)-**12** at 386 and 389 nm, respectively. These results are consistent with the presence of hydrogen bonding between the hydroxy group of **48** and the phenoxide oxygen of the hosts.

3.3 Enantiomer recognition ability of phenolic crown ethers and podand

In order to investigate chiral recognition ability of the hosts, chiral amines **51**, **52**, **53**, **54**, and **55** were selected as guests. *N*,α-dimethylphenylethylamine (**51**) has a methyl group at the α-position of **46** and can be regarded as its chiral derivative. Pyrrolidine methanol (**52**) is a secondary ethanolamine derivative with a cyclic structure. 2-(Isopropylamino)-2-phenylethanol (**53**) and 2-(isopropylamino)-1-phenylethanol (**54**) have a chiral center at α and β position of an amino group, respectively. *N*-isopropyl group of **53** and **54** was selected because of the ease in preparation of both enantiomers from commercially available materials and because of the fact that many of the biologically active secondary amines possess this group.[5] Compound **53** is regarded as a *N*-isopropylated derivative of phenylglycinol, which was reported to show excellent binding ability and enantiomer selectivity toward pseudo-18-crown-6 hosts like (*S*,*S*)-**7**.[3a,4a,4c,6] Many of biologically active secondary amines have a chiral center at β-position of an amino group as shown in Figures 1.1 and 1.2[5] like guest **54**. Propranolol (**55**) is one of commercially produced biologically active secondary amines, and its biological activities are known to be different from those of the corresponding enantiomers; (*S*)- isomer is a β-blocker and an arrhythmias while (*R*)- isomer is a contraceptive.

The binding constants and the enantiomer selectivity of the hosts were determined for hosts (*S*,*S*)-**10**, (*S*,*S*)-**11**, and (*R*,*R*)-**12** with the chiral amines (Table 3.2). The measurements were carried out at 15 °C because of the relatively small binding constants at 30 °C except for the case of **52**. Both enantiomers of **51**, **52**, and **55** are commercially

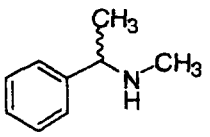

51

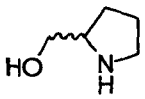

52

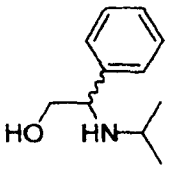

53

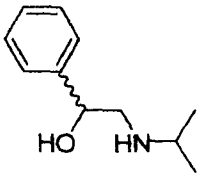

54

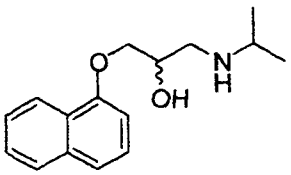

55

available. Amines **53** and **54** were prepared by *N*-isopropylation of the corresponding primary amines according to the reported procedure.[7]

Table 3.2 Binding constants and enantiomer selectivities in complexation of (*S*,*S*)-**9**, (*S*,*S*)-**10**, (*S*,*S*)-**11**, and (*R*,*R*)-**12** with **51**, **52**, **53**, **54**, and **55**.

		(*S*,*S*)-**9** [a]	(*S*,*S*)-**10**	(*S*,*S*)-**11** [a]	(*R*,*R*)-**12** [b]
	K_S	<1	(1.8±0.1)×10 [a]	7.5±0.2	(1.0±0.1)×10^2
51 [c]	K_R	<1	8.8±0.3 [a]	4.5±0.2	(7.2±0.2)×10
	K_S/K_R	–	2.0	1.7	1.4
	K_S	–	(1.6±0.1)×10^2 [b]	–	(9.8±0.7)×10^2
52 [d]	K_R	–	(1.3±0.1)×10^2 [b]	–	(8.9±0.7)×10^2
	K_S/K_R	–	1.2		1.1
	K_S	–	<1 [a]	–	(5.3±0.2)×10
53 [c]	K_R	–	<1 [a]	–	(4.7±0.5)×10
	K_S/K_R	–	–	–	1.1
	K_S	–	(1.6±0.1)×10 [a]	–	(3.1±0.2)×10^2
54 [c]	K_R	–	(2.6±0.1)×10 [a]	–	(1.8±0.1)×10^2
	K_S/K_R	–	0.6	–	1.7
	K_S	–	(5.3±0.1)×10 [a]	(1.8±0.1)×10	(2.3±0.1)×10^2
55 [c]	K_R	–	(3.1±0.2)×10 [a]	(1.5±0.1)×10	(3.7±0.1)×10^2
	K_S/K_R	–	1.7	1.2	0.6

[a] measured by ^{1}H NMR spectroscopy (270 MHz) in $CDCl_3$.
[b] measured by UV-visible spectroscopy in $CHCl_3$.
[c] measured at 15 °C.
[d] measured at 30 °C.

First, the binding ability and enantiomer selectivity of (*S*,*S*)-**9**, (*S*,*S*)-**10**, (*S*,*S*)-**11**, and (*R*,*R*)-**12** toward **51** are compared. While pseudo-18-crown-6 (*S*,*S*)-**9** formed a complex with achiral amine **46** with a binding constant of 14 M^{-1}, it did not bind *S* and *R* enantiomers of **51** (K<1 M^{-1}). Thus, the introduction of a methyl group in the guest amine reduced the binding ability of (*S*,*S*)-**9** dramatically, suggesting a severe steric repulsion between the α-methyl group of **51** and the host. Because of the small binding ability of

(*S,S*)-**9** toward this chiral secondary amine, its binding constants with other chiral secondary amine were not determined. With pseudo-24-crown-8 (*S,S*)-**10**, although the binding constants with *S* and *R* enantiomers of **51** were considerably reduced (18 and 8.8 M^{-1}, respectively) compared to that with **46**, moderate degree of enantiomer selectivity was observed (K_S/K_R=2.0). Similarly, pseudo-27-crown-9 (*S,S*)-**11** exhibited moderate degree of enantiomer selectivity (K_S/K_R=1.7). In contrast to crown ethers (*S,S*)-**9**, (*S,S*)-**10**, and (*S,S*)-**11**, the binding constants of podand (*R,R*)-**12** with **51** (K_S=100 M^{-1}, K_R=72 M^{-1}) scarcely decreased from that with achiral amine **46**, resulting in the relatively low enantiomer selectivity (K_S/K_R=1.4). The binding constants of pseudo crown ether (*S,S*)-**10** and podand (*R,R*)-**12** with **52** were next examined. In both cases, although the binding constants are larger than those with **51**, enantiomer selectivities are relatively small. The binding constants toward **53** and **54** were also measured by using hosts (*S,S*)-**10** and (*R,R*)-**12** which showed relatively high binding ability toward **51**. However, (*S,S*)-**10** did not bind both enantiomers of α-substituted **53** (K<1 M^{-1}). On the contrary, (*S,S*)-**10** formed complexes with *S* and *R* enantiomers of β-substituted **54** with binding constants 16 M^{-1} and 26 M^{-1}, respectively, and moderate degree of enantiomer selectivity (K_S/K_R=0.6) was observed. For podand (*R,R*)-**12**, although it binds α-substituted **53**, the enantiomer selectivity is marginal. On the other hand, its binding constants with *S* and *R* enantiomers of β-substituted **54** are considerably large, and moderate degree of enantiomer selectivity (K_S/K_R=1.7) is observed. The relatively low binding abilities of (*S,S*)-**10** and (*R,R*)-**12** toward **53** suggest a severe steric repulsion between the α-phenyl group and the host. Since (*S,S*)-**10** and (*R,R*)-**12** showed relatively high binding constants and enantiomer selectivities toward β-substituted ethanolamine **54**, we employed propranolol (**55**) as a guest, which is one of the well-known biologically active aminoalcohols possessing a hydroxy group on a chiral center at β-position of the amino group. In this case, pseudo-27-crown-9 (*S,S*)-**11** was also examined in addition to (*S,S*)-**10** and (*R,R*)-**12**. As we expected, (*S,S*)-**10** and (*R,R*)-**12** showed relatively high binding ability and moderate degree of enantiomer selectivity (K_S/K_R=1.7 and 0.6, respectively). In the case of (*S,S*)-**11**, however, both the binding constants and enantiomer selectivity are smaller.

3.4 Interpretation of enantiomer selectivities in complexation of phenolic crown ethers and podands with secondary amines

Regarding the predictable *R/S*-selectivities of pseudo-18-crown-6 ethers governed by enthalpy,[6] Naemura, Hirose, and Tobe have proposed an explanation in terms of a steric repulsion between the ligand of the amine and the hosts on the basis of CPK molecular model examination of the complex. The enantiomer selectivities of (*S,S*)-**10** and (*R,R*)-**12** are interpreted on the same ground. Although both hosts (*S,S*)-**10** and (*R,R*)-**12** have more flexible structures than that of pseudo-18-crown-6, moderate enantiomer selectivities of

(*S*,*S*)-**10** and (*R*,*R*)-**12** were observed toward amines **51**, **54**, and **55** (K_S/K_R>1.7 or <0.6) except for the combination of (*R*,*R*)-**12** with **51**.

In Figure 3.4 (a), predicted geometries **56** and **57** are illustrated for the complexes (*S*,*S*)-**10** : (*S*)-**51** and (*S*,*S*)-**10** : (*R*)-**51**, respectively, assuming the following issues: (i) The pheoxide oxygen atom participates in binding the amine. (ii) The phenyl substituents of the host occupy a pseudo-equatrial positions,[8] making the O-6 oxygen (shown by the arrow in Figure 3.4 (a)) form O···H–N$^+$ hydrogen bond with the ammonium cation nested on the cavity of the crown ether. (iii) The protonated amine (**51**H$^+$) adopts a conformation in which the bulkiest groups are located in anti position. On the basis of these assumptions, two hydrogen atoms on ammonium nitrogen of (*S*)-**51**H$^+$ form hydrogen bondings with phenoxide oxygen and O-6 oxygen. The position of the methyl group on nitrogen atom is then on the 11 o'clock position. Consequently, the phenyl group of (*S*)-**51**H$^+$ is located at the anti position of the *N*-methyl group, thereby adopting the 5 o'clock position. Thus, in complex **57**, the α-methyl group of (*S*)-**51**H$^+$ is located at the less hindered 9 o'clock position of (*S*,*S*)-**10** and the smallest group on the α-position (hydrogen atom) is located at the most congested 2 o'clock position. On the other hand, in the case with (*R*)-**51**H$^+$, the complex must be destabilized because either of the following two requirements cannot be satisfied: (i) The bulkiest phenyl group is located at the anti position of the *N*-methyl group. (ii) The smallest group (hydrogen) is located at the most conjested 2 o'clock position. If the bulkiest phenyl group is located at less hindered 5 o'clock position, the second requirement is not fulfilled. The conformer shown as **57** having phenyl group at the 9 o'clock position does not fulfill the first requirement. On the basis of these conditions, the enantiomer selectivity of (*S*,*S*)-**10** toward (*S*)-**51** can be explained.

The predicted geometries **58** and **59** are illustrated for complexes (*S*,*S*)-**10** : (*R*)-**54**, (*S*,*S*)-**10** : (*S*)-**55**, (*S*,*S*)-**10** : (*S*)-**54**, and (*S*,*S*)-**10** : (*R*)-**55** (Figure 3.4 (b)). Here, in addition to the assumptions to draw the geometries of the complexes **56** and **57**, hydrogen bonding of the hydroxy group of the ethanolamine with the phenoxide oxygen atom of the host is taken into account. With this assumption in mind, the *R*/*S* selectivities of **54** and **55** are interpreted as arising from steric repulsion between the substituent on the β-position of amine and phenyl barrier. As shown in Figure 3.4 (b), complex **58** must be more stable than complex **59**. The *R*/*S* selectivities of the combination of podand (*R*,*R*)-**12** with ethanolamine derivatives **54** and **55** are analogously rationalized (Figure 3.4 (c)). Complex **60** ((*R*,*R*)-**12** : (*R*)-**54** and (*R*,*R*)-**12** : (*S*)-**55**) should be destabilized compared to the diastereomeric complex **61** ((*R*,*R*)-**12** : (*S*)-**54** and (*R*,*R*)-**12** : (*R*)-**55**) by the steric interaction between the substituent R and the phenyl barrier of the host.

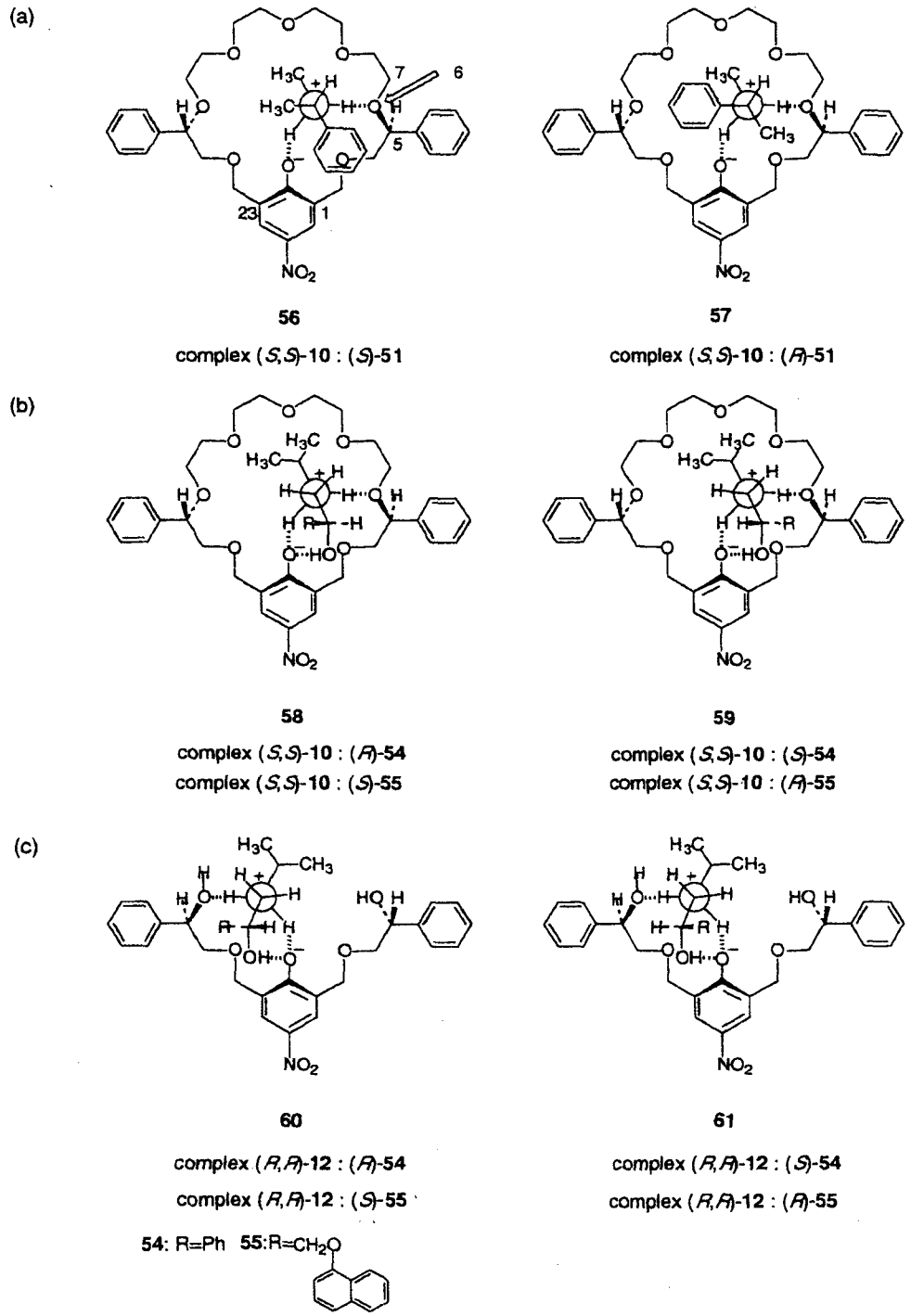

Figure 3.4 Predicted geometries of complexes **56**, **57**, **58**, **59**, **60**, and **61**.

In order to obtain spectroscopic support for the above explanation, ^{1}H NMR spectra were examined in detail. However, in the case of podand (*R*,*R*)-**12**, because of its limited solubility, the ^{1}H NMR investigations were not undertaken. For the complexes of (*S*,*S*)-**10**, though the author first attempted to measure NOE between the host and guest protons, it was not possible to observe NOE probably due to the presence of many conformers other than those shown in Figure 3.4 which are exchanging rapidly. Consequently, complexation induced shifts (CISs), the difference between the chemical shifts of uncomplexed host (or guest) and those of complexed host (or guest), were next calculated. The data obtained for complexes **56** and **57** are shown in Figrure 3.5. Here the signals of proton H5 and H19, H2β and H22α, and H2α and H22β exchange each other rapidly on the NMR time scale, that the signals appear as time-averaged ones. With regard to complexes **58** and **59**, however, useful CIS data were not obtained because the aromatic ring of guest is not located close enough to induce anisotropoic effect.

In complexes **56** and **57**, CISs of H2β and H22β show large negative values. To confirm if the large negative values of CISs of H2β and H22β are due to the anisotropic shielding effect of the guest amines or not, the CISs were calculated for complexes of (*S*,*S*)-**10** with *N*-methylisopropylamine that has no aromatic ring. Since both of H2β and H22β of the complex between (*S*,*S*)-**10** and *N*-methylisopropylamine show large upfield shifts (–0.45 and –0.24 ppm, respectively), the large upfield shift of H2β and H22β for the complexes **56** and **57** are ascribed to conformational change of the nitrophenol moiety upon complexation. Therefore, CISs of H2β and H22β are not suitable to probe the anisotropic shielding effect of an aromatic ring on guest molecules. On the other hand, CIS of H19 caused by complexation with *N*-methylisopropylamine is small (–0.08 ppm) because it is not close to the nitrophenol moiety. For the reason described above, proton H19 is suitable to probe the anisotropic shielding effect of the phenyl ring of guest **51H**$^+$. As shown in Figure 3.5, proton H19 shows larger upfield shift with (*R*)-**51** than that with (*S*)-**51** ($\Delta_{R\text{-}S}$CIS=–0.11), indicating that it suffers anisotropic shielding from phenyl ring of (*R*)-**51** more effectively than that from (*S*)-**51**. These results are in agreement with the proposed conformations shown in Figure 3.5.

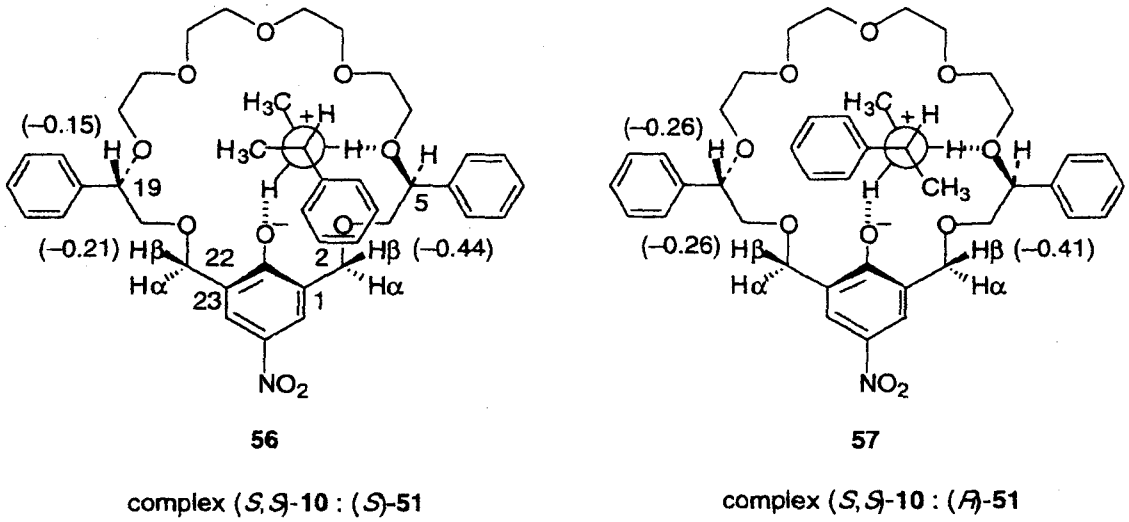

Figure 3.5 Observed complexation induced shifts (CISs) of H22β, H19, and H2β for complexes of **56** and **57**. CISs of H2α, H5, and H22α which are time-averaged with those of H22β, H19, and H2β, respectively, are not shown.

3.5 Conclusion

There exist many biologically active secondary amines as with primary amines and their activities are different from the corresponding enantiomers. Despite the abundance of reports on chiral recognition of primary amines, little has been reported about chiral recognition of secondary amines. In this connection, the author embarked a project to prepare host molecules capable of not only binding secondary amines but also recognizing their chirality.

The author designed chiral pseudo-crown ethers such as pseudo-24-crown-8 (*S*,*S*)-**10** and pseudo-27-crown-9 (*S*,*S*)-**11** having a *p*-nitrophenolic hydroxy group and a macrocyclic ring larger than that of pseudo-18-crown-6 ethers, which have been shown to possess excellent binding and chiral recognition abilities toward primary amines. Moreover, more flexible podands such as (*R*,*R*)-**12** and (*R*,*R*)-**13** with an open chain structure were also designed. The synthesis of the hosts was efficiently undertaken starting from the commercially available (*S*)- and (*R*)-mandelic acid. The binding and chiral recognition abilities of hosts toward secondary amines were next investigated. Pseudo-24-crown-8 (*S*,*S*)-**10** and podand (*R*,*R*)-**12** turned out to be better binders for secondary amines than the other hosts. Moreover, hosts (*S*,*S*)-**10** and (*R*,*R*)-**12** showed moderate degree of chiral recognition abilities toward a few secondary amines. The explanations in terms of a steric repulsion between the ligand of the amine and the hosts on the basis of CPK molecular model examination of the complex was proposed, which was supported by the NMR spectroscopic observations. In addition, in order to apply to the chiral stationary

phase for secondary amines, (*S*,*S*)-**14** having a carboxyl group at the para position of the inner methoxy group was prepared.

The author hope not only that some of the compounds investigated in this thesis would find their useful application in various areas in near future, but also that the results on the whole would contribute to the development of host-guest chemistry particularly in the area of chiral recognition.

3.6 Experimental section

3.6.1 Synthesis of chiral secondary amines

(*R*)-2-(Isopropylamino)-2-phenylethanol (*R*)-53

To a solution of (*R*)-2-amino-2-phenylethanol (900 mg, 6.56 mmol) in ethanol (10 mL), acetone (1.2 mL, 10.9 mmol) was added and the reaction mixture was stirred for 30 min at room temperature. After all the starting amine had been vanished as indicated by gas chromatography, sodium borohydride (370 mg, 9.78 mmol) was added with ice-cooling. After being stirred for 30 min, 1 N HCl was added dropwise to adjust the solution to pH 1, and the solvent was removed under reduced pressure. 5 M aqueous KOH solution was added to adjust the solution to pH 11, and the mixture was extracted with CH_2Cl_2. The solution was dried over anhydrous $MgSO_4$ and the solvent was removed under reduced pressure. The crude product was recrystallized from hexane to give (*R*)-**53** (980 mg, 83% yield) as colorless prisms: mp 76–78 °C; $[\alpha]_D^{31}$=–68.7 (*c* 1.05, EtOH); IR (KBr) 3270, 1472, 1169, 1134, 1064, 1041, 701 cm^{-1}; ^1H NMR ($CDCl_3$, 270 MHz) δ 1.02 (d, *J*=6.2 Hz, 3H, CH_3), 1.04 (d, *J*=6.2 Hz, 3H, CH_3), 2.68–2.82 (m, 1H, $CH(CH_3)_2$) 3.46 (dd, *J*=8.7, 11 Hz, 1H, CH_2OH), 3.67 (dd, *J*=4.7, 11 Hz, 1H, CH_2OH), 3.86 (dd, *J*=4.7, 8.7 Hz, 1H, *C*HPh), 7.24–7.38 (m, 5H, C_6H_5); MS (EI) *m/z* 148 (M^+–CH_2OH). Anal. Calcd for $C_{11}H_{17}NO$: C, 73.70; H, 9.56; N, 7.81. Found: C, 73.84; H, 9.65; N, 7.87.

(*S*)-2-(Isopropylamino)-2-phenylethanol (*S*)-53

In a manner similar to that described for the preparation of (*R*)-**53**, reaction of (*S*)-2-amino-2-phenylethanol (1.00 g, 7.29 mmol) with acetone followed by sodium borohydride gave (*S*)-**53** (0.925 g, 77% yield) as colorless prisms after recrystallization: mp 76–78 °C; $[\alpha]_D^{31}$=+66.7 (*c* 0.91, EtOH); IR (KBr) 3270, 1472, 1169, 1134, 1064, 1041, 701 cm^{-1}; ^1H NMR ($CDCl_3$, 270 MHz) δ 1.02 (d, *J*=6.2 Hz, 3H, $CHCH_3$), 1.04 (d, *J*=6.2 Hz, 3H, $CHCH_3$), 2.67–2.81 (m, 1H, $CH(CH_3)_2$), 3.46 (dd, *J*=8.7, 11 Hz, 1H, CH_2OH), 3.67 (dd, *J*=4.7, 11 Hz, 1H, CH_2OH), 3.86 (dd, *J*=4.7, 8.7 Hz, 1H, *C*HPh), 7.24–7.38(m, 5H, C_6H_5); MS (EI) *m/z* 148 (M^+–CH_2OH). Anal. Calcd for $C_{11}H_{17}NO$: C, 73.70; H, 9.56; N, 7.81. Found: C, 73.66; H, 9.63; N, 7.91.

(*R*)-2-(Isopropylamino)-1-phenylethanol (*R*)-54

To a solution of (*R*)-2-amino-1-phenylethanol (975 mg, 7.12 mmol) in ethanol (10 mL), acetone (1.0 mL, 10.9 mmol) was added and the reaction mixture was stirred for 1 h at room temperature. After all the starting amine had been vanished as indicated by gas chromatography, sodium borohydride (410 mg, 10.8 mmol) was added with ice-cooling. After being stirred for 1 h, 1 N HCl was added dropwise to adjust the solution to pH 1, and the solvent was removed under reduced pressure. 5 M aqueous KOH solution was added to adjust the solution to pH 11, and the mixture was extracted with CH_2Cl_2. The solution was dried over anhydrous $MgSO_4$ and the solvent was removed under reduced pressure. The crude product was recrystallized from hexane to give (*R*)-**54** (904 mg, 71% yield) as colorless needles, mp 83–85 °C; $[\alpha]_D^{28}$=–26.7 (*c* 1.03, EtOH); IR (KBr) 3293, 2968, 1604, 1450, 1345, 1088, 1062, 701 cm^{-1}; ^1H NMR ($CDCl_3$, 270 MHz) δ 1.07 (d, *J*=6.2 Hz, 6H, $CHCH_3$), 2.76–2.87 (m, 1H, $CH(CH_3)_2$), 2.65 (dd, *J*=8.9,12 Hz, 1H, CH_2OH), 2.94 (dd, *J*=3.7, 12 Hz, 1H, CH_2OH), 4.65 (dd, *J*=3.7, 8.9 Hz, 1H, *CH*Ph), 7.23–7.39 (m, 5H, C_6H_5); MS (EI) *m/z* 180 (M^+–CH_2OH). Anal. Calcd for $C_{11}H_{17}NO$: C, 73.70; H, 9.56; N, 7.81. Found: C, 73.74; H, 9.70; N, 7.81.

(*S*)-2-(Isopropylamino)-1-phenylethanol (*S*)-54

In a manner similar to that described for the preparation of (*R*)-**54**, reaction of (*S*)-2-amino-1-phenylethanol (979 mg, 7.14 mmol) with acetone followed by sodium borohydride gave (*S*)-**54** (973 mg, 76% yield) as colorless needles after recrystallization: mp 82–83 °C; $[\alpha]_D^{28}$=+28.3 (*c* 1.10, EtOH); IR (KBr) 3293, 2968, 1604, 1450, 1345, 1088, 1062, 701 cm^{-1}; ^1H NMR ($CDCl_3$, 270 MHz) δ 1.07 (d, *J*=6.2 Hz, 6H, $CH(CH_3)_2$), 2.77–2.89 (m, 1H, $CH(CH_3)_2$), 2.66 (dd, *J*=8.9, 12 Hz, 1H, CH_2OH), 2.95 (dd, *J*=3.7, 12 Hz, 1H, CH_2OH), 4.66 (dd, *J*=3.7, 8.9 Hz, 1H, *CH*Ph), 7.22–7.39(m, 5H, C_6H_5); MS (EI) *m/z* 180 (M^+–CH_2OH). Anal. Calcd for $C_{11}H_{17}NO$: C, 73.70; H, 9.56; N, 7.81. Found: C, 73.52; H, 9.53; N, 7.82.

3.6.2 Determination of association constants by the ^1H NMR titration method

The titration experiment for complexation of host (*S*,*S*)-**10** with chiral amine (*S*)-**51** is described here as an example for determination of binding constants by ^1H-NMR spectroscopy. A solution of (*S*,*S*)-**10** (22.3 mM) and a solution of (*S*)-**51** (81.1 mM) each in $CDCl_3$ were prepared. An initial ^1H NMR spectrum of 600 μL of this host (*S*,*S*)-**10** solution was recorded. Samples were made by adding the guest solutions to the host solution. Namely, a 600 μL portion of the host solution and 0.0, 10, 20, 30, 40, 50, 60, 80, 100, 130, 160, and 200 μL portions of the guest (*S*)-**51** solution were mixed. Then, spectra of these samples were recorded. The association constant for the complex of (*S*,*S*)-**10** with (*S*)-**51** was calculated by the non-linear least-squares method following the chemical shift

of one of the benzylic protons (H22β and H22α or H22α and H22β shown in Figure 3.6) of (*S*,*S*)-**10**. The results are listed in Tables 3.3–3.17 and Figures 3.6–3.20.

3.6.3 Determination of association constants by the UV-vis titration method

The titration experiment for complexation of host (*R*,*R*)-**12** with chiral amine (*R*)-**54** is described here as an example for determination of binding constants by UV-visible spectroscopy. A solution of (*R*,*R*)-**12** in $CHCl_3$ was prepared and an initial UV spectrum of this solution was recorded. The concentration was calculated to be 0.036 mM based on its molar extinction coefficient. Separately, a solution of (*R*)-**54** in $CHCl_3$ was prepared. Samples were made by adding the guest solution to the host solution and diluted with $CHCl_3$ to make the total volume up to 4.0 mL, so that the concentrations of the guest in each samples were 0.0, 2.0, 5.0, 8.0, 14, 20 mM, respectively. The concentration of the host was kept constant 0.036 mM in each sample. Then, spectra of these five different solutions were recorded. The binding constants were calculated from absorption intensity of the complex at the absorption maximum (388 nm) based on the Rose-Drago method using the spreadsheet in reference 1b. The results are listed in Tables 3.18–3.39 and Figures 3.21–3.42.

3.6.4 ^{1}H NMR titration and UV-vis titration data for determining binding constants

^{1}H NMR titration and UV-vis titration data for determining binding constants are tabulated in Tables 3.3–3.17, Figures 3.6–3.20 and in Tables 3.18–3.39, Figures 3.21–3.42, respectively.

Table 3.3 Tabulated ^{1}H NMR titration data of **9** with **46** in $CDCl_3$ at 15°C, calculated association constant, and calculated chemical shift of the complex.

	$[H]_t$ (M) [a]	$[G]_t$ (M) [b]	$[G]_t$ / $[H]_t$	[C] / $[H]_t$ [c]	δ (ppm) [d]
1	0.0127	0	0	0	4.826
2	0.0125	0.0070	0.6	0.09	4.808
3	0.0123	0.0138	1.1	0.15	4.798
4	0.0121	0.0205	1.7	0.20	4.789
5	0.0119	0.0269	2.3	0.25	4.779
6	0.0118	0.0331	2.8	0.30	4.771
7	0.0116	0.0392	3.4	0.34	4.764
8	0.0113	0.0508	4.5	0.40	4.752
9	0.0110	0.0618	5.6	0.46	4.743
10	0.0106	0.0773	7.3	0.51	4.734
					δ_{cump}=4.65
					K =14±1.7

[a] Total concentration of **9**.

[b] Total concentration of **46**.

[c] The complexation ratio for the complex of **9** with **46**.

[d] Observed chemical shifts for one of the benzylic protons of **9**.

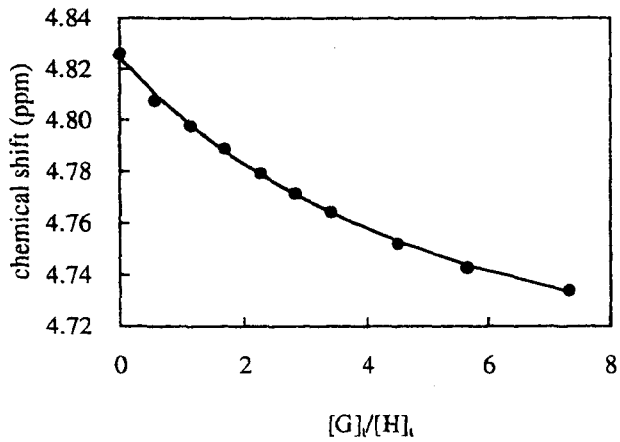

Figure 3.6 ^{1}H NMR titration curve for the complexation of **9** with **46**.

Table 3.4 Tabulated ^{1}H NMR titration data of **10** with **46** in $CDCl_3$ at 15°C, calculated association constant, and calculated chemical shift of the complex.

	$[H]_t$ (M) [a]	$[G]_t$ (M) [b]	$[G]_t$ / $[H]_t$	[C] / $[H]_t$ [c]	δ (ppm) [d]
1	0.0130	0	0	0	4.876
2	0.0128	0.0067	0.5	0.17	4.796
3	0.0126	0.0133	1.1	0.30	4.733
4	0.0124	0.0196	1.6	0.41	4.684
5	0.0122	0.0258	2.1	0.48	4.648
6	0.0121	0.0317	2.6	0.53	4.627
7	0.0119	0.0375	3.2	0.58	4.605
8	0.0116	0.0487	4.2	0.65	4.568
9	0.0113	0.0592	5.3	0.71	4.544
10	0.0108	0.0740	6.8	0.75	4.522
11	0.0104	0.0878	8.4	0.79	4.507
12	0.0099	0.1045	10.5	0.82	4.492
					δ_{comp}=4.41
					K =46 ± 1.4

[a] Total concentration of **10**.

[b] Total concentration of **46**.

[c] The complexation ratio for the complex of **10** with **46**.

[d] Observed chemical shifts for one of the benzylic protons of **10**.

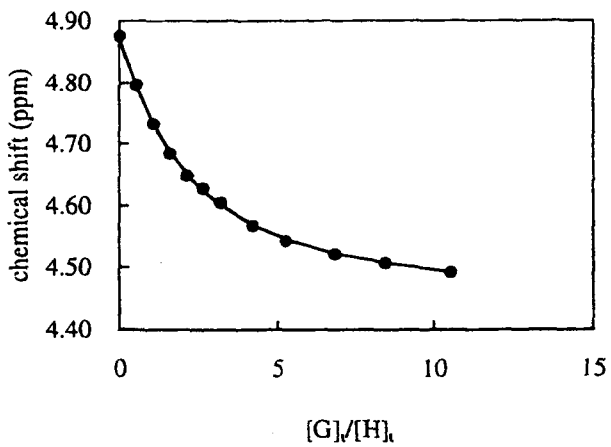

Figure 3.7 ^{1}H NMR titration curve for the complexation of **10** with **46**.

Table 3.5 Tabulated ^{1}H NMR titration data of **11** with **46** in $CDCl_3$ at 15°C, calculated association constant, and calculated chemical shift of the complex.

	$[H]_t$ (M) [a]	$[G]_t$ (M) [b]	$[G]_t$ / $[H]_t$	[C] / $[H]_t$ [c]	δ (ppm) [d]
1	0.0083	0	0	0	4.733
2	0.0082	0.0143	1.8	0.20	4.671
3	0.0080	0.0282	3.5	0.34	4.627
4	0.0079	0.0416	5.3	0.44	4.598
5	0.0078	0.0546	7.0	0.50	4.577
6	0.0077	0.0672	8.8	0.56	4.560
7	0.0076	0.0794	10.5	0.61	4.548
8	0.0073	0.1027	14.0	0.66	4.530
9	0.0071	0.1247	17.5	0.71	4.517
10	0.0068	0.1555	22.8	0.75	4.506
11	0.0066	0.1838	28.0	0.78	4.497
12	0.0062	0.2183	35.0	0.81	4.490
					δ_{comp}=4.44
					K =22±0.1

[a] Total concentration of **11**.

[b] Total concentration of **46**.

[c] The complexation ratio for the complex of **11** with **46**.

[d] Observed chemical shifts for one of the benzylic protons of **11**.

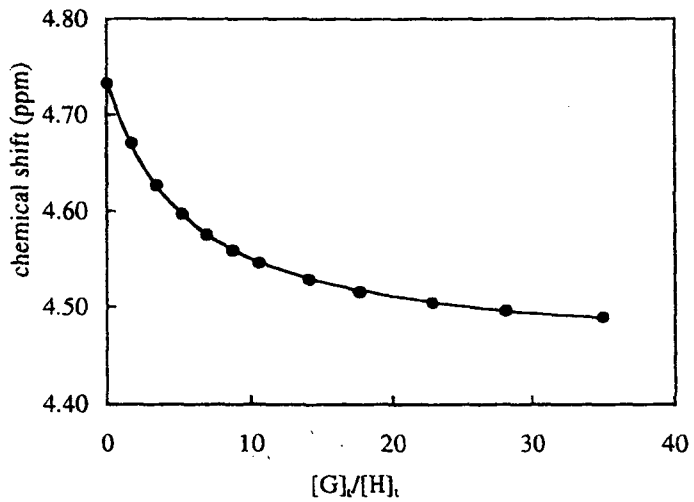

Figure 3.8 ^{1}H NMR titration curve for the complexation of **11** with **46**.

Table 3.6 Tabulated ^{1}H NMR titration data of **13** with **47** in $CDCl_3$ at 30°C, calculated association constant, and calculated chemical shift of the complex.

	$[H]_t$ (mM) [a]	$[G]_t$ (mM) [b]	$[G]_t$ / $[H]_t$	$[C]$ / $[H]_t$ [c]	δ (ppm) [d]
1	0.0054	0.0439	8.2	0.22	4.694
2	0.0052	0.0851	16.4	0.33	4.665
3	0.0050	0.1238	24.6	0.42	4.640
4	0.0049	0.1603	32.8	0.49	4.622
5	0.0047	0.1946	41.0	0.55	4.604
6	0.0046	0.2270	49.2	0.59	4.596
7	0.0044	0.2724	61.5	0.62	4.586
8	0.0043	0.3143	73.8	0.67	4.573
9	0.0041	0.3531	86.1	0.69	4.569
10	0.0039	0.4006	102.5	0.70	4.565
11	0.0037	0.4540	122.9	0.73	4.559
					δ_{comp}=4.49
					K =6.2±0.8

[a] Total concentration of **13**.

[b] Total concentration of **47**.

[c] The complexation ratio for the complex of **13** with **47**.

[d] Observed chemical shifts for one of the benzylic protons of **13**.

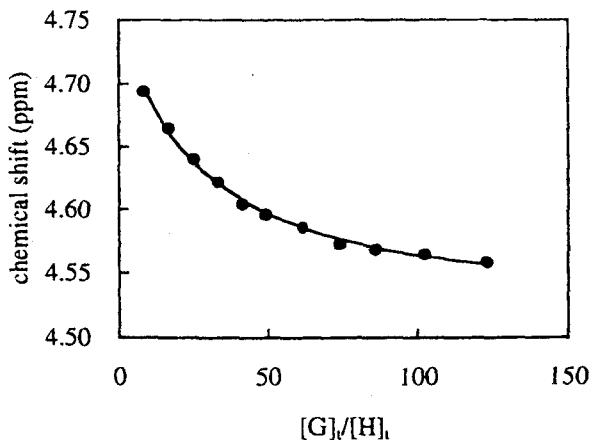

Figure 3.9 ^{1}H NMR titration curve for the complexation of **13** with **47**.

Table 3.7 Tabulated ^{1}H NMR titration data of **13** with **48** in $CDCl_3$ at 30°C, calculated association constant, and calculated chemical shift of the complex.

	$[H]_t$ (mM) [a]	$[G]_t$ (mM) [b]	$[G]_t$ / $[H]_t$	[C] / $[H]_t$ [c]	δ (ppm) [d]
1	0.0055	0.0025	0.4	0.04	3.323
2	0.0053	0.0048	0.9	0.07	3.321
3	0.0052	0.0069	1.3	0.10	3.319
4	0.0050	0.0090	1.8	0.13	3.317
5	0.0049	0.0109	2.2	0.16	3.316
6	0.0046	0.0154	3.4	0.21	3.313
7	0.0043	0.0193	4.5	0.25	3.310
8	0.0041	0.0228	5.6	0.28	3.308
9	0.0039	0.0259	6.7	0.31	3.306
10	0.0037	0.0287	7.8	0.33	3.305
11	0.0035	0.0313	8.9	0.36	3.304
					δ_{comp}=3.27
					K =18±2.4

[a] Total concentration of **13**.

[b] Total concentration of **48**.

[c] The complexation ratio for the complex of **13** with **48**.

[d] Observed chemical shifts for the methoxy proton of **13**.

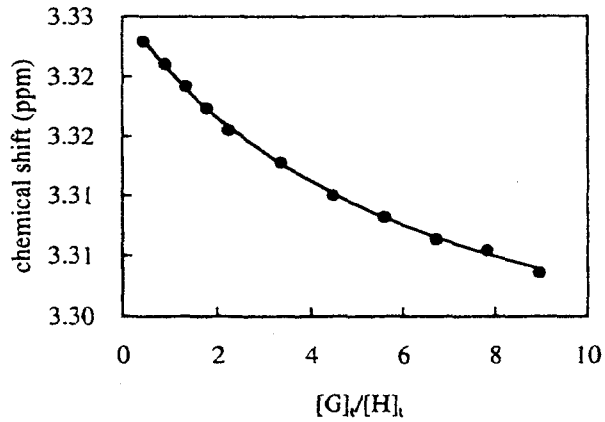

Figure 3.10 ^{1}H NMR titration curve for the complexation of **13** with **48**.

Table 3.8 Tabulated ^{1}H NMR titration data of **10** with (*S*)-**51** in $CDCl_3$ at 15 °C, calculated association constant, and calculated chemical shift of the complex.

	$[H]_t$ (M) [a]	$[G]_t$ (M) [b]	$[G]_t$ / $[H]_t$	[C] / $[H]_t$ [c]	δ (ppm) [d]
1	0.0223	0	0	0	4.864
2	0.0220	0.0133	0.6	0.17	4.788
3	0.0216	0.0262	1.2	0.28	4.739
4	0.0213	0.0386	1.8	0.36	4.705
5	0.0209	0.0507	2.4	0.42	4.677
6	0.0206	0.0624	3.0	0.49	4.646
7	0.0203	0.0737	3.6	0.54	4.627
8	0.0197	0.0954	4.8	0.60	4.598
9	0.0191	0.1159	6.1	0.66	4.576
10	0.0184	0.1445	7.9	0.71	4.552
11	0.0176	0.1708	9.7	0.74	4.537
12	0.0167	0.2028	12.1	0.78	4.522
					δ_{comp}=4.43
					K =18±0.9

[a] Total concentration of **10**.

[b] Total concentration of (*S*)-**51**.

[c] The complexation ratio for the complex of **10** with (*S*)-**51**.

[d] Observed chemical shifts for one of the benzylic protons of **10**.

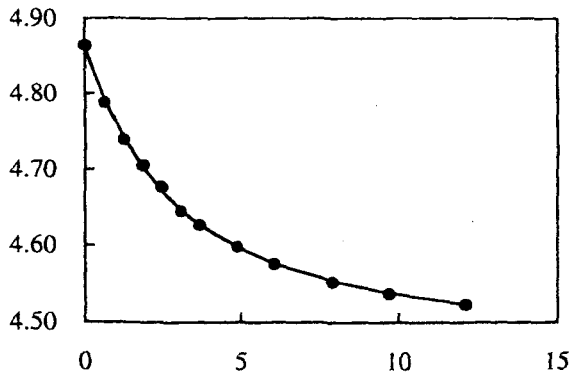

Figure 3.11 ^{1}H NMR titration curve for the complexation of **10** with (*S*)-**51**.

Table 3.9 Tabulated ^{1}H NMR titration data of **10** with (*R*)-**51** in $CDCl_3$ at 15 °C, calculated association constant, and calculated chemical shift of the complex.

	$[H]_t$ (M) [a]	$[G]_t$ (M) [b]	$[G]_t$ / $[H]_t$	[C] / $[H]_t$ [c]	δ (ppm) [d]
1	0.0223	0	0	0	4.864
2	0.0220	0.0133	0.6	0.09	4.825
3	0.0216	0.0262	1.2	0.17	4.795
4	0.0213	0.0386	1.8	0.23	4.770
5	0.0209	0.0507	2.4	0.28	4.749
6	0.0206	0.0624	3.0	0.32	4.731
7	0.0203	0.0737	3.6	0.37	4.715
8	0.0197	0.0954	4.8	0.43	4.688
9	0.0191	0.1159	6.1	0.49	4.664
10	0.0184	0.1445	7.9	0.54	4.645
11	0.0176	0.1708	9.7	0.59	4.625
12	0.0167	0.2028	12.1	0.62	4.610
					δ_{comp}=4.46
					K =8.8±0.3

[a] Total concentration of **10**.

[b] Total concentration of (*R*)-**51**.

[c] The complexation ratio for the complex of **10** with (*R*)-**51**.

[d] Observed chemical shifts for one of the benzylic protons of **10**.

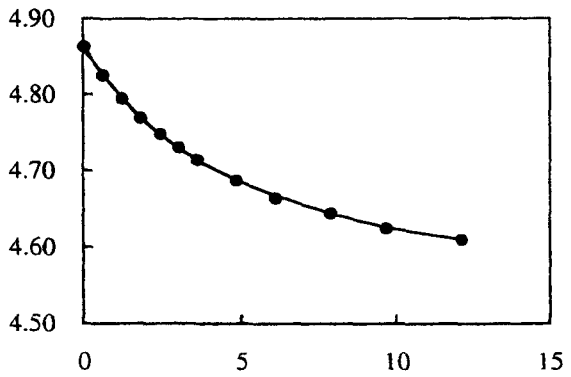

Figure 3.12 ^{1}H NMR titration curve for the complexation of **10** with (*R*)-**51**.

Table 3.10 Tabulated ^{1}H NMR titration data of **10** with (*S*)-**54** in $CDCl_3$ at 15 °C, calculated association constant, and calculated chemical shift of the complex.

	$[H]_t$ (M) [a]	$[G]_t$ (M) [b]	$[G]_t$ / $[H]_t$	[C] / $[H]_t$ [c]	δ (ppm) [d]
1	0.0092	0	0	0	4.862
2	0.0090	0.0104	1.1	0.11	4.812
3	0.0089	0.0204	2.3	0.22	4.761
4	0.0087	0.0301	3.4	0.31	4.716
5	0.0086	0.0395	4.6	0.37	4.689
6	0.0085	0.0487	5.7	0.41	4.671
7	0.0084	0.0575	6.9	0.45	4.651
8	0.0081	0.0744	9.2	0.53	4.617
9	0.0079	0.0904	11.5	0.58	4.593
10	0.0076	0.1127	14.9	0.63	4.568
11	0.0072	0.1345	18.6	0.67	4.547
12	0.0069	0.1594	23.2	0.71	4.531
					δ_{comp}=4.39
					K =16±1.1

[a] Total concentration of **10**.

[b] Total concentration of (*S*)-**54**.

[c] The complexation ratio for the complex of **10** with (*S*)-**54**.

[d] Observed chemical shifts for one of the benzylic protons of **10**.

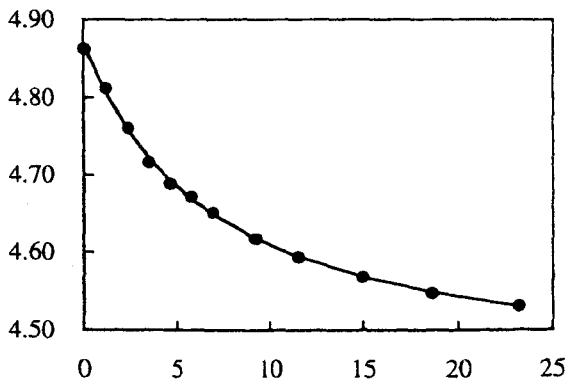

Figure 3.13 ^{1}H NMR titration curve for the complexation of **10** with (*S*)-**54**.

Table 3.11 Tabulated ^{1}H NMR titration data of **10** with (*R*)-**54** in $CDCl_3$ at 15 °C, calculated association constant, and calculated chemical shift of the complex.

	$[H]_t$ (M) [a]	$[G]_t$ (M) [b]	$[G]_t$ / $[H]_t$	[C] / $[H]_t$ [c]	δ (ppm) [d]
1	0.0096	0	0	0	4.874
2	0.0095	0.0087	0.9	0.16	4.802
3	0.0093	0.0172	1.8	0.28	4.746
4	0.0092	0.0254	2.8	0.37	4.706
5	0.0090	0.0333	3.7	0.44	4.675
6	0.0089	0.0410	4.6	0.50	4.648
7	0.0088	0.0485	5.5	0.53	4.634
8	0.0085	0.0627	7.4	0.61	4.597
9	0.0083	0.0762	9.2	0.65	4.577
10	0.0079	0.0949	12.0	0.70	4.554
11	0.0076	0.1122	14.8	0.74	4.540
12	0.0072	0.1333	18.4	0.77	4.525
					δ_{comp}=4.42
					K =26±0.7

[a] Total concentration of **10**.

[b] Total concentration of (*R*)-**54**.

[c] The complexation ratio for the complex of **10** with (*R*)-**54**.

[d] Observed chemical shifts for one of the benzylic protons of **10**.

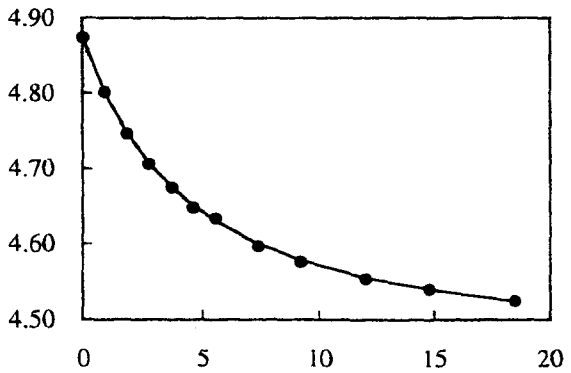

Figure 3.14 ^{1}H NMR titration curve for the complexation of **10** with (*R*)-**54**.

Table 3.12 Tabulated ^{1}H NMR titration data of **10** with (*S*)-**55** in $CDCl_3$ at 15 °C, calculated association constant, and calculated chemical shift of the complex.

	$[H]_t$ (M) [a]	$[G]_t$ (M) [b]	$[G]_t$ / $[H]_t$	[C] / $[H]_t$ [c]	δ (ppm) [d]
1	0.0118	0	0	0	4.866
2	0.0116	0.0047	0.4	0.15	4.790
3	0.0114	0.0093	0.8	0.26	4.741
4	0.0113	0.0137	1.2	0.35	4.701
5	0.0111	0.0180	1.6	0.41	4.674
6	0.0109	0.0222	2.0	0.47	4.647
7	0.0108	0.0263	2.4	0.52	4.626
8	0.0105	0.0341	3.2	0.59	4.594
9	0.0102	0.0414	4.1	0.64	4.569
10	0.0098	0.0518	5.3	0.70	4.542
11	0.0095	0.0614	6.5	0.74	4.523
12	0.0090	0.0731	8.1	0.78	4.505
					δ_{comp}=4.41
					K =53 ± 1.4

[a] Total concentration of **10**.

[b] Total concentration of (*S*)-**55**.

[c] The complexation ratio for the complex of **10** with (*S*)-**55**.

[d] Observed chemical shifts for one of the benzylic protons of **10**.

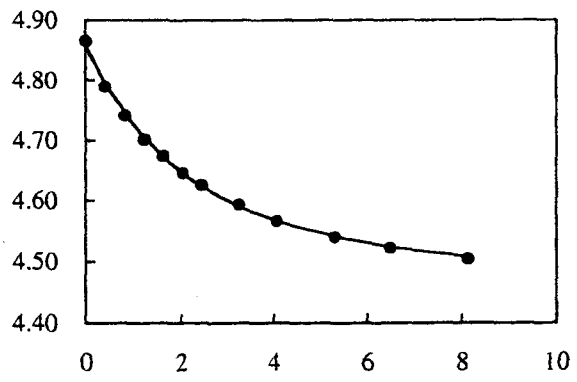

Figure 3.15 ^{1}H NMR titration curve for the complexation of **10** with (*S*)-**55**.

Table 3.13 Tabulated ^{1}H NMR titration data of **10** with (*R*)-**55** in $CDCl_3$ at 15 °C, calculated association constant, and calculated chemical shift of the complex.

	$[H]_t$ (M) [a]	$[G]_t$ (M) [b]	$[G]_t$ / $[H]_t$	[C] / $[H]_t$ [c]	δ (ppm) [d]
1	0.0123	0	0	0	4.870
2	0.0121	0.0046	0.4	0.07	4.825
3	0.0119	0.0091	0.8	0.12	4.788
4	0.0117	0.0135	1.1	0.15	4.755
5	0.0116	0.0177	1.5	0.20	4.731
6	0.0114	0.0218	1.9	0.24	4.716
7	0.0112	0.0258	2.3	0.27	4.696
8	0.0109	0.0335	3.1	0.33	4.663
9	0.0106	0.0408	3.8	0.37	4.638
10	0.0102	0.0510	5.0	0.42	4.612
11	0.0099	0.0604	6.1	0.46	4.592
12	0.0094	0.0720	7.7	0.51	4.572
					δ_{comp}=4.43
					K =31 ± 1.8

[a] Total concentration of **10**.

[b] Total concentration of (*R*)-**55**.

[c] The complexation ratio for the complex of **10** with (*R*)-**55**.

[d] Observed chemical shifts for one of the benzylic protons of **10**.

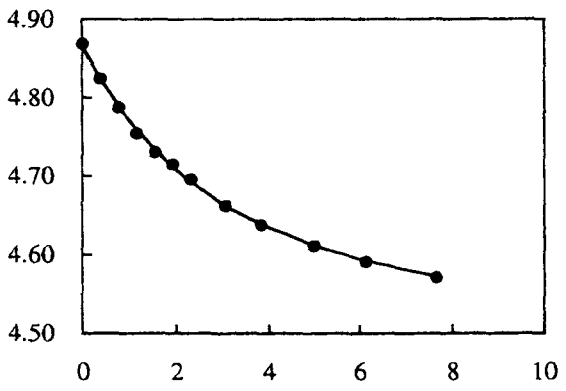

Figure 3.16 ^{1}H NMR titration curve for the complexation of **10** with (*R*)-**55**.

Table 3.14 Tabulated ^{1}H NMR titration data of **11** with (*S*)-**51** in $CDCl_3$ at 15 °C, calculated association constant, and calculated chemical shift of the complex.

	$[H]_t$ (M) [a]	$[G]_t$ (M) [b]	$[G]_t$ / $[H]_t$	[C] / $[H]_t$ [c]	δ (ppm) [d]
1	0.0069	0	0	0	4.731
2	0.0067	0.0186	2.8	0.11	4.707
3	0.0066	0.0365	5.5	0.21	4.688
4	0.0065	0.0539	8.3	0.28	4.672
5	0.0064	0.0708	11.0	0.33	4.662
6	0.0063	0.0871	13.8	0.39	4.650
7	0.0062	0.1030	16.5	0.43	4.641
8	0.0060	0.1332	22.0	0.50	4.628
9	0.0059	0.1618	27.5	0.54	4.618
10	0.0056	0.2017	35.8	0.60	4.606
11	0.0054	0.2384	44.0	0.63	4.599
12	0.0051	0.2831	55.1	0.68	4.590
					δ_{comp}=4.52
					K =7.5±0.2

[a] Total concentration of **11**.

[b] Total concentration of (*S*)-**51**.

[c] The complexation ratio for the complex of **11** with (*S*)-**51**.

[d] Observed chemical shifts for one of the benzylic protons of **11**.

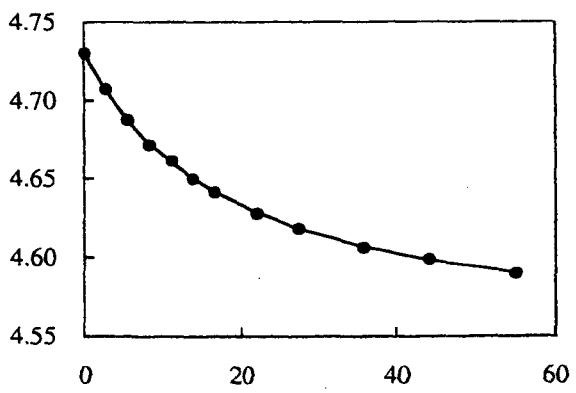

Figure 3.17 ^{1}H NMR titration curve for the complexation of **11** with (*S*)-**51**.

Table 3.15 Tabulated ^{1}H NMR titration data of **11** with (*R*)-**51** in $CDCl_3$ at 15 °C, calculated association constant, and calculated chemical shift of the complex.

	$[H]_t$ (M) [a]	$[G]_t$ (M) [b]	$[G]_t$ / $[H]_t$	[C] / $[H]_t$ [c]	δ (ppm) [d]
1	0.0069	0	0	0	4.735
2	0.0068	0.0153	2.2	0.07	4.719
3	0.0067	0.0301	4.5	0.12	4.707
4	0.0066	0.0444	6.7	0.15	4.699
5	0.0065	0.0583	9.0	0.20	4.688
6	0.0064	0.0718	11.2	0.24	4.679
7	0.0063	0.0848	13.5	0.27	4.672
8	0.0061	0.1098	17.9	0.33	4.658
9	0.0059	0.1333	22.4	0.37	4.648
10	0.0057	0.1662	29.2	0.42	4.637
11	0.0055	0.1965	35.9	0.46	4.627
12	0.0052	0.2333	44.9	0.51	4.617
					$\delta_{complex}$=4.50
					K =4.5±0.2

[a] Total concentration of **11**.

[b] Total concentration of (*R*)-**51**.

[c] The complexation ratio for the complex of **11** with (*R*)-**51**.

[d] Observed chemical shifts for one of the benzylic protons of **11**.

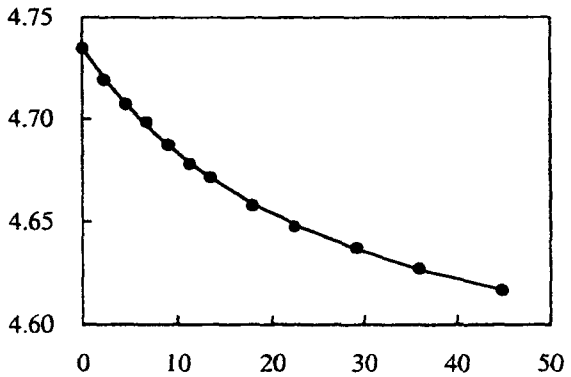

Figure 3.18 ^{1}H NMR titration curve for the complexation of **11** with (*R*)-**51**.

Table 3.16 Tabulated ^{1}H NMR titration data of **11** with (*S*)-**55** in $CDCl_3$ at 15 °C, calculated association constant, and calculated chemical shift of the complex.

	$[H]_t$ (M) [a]	$[G]_t$ (M) [b]	$[G]_t$ / $[H]_t$	[C] / $[H]_t$ [c]	δ (ppm) [d]
1	0.0070	0	0	0	4.837
2	0.0069	0.0067	1.0	0.10	4.806
3	0.0068	0.0133	1.9	0.18	4.781
4	0.0067	0.0196	2.9	0.24	4.760
5	0.0066	0.0257	3.9	0.30	4.743
6	0.0065	0.0316	4.9	0.35	4.728
7	0.0064	0.0374	5.8	0.39	4.715
8	0.0062	0.0484	7.8	0.46	4.693
9	0.0060	0.0587	9.7	0.50	4.678
10	0.0058	0.0732	12.6	0.56	4.660
11	0.0056	0.0866	15.6	0.60	4.647
12	0.0053	0.1028	19.5	0.64	4.635
					δ_{comp}=4.52
					K =18±0.3

[a] Total concentration of **11**.

[b] Total concentration of (*S*)-**55**.

[c] The complexation ratio for the complex of **11** with (*S*)-**55**.

[d] Observed chemical shifts for one of the benzylic protons of **11**.

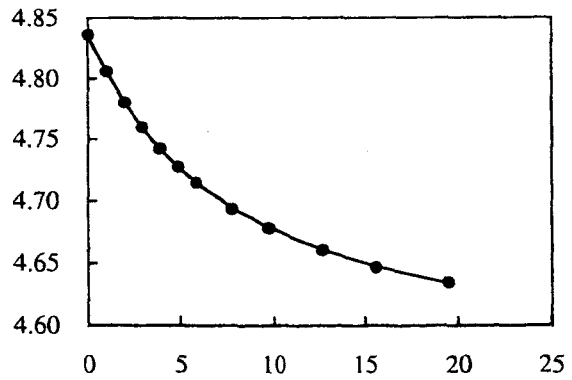

Figure 3.19 ^{1}H NMR titration curve for the complexation of **11** with (*S*)-**55**.

Table 3.17 Tabulated ^{1}H NMR titration data of **11** with (*R*)-**55** in $CDCl_3$ at 15 °C, calculated association constant, and calculated chemical shift of the complex.

	$[H]_t$ (M) [a]	$[G]_t$ (M) [b]	$[G]_t$ / $[H]_t$	[C] / $[H]_t$ [c]	δ (ppm) [d]
1	0.0062	0	0	0	4.831
2	0.0061	0.0092	1.5	0.11	4.796
3	0.0060	0.0182	3.0	0.20	4.767
4	0.0059	0.0268	4.6	0.28	4.743
5	0.0058	0.0352	6.1	0.34	4.723
6	0.0057	0.0434	7.6	0.39	4.707
7	0.0056	0.0512	9.1	0.44	4.690
8	0.0054	0.0663	12.2	0.51	4.668
9	0.0053	0.0805	15.2	0.55	4.654
10	0.0051	0.1004	19.8	0.59	4.639
11	0.0049	0.1187	24.4	0.64	4.623
12	0.0046	0.1409	30.5	0.67	4.613
					δ_{comp}=4.51
					K =15±0.8

[a] Total concentration of **11**.

[b] Total concentration of (*R*)-**55**.

[c] The complexation ratio for the complex of **11** with (*R*)-**55**.

[d] Observed chemical shifts for one of the benzylic protons of **11**.

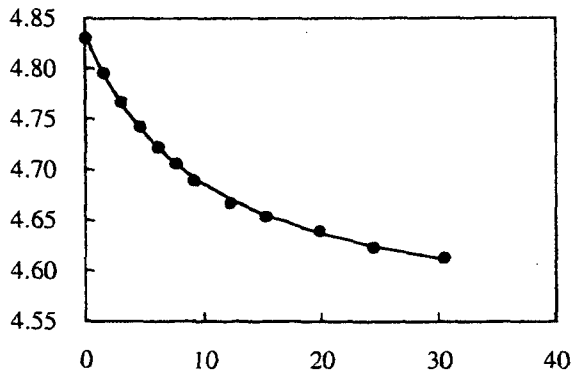

Figure 3.20 ^{1}H NMR titration curve for the complexation of **11** with (*R*)-**55**.

Table 3.18 Tabulated UV-vis titration data of **9** with **47** in $CHCl_3$ at 30°C, and calculated association constant.

	$[H]_t$ (M) [a]	$[G]_t$ (M) [b]	$[G]_t$ / $[H]_t$	[C] / $[H]_t$ [c]	abs. [d]
1	0.00003230	0	0	0	0.0066
2	0.00003230	0.00004	1.2	0.22	0.160
3	0.00003230	0.00011	3.5	0.49	0.343
4	0.00003230	0.00019	5.8	0.62	0.430
5	0.00003230	0.00030	9.3	0.73	0.504
6	0.00003230	0.00045	14.0	0.80	0.553
					K =9900±510

[a] Total concentration of **9**.

[b] Total concentration of **47**.

Suitable range of $[G]_t$ for titration was calculated from dissociation constant (K_d) according to the reference 2. ($K_d/10 < [G]_t < 10K_d$)

$K_d = 0.0001$ $\quad 0.00001 < [G]_t < 0.00101$

$K = 9900$

[c] The complexation ratio for the complex of **9** with **47**.

[d] Observed at absorption maxima (397 nm) for the complex of **9** with **47**.

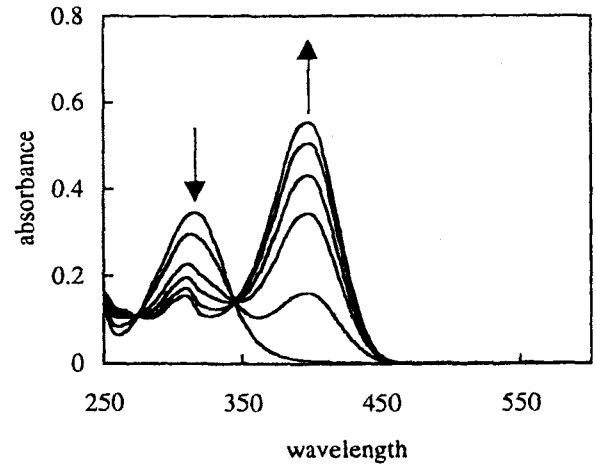

Figure 3.21 UV-vis spectral change of **9** upon addition of **47** in $CHCl_3$.

Table 3.19 Tabulated UV-vis titration data of **9** with **48** in $CHCl_3$ at 30°C, and calculated association constant.

	$[H]_t$ (M) [a]	$[G]_t$ (M) [b]	$[G]_t$ / $[H]_t$	[C] / $[H]_t$ [c]	abs. [d]
1	0.00003572	0	0	0	0.0092
2	0.00003572	0.00378	106	0.23	0.241
3	0.00003572	0.00755	212	0.37	0.334
4	0.00003572	0.00907	254	0.41	0.416
5	0.00003572	0.01133	317	0.47	0.458
6	0.00003572	0.01511	423	0.54	0.487
					K =79±9.9

[a] Total concentration of **9**.

[b] Total concentration of **48**.

Suitable range of $[G]_t$ for titration was calculated from dissociation constant (K_d) according to the reference 2. ($K_d/10 < [G]_t < 10K_d$)

K_d = 0.0127 0.00127 < $[G]_t$ < 0.12658

K = 79

[c] The complexation ratio for the complex of **9** with **48**.

[d] Observed at absorption maxima (402 nm) for the complex of **9** with **48**.

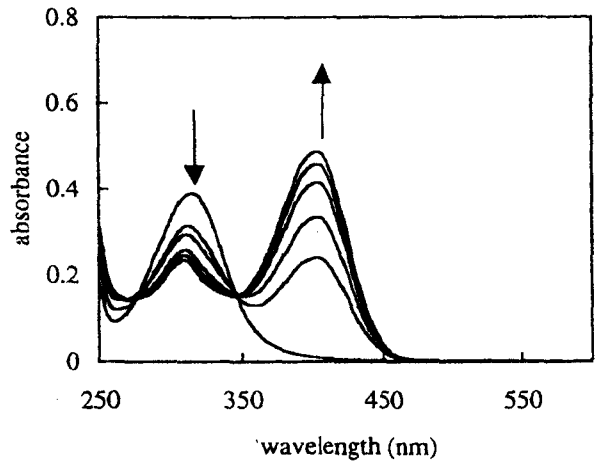

Figure 3.22 UV-vis spectral change of **9** upon addition of **48** in $CHCl_3$.

Table 3.20 Tabulated UV-vis titration data of **10** with **47** in $CHCl_3$ at 30°C, and calculated association constant.

	$[H]_t$ (M) [a]	$[G]_t$ (M) [b]	$[G]_t$ / $[H]_t$	[C] / $[H]_t$ [c]	abs. [d]
1	0.00004208	0	0	0	0.0095
2	0.00004208	0.00063	14.9	0.19	0.149
3	0.00004208	0.00188	44.6	0.41	0.311
4	0.00004208	0.00313	74.4	0.53	0.404
5	0.00004208	0.00501	119.0	0.65	0.493
6	0.00004208	0.00626	148.7	0.70	0.529
					K =370±14

[a] Total concentration of **10**.

[b] Total concentration of **47**.

Suitable range of $[G]_t$ for titration was calculated from dissociation constant (K_d) according to the reference 2. ($K_d/10 < [G]_t < 10K_d$)

$K_d = 0.0027$ $\quad 0.00027 < [G]_t < 0.02703$

$K = 370$

[c] The complexation ratio for the complex of **10** with **47**.

[d] Observed at absorption maxima (401 nm) for the complex of **10** with **47**.

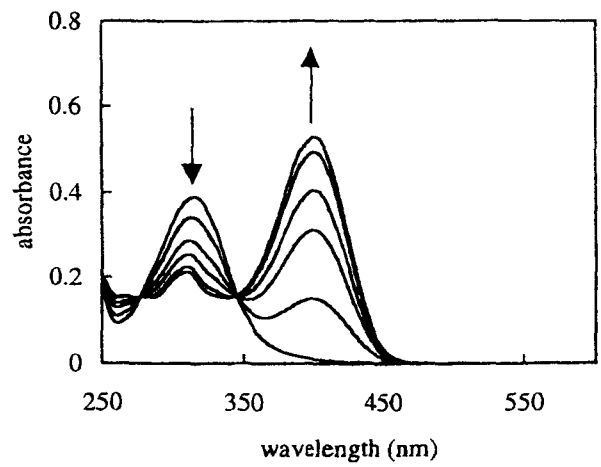

Figure 3.23 UV-vis spectral change of **10** upon addition of **47** in $CHCl_3$.

Table 3.21 Tabulated UV-vis titration data of **10** with **48** in $CHCl_3$ at 30°C, and calculated association constant.

	$[H]_t$ (M) [a]	$[G]_t$ (M) [b]	$[G]_t$ / $[H]_t$	[C] / $[H]_t$ [c]	abs. [d]
1	0.0000421	0	0	0	0.009
2	0.0000421	0.00191	45	0.31	0.241
3	0.0000421	0.00318	75	0.44	0.334
4	0.0000421	0.00508	121	0.55	0.416
5	0.0000421	0.00635	151	0.61	0.458
6	0.0000421	0.00762	181	0.65	0.487
					K =245±14

[a] Total concentration of **10**.

[b] Total concentration of **48**.

Suitable range of $[G]_t$ for titration was calculated from dissociation constant (K_d) according to the reference 2. ($K_d/10 < [G]_t < 10K_d$)

K_d = 0.00408 0.00041 < $[G]_t$ < 0.04082

K = 245

[c] The complexation ratio for the complex of **10** with **48**.

[d] Observed at absorption maxima (402 nm) for the complex of **10** with **48**.

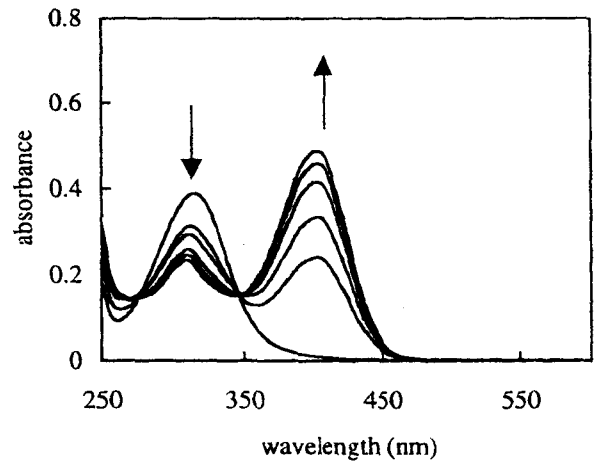

Figure 3.24 UV-vis spectral change of **10** upon addition of **48** in $CHCl_3$.

Table 3.22 Tabulated UV-vis titration data of **10** with **50** in $CHCl_3$ at 30°C, and calculated association constant.

	$[H]_t$ (M) [a]	$[G]_t$ (M) [b]	$[G]_t$ / $[H]_t$	[C] / $[H]_t$ [c]	abs. [d]
1	0.00005700	0	0	0	0.0090
2	0.00005700	0.01200	211	0.21	0.250
3	0.00005700	0.03000	526	0.38	0.446
4	0.00005700	0.06000	1053	0.56	0.659
5	0.00005700	0.09000	1579	0.65	0.770
6	0.00005700	0.12000	2105	0.72	0.851
					K =21±2.1

[a] Total concentration of **10**.

[b] Total concentration of **50**.

Suitable range of $[G]_t$ for titration was calculated from dissociation constant (K_d) according to the reference 2. ($K_d/10 < [G]_t < 10K_d$)

$K_d = 0.04762$ $\quad 0.00476 < [G]_t < 0.47619$

$K = 21$

[c] The complexation ratio for the complex of **10** with **50**.

[d] Observed at absorption maxima (405 nm) for the complex of **10** with **50**.

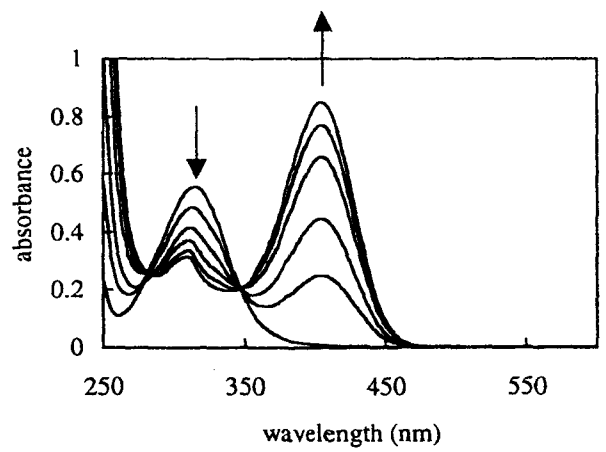

Figure 3.25 UV-vis spectral change of **10** upon addition of **50** in $CHCl_3$.

Table 3.23 Tabulated UV-vis titration data of **11** with **48** in $CHCl_3$ at 30°C, and calculated association constant.

	$[H]_t$ (M) [a]	$[G]_t$ (M) [b]	$[G]_t$ / $[H]_t$	[C] / $[H]_t$ [c]	abs. [d]
1	0.00004208	0	0	0	0.0060
2	0.00004208	0.00471	112	0.31	0.234
3	0.00004208	0.00589	140	0.36	0.270
4	0.00004208	0.00707	168	0.40	0.302
5	0.00004208	0.00883	210	0.46	0.342
6	0.00004208	0.01178	280	0.53	0.395
					K =95±1.5

[a] Total concentration of **11**.

[b] Total concentration of **48**.

Suitable range of $[G]_t$ for titration was calculated from dissociation constant (K_d) according to the reference 2. ($K_d/10 < [G]_t < 10K_d$)

K_d = 0.01053 0.00105 < $[G]_t$ < 0.10526

K = 95

[c] The complexation ratio for the complex of **11** with **48**.

[d] Observed at absorption maxima (401 nm) for the complex of **11** with **48**.

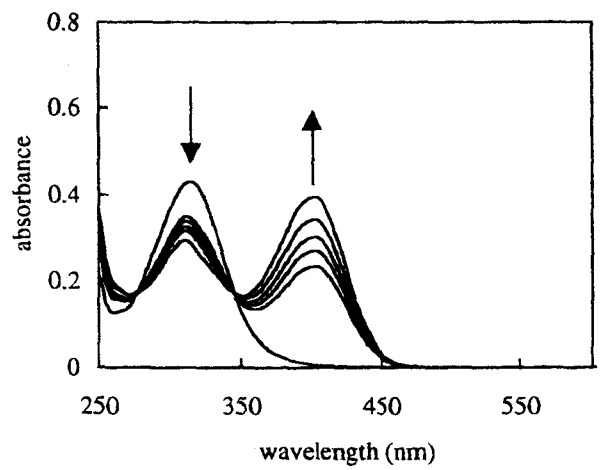

Figure 3.26 UV-vis spectral change of **11** upon addition of **48** in $CHCl_3$.

Table 3.24 Tabulated UV-vis titration data of **12** with **46** in $CHCl_3$ at 15°C, and calculated association constant.

	$[H]_t$ (M) [a]	$[G]_t$ (M) [b]	$[G]_t$ / $[H]_t$	[C] / $[H]_t$ [c]	abs. [d]
1	0.00003641	0	0	0	0.00298
2	0.00003641	0.00241	66	0.21	0.148
3	0.00003641	0.00963	265	0.51	0.350
4	0.00003641	0.01445	397	0.60	0.412
5	0.00003641	0.02409	662	0.73	0.496
6	0.00003641	0.03613	992	0.81	0.551
					K =110±7.4

[a] Total concentration of **12**.

[b] Total concentration of **46**.

Suitable range of $[G]_t$ for titration was calculated from dissociation constant (K_d) according to the reference 2. ($K_d/10 < [G]_t < 10K_d$)

K_d = 0.00909 0.00091 < $[G]_t$ < 0.09091

K = 110

[c] The complexation ratio for the complex of **12** with **46**.

[d] Observed at absorption maxima (392 nm) for the complex of **12** with **46**.

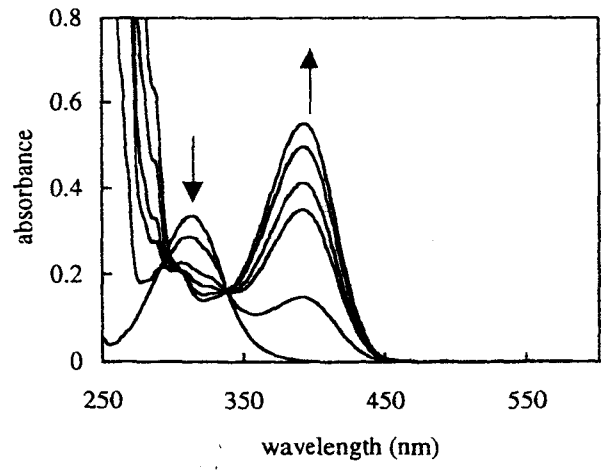

Figure 3.27 UV-vis spectral change of **12** upon addition of **46** in $CHCl_3$.

Table 3.25 Tabulated UV-vis titration data of **12** with **47** in $CHCl_3$ at 30°C, and calculated association constant.

	$[H]_t$ (M) [a]	$[G]_t$ (M) [b]	$[G]_t$ / $[H]_t$	[C] / $[H]_t$ [c]	abs. [d]
1	0.00003410	0	0	0	0.0029
2	0.00003410	0.00488	143	0.14	0.141
3	0.00003410	0.00684	200	0.19	0.183
4	0.00003410	0.00977	286	0.25	0.242
5	0.00003410	0.01465	430	0.34	0.323
6	0.00003410	0.01953	573	0.40	0.386
					K =35±3.2

[a] Total concentration of **12**.

[b] Total concentration of **47**.

Suitable range of $[G]_t$ for titration was calculated from dissociation constant (K_d) according to the reference 2. ($K_d/10 < [G]_t < 10K_d$)

$K_d = 0.02857$ $\quad 0.00286 < [G]_t < 0.28571$

$K = 35$

[c] The complexation ratio for the complex of **12** with **47**.

[d] Observed at absorption maxima (390 nm) for the complex of **12** with **47**.

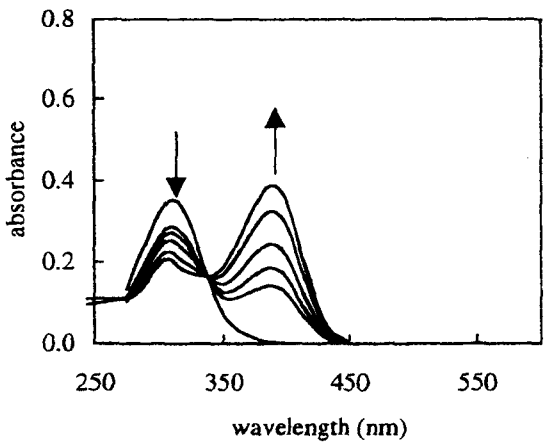

Figure 3.28 UV-vis spectral change of **12** upon addition of **47** in $CHCl_3$.

Table 3.26. Tabulated UV-vis titration data of **12** with **48** in $CHCl_3$ at 30°C, and calculated association constant.

	$[H]_t$ (M) [a]	$[G]_t$ (M) [b]	$[G]_t$ / $[H]_t$	[C] / $[H]_t$ [c]	abs. [d]
1	0.00004369	0	0	0	0.0044
2	0.00004369	0.00327	75	0.42	0.378
3	0.00004369	0.00409	94	0.47	0.421
4	0.00004369	0.00491	112	0.52	0.464
5	0.00004369	0.00613	140	0.58	0.514
6	0.00004369	0.00818	187	0.65	0.577
					K =220±18

[a] Total concentration of **12**.

[b] Total concentration of **48**.

Suitable range of $[G]_t$ for titration was calculated from dissociation constant (K_d) according to the reference 2. ($K_d/10 < [G]_t < 10K_d$)

$K_d = 0.00455$ $\quad 0.00045 < [G]_t < 0.04545$

$K = 220$

[c] The complexation ratio for the complex of **12** with **48**.

[d] Observed at absorption maxima (386 nm) for the complex of **12** with **48**.

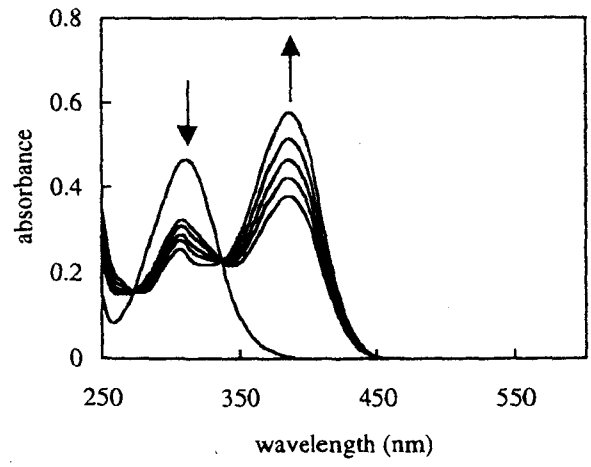

Figure 3.29 UV-vis spectral change of **12** upon addition of **48** in $CHCl_3$.

Table 3.27 Tabulated UV-vis titration data of **12** with **50** in $CHCl_3$ at 30°C, and calculated association constant.

	$[H]_t$ (M) [a]	$[G]_t$ (M) [b]	$[G]_t$ / $[H]_t$	[C] / $[H]_t$ [c]	abs. [d]
1	0.00003030	0	0	0	0.0042
2	0.00003030	0.00160	52.8	0.12	0.070
3	0.00003030	0.00400	132.0	0.26	0.144
4	0.00003030	0.00800	264.0	0.40	0.220
5	0.00003030	0.01200	396.0	0.51	0.276
6	0.00003030	0.01600	528.0	0.58	0.313
					K =89±4.9

[a] Total concentration of **12**.

[b] Total concentration of **50**.

Suitable range of $[G]_t$ for titration was calculated from dissociation constant (K_d) according to the reference 2. ($K_d/10 < [G]_t < 10K_d$)

$K_d = 0.01124$ $\quad 0.00112 < [G]_t < 0.11236$

$K = 89$

[c] The complexation ratio for the complex of **12** with **50**.

[d] Observed at absorption maxima (388 nm) for the complex of **12** with **50**.

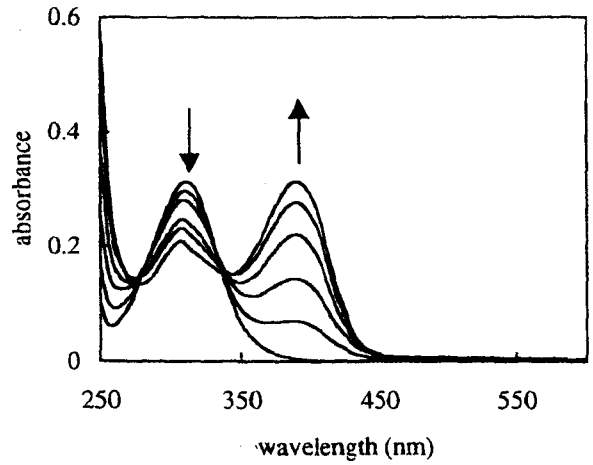

Figure 3.30 UV-vis spectral change of **12** upon addition of **50** in $CHCl_3$.

Table 3.28 Tabulated UV-vis titration data of **10** with (S)-**52** in $CHCl_3$ at 30 °C, and calculated association constant.

	$[H]_t$ (M) [a]	$[G]_t$ (M) [b]	$[G]_t$ / $[H]_t$	[C] / $[H]_t$ [c]	abs. [d]
1	0.0000418	0	0	0	0.015
2	0.0000418	0.00221	53	0.26	0.205
3	0.0000418	0.00368	88	0.37	0.285
4	0.0000418	0.00590	141	0.48	0.369
5	0.0000418	0.00737	176	0.54	0.407
6	0.0000418	0.01105	264	0.64	0.484
					K =160±6.4

[a] Total concentration of **10**.

[b] Total concentration of (S)-**52**.

Suitable range of $[G]_t$ for titration was calculated from dissociation constant (K_d) according to the reference 2. (K_d /10 < $[G]_t$ < 10K_d)

K_d = 0.00625 0.00063 < $[G]_t$ < 0.06250

K = 160

[c] The complexation ratio for the complex of **10** with (S)-**52**.

[d] Observed at absorption maxima (396 nm) for the complex of **10** with (S)-**52**.

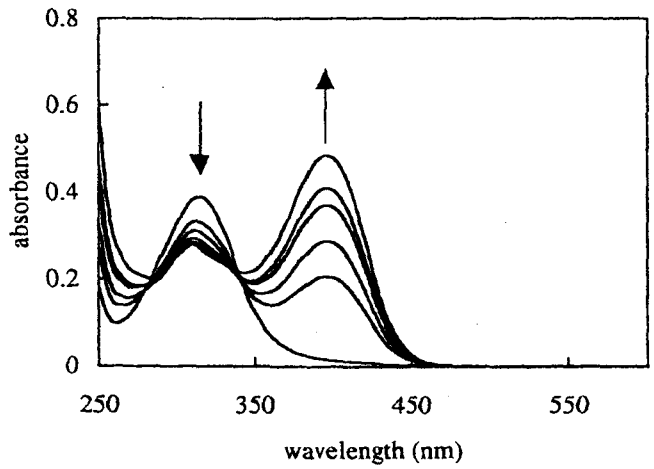

Figure 3.31 UV-vis spectral change of **10** upon addition of (S)-**52** in $CHCl_3$.

Table 3.29 Tabulated UV-vis titration data of **10** with (*R*)-**52** in $CHCl_3$ at 30°C, and calculated association constant.

	$[H]_t$ (M) [a]	$[G]_t$ (M) [b]	$[G]_t$ / $[H]_t$	[C] / $[H]_t$ [c]	abs. [d]
1	0.0000418	0	0	0	0.015
2	0.0000418	0.00326	78	0.30	0.478
3	0.0000418	0.00544	130	0.42	0.234
4	0.0000418	0.00870	208	0.53	0.322
5	0.0000418	0.01088	260	0.58	0.403
6	0.0000418	0.01306	312	0.63	0.444
					K =130±7.3

[a] Total concentration of **10**.

[b] Total concentration of (*R*)-**52**.

Suitable range of $[G]_t$ for titration was calculated from dissociation constant (K_d) according to the reference 2. ($K_d/10 < [G]_t < 10K_d$)

$K_d = 0.00769$ $\quad 0.00077 < [G]_t < 0.07692$

$K = 130$

[c] The complexation ratio for the complex of **10** with (*R*)-**52**.

[d] Observed at absorption maxima (397 nm) for the complex of **10** with (*R*)-**52**.

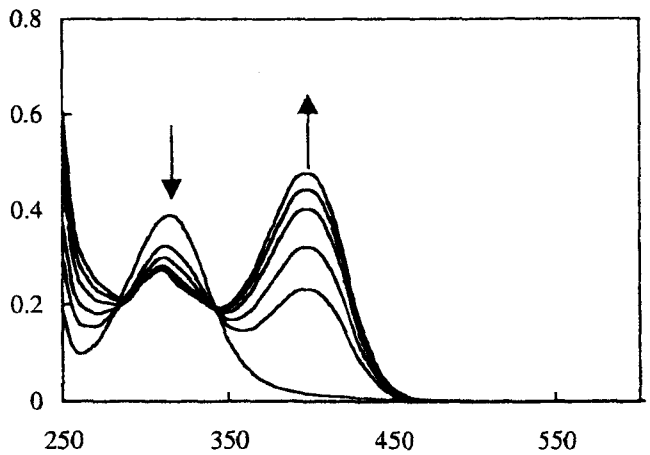

Figure 3.32 UV-vis spectral change of **10** upon addition of (*R*)-**52** in $CHCl_3$.

Table 3.30 Tabulated UV-vis titration data of **12** with (*S*)-**51** in $CHCl_3$ at 15 °C, and calculated association constant.

	$[H]_t$ (M) [a]	$[G]_t$ (M) [b]	$[G]_t$ / $[H]_t$	[C] / $[H]_t$ [c]	abs. [d]
1	0.00004096	0	0	0	0.0037
2	0.00004096	0.00394	96	0.29	0.232
3	0.00004096	0.00657	160	0.40	0.322
4	0.00004096	0.01051	257	0.52	0.414
5	0.00004096	0.01314	321	0.57	0.457
6	0.00004096	0.01970	481	0.67	0.534
					K =100±1.4

[a] Total concentration of **12**.

[b] Total concentration of (*S*)-**51**.

Suitable range of $[G]_t$ for titration was calculated from dissociation constant (K_d) according to the reference 2. (K_d /10 < $[G]_t$ < 10K_d)

K_d = 0.01000 0.00100 < $[G]_t$ < 0.10000

K = 100

[c] The complexation ratio for the complex of **12** with (*S*)-**51**.

[d] Observed at absorption maxima (392 nm) for the complex of **12** with (*S*)-**51** .

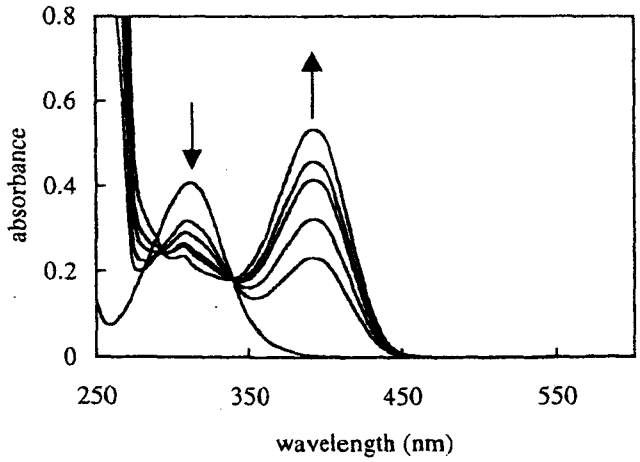

Figure 3.33 UV-vis spectral change of **12** upon addition of (*S*)-**51** in $CHCl_3$.

Table 3.31 Tabulated UV-vis titration data of **12** with (*R*)-**51** in $CHCl_3$ at 15 °C, and calculated association constant.

	$[H]_t$ (M) [a]	$[G]_t$ (M) [b]	$[G]_t$ / $[H]_t$	[C] / $[H]_t$ [c]	abs. [d]
1	0.00004096	0	0	0	0.0037
2	0.00004096	0.00492	120	0.26	0.207
3	0.00004096	0.00738	180	0.34	0.276
4	0.00004096	0.01230	300	0.47	0.372
5	0.00004096	0.01968	480	0.58	0.464
6	0.00004096	0.02460	601	0.63	0.503
					K =72±2.3

[a] Total concentration of **12**.

[b] Total concentration of (*R*)-**51**.

Suitable range of $[G]_t$ for titration was calculated from dissociation constant (K_d) according to the reference 2. (K_d /10 < $[G]_t$ < 10K_d)

K_d = 0.01389 0.00139 < $[G]_t$< 0.13889

K = 72

[c] The complexation ratio for the complex of **12** with (*R*)-**51**.

[d] Observed at absorption maxima (392 nm) for the complex of **12** with (*R*)-**51** .

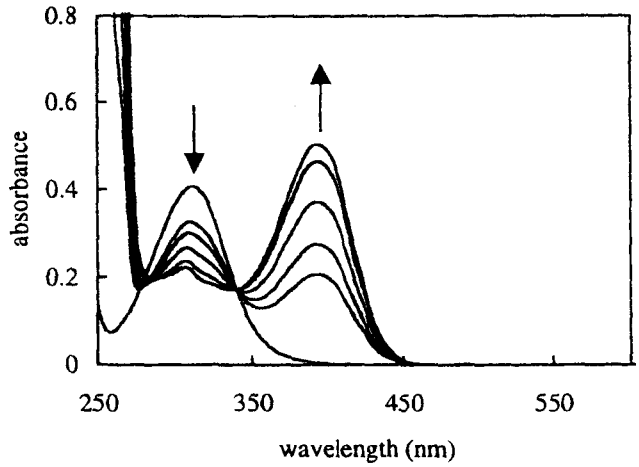

Figure 3.34 UV-vis spectral change of **12** upon addition of (*R*)-**51** in $CHCl_3$.

Table 3.32 Tabulated UV-vis titration data of **12** with (*S*)-**52** in $CHCl_3$ at 30 °C, and calculated association constant.

	$[H]_t$ (M) [a]	$[G]_t$ (M) [b]	$[G]_t$ / $[H]_t$	[C] / $[H]_t$ [c]	abs. [d]
1	0.00003841	0	0	0	0.0060
2	0.00003841	0.00037	10	0.27	0.199
3	0.00003841	0.00075	20	0.42	0.308
4	0.00003841	0.00112	29	0.51	0.376
5	0.00003841	0.00187	49	0.65	0.477
6	0.00003841	0.00375	98	0.79	0.582
					K =980±71

[a] Total concentration of **12**.

[b] Total concentration of (*S*)-**52**.

Suitable range of $[G]_t$ for titration was calculated from dissociation constant (K_d) according to the reference 2. ($K_d/10 < [G]_t < 10K_d$)

K_d = 0.00102 0.00010 < $[G]_t$ < 0.01020

K = 980

[c] The complexation ratio for the complex of **12** with (*S*)-**52**.

[d] Observed at absorption maxima (387 nm) for the complex of **12** with (*S*)-**52** .

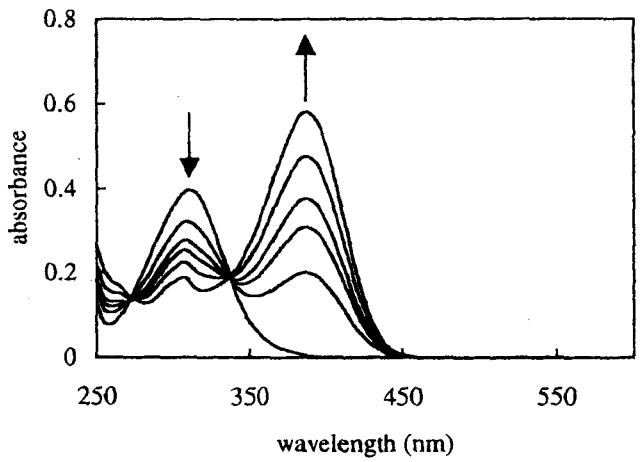

Figure 3.35 UV-vis spectral change of **12** upon addition of (*S*)-**52** in $CHCl_3$.

Table 3.33 Tabulated UV-vis titration data of **12** with (*R*)-**52** in $CHCl_3$ at 30 °C, and calculated association constant.

	$[H]_t$ (M) [a]	$[G]_t$ (M) [b]	$[G]_t$ / $[H]_t$	[C] / $[H]_t$ [c]	abs. [d]
1	0.00003841	0	0	0	0.0060
2	0.00003841	0.00038	10	0.24	0.191
3	0.00003841	0.00077	20	0.40	0.313
4	0.00003841	0.00115	30	0.50	0.388
5	0.00003841	0.00192	50	0.62	0.476
6	0.00003841	0.00384	100	0.76	0.588
					K =890±65

[a] Total concentration of **12**.

[b] Total concentration of (*R*)-**52**.

Suitable range of $[G]_t$ for titration was calculated from dissociation constant (K_d) according to the reference 2. (K_d /10 < $[G]_t$ < 10K_d)

K_d = 0.00112 0.00011 < $[G]_t$ < 0.01124

K = 890

[c] The complexation ratio for the complex of **12** with (*R*)-**52**.

[d] Observed at absorption maxima (387 nm) for the complex of **12** with (*R*)-**52**.

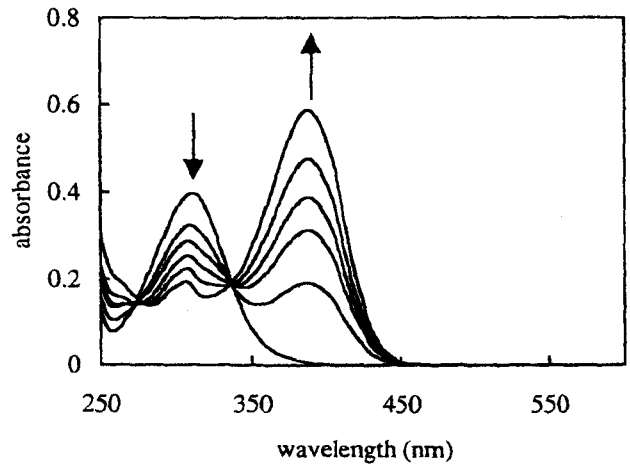

Figure 3.36 UV-vis spectral change of **12** upon addition of (*R*)-**52** in $CHCl_3$.

Table 3.34 Tabulated UV-vis titration data of **12** with (*S*)-**53** in $CHCl_3$ at 15 °C, and calculated association constant.

	$[H]_t$ (M) [a]	$[G]_t$ (M) [b]	$[G]_t$ / $[H]_t$	[C] / $[H]_t$ [c]	abs. [d]
1	0.00004660	0	0	0	0.0054
2	0.00004660	0.01450	311	0.43	0.381
3	0.00004660	0.02310	496	0.55	0.483
4	0.00004660	0.02890	620	0.60	0.527
5	0.00004660	0.04330	929	0.70	0.607
6	0.00004660	0.05780	1240	0.76	0.658
					K =53 ± 1.7

[a] Total concentration of **12**.

[b] Total concentration of (*S*)-**53**.

Suitable range of $[G]_t$ for titration was calculated from dissociation constant (K_d) according to the reference 2. (K_d /10 < $[G]_t$ < 10K_d)

K_d = 0.01887 0.00189 < $[G]_t$ < 0.18868

K = 53

[c] The complexation ratio for the complex of **12** with (*S*)-**53**.

[d] Observed at absorption maxima (386 nm) for the complex of **12** with (*S*)-**53** .

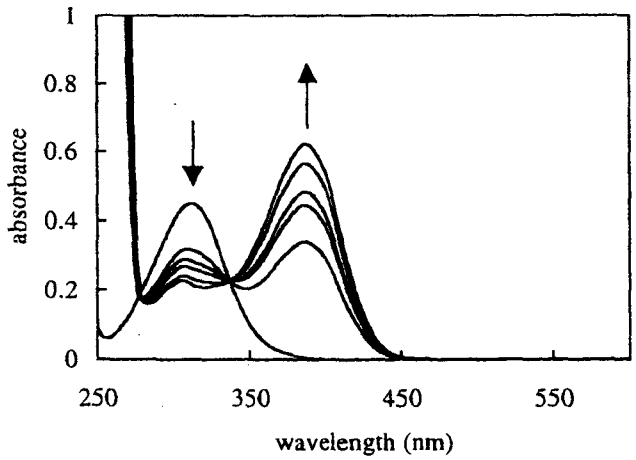

Figure 3.37 UV-vis spectral change of **12** upon addition of (*S*)-**53** in $CHCl_3$.

Table 3.35 Tabulated UV-vis titration data of **12** with (*R*)-**53** in $CHCl_3$ at 15 °C, and calculated association constant.

	$[H]_t$ (M) [a]	$[G]_t$ (M) [b]	$[G]_t$ / $[H]_t$	[C] / $[H]_t$ [c]	abs. [d]
1	0.00004660	0	0	0	0.0041
2	0.00004660	0.01420	305	0.40	0.341
3	0.00004660	0.02276	488	0.52	0.445
4	0.00004660	0.02840	609	0.57	0.484
5	0.00004660	0.04270	916	0.66	0.567
6	0.00004660	0.05690	1221	0.73	0.623
					K =47±4.5

[a] Total concentration of **12**.

[b] Total concentration of (*R*)-**53**.

Suitable range of $[G]_t$ for titration was calculated from dissociation constant (K_d) according to the reference 2. (K_d /10 < $[G]_t$ < 10K_d)

K_d = 0.02128 0.00213 < $[G]_t$ < 0.21277

K = 47

[c] The complexation ratio for the complex of **12** with (*R*)-**53**.

[d] Observed at absorption maxima (387 nm) for the complex of **12** with (*R*)-**53** .

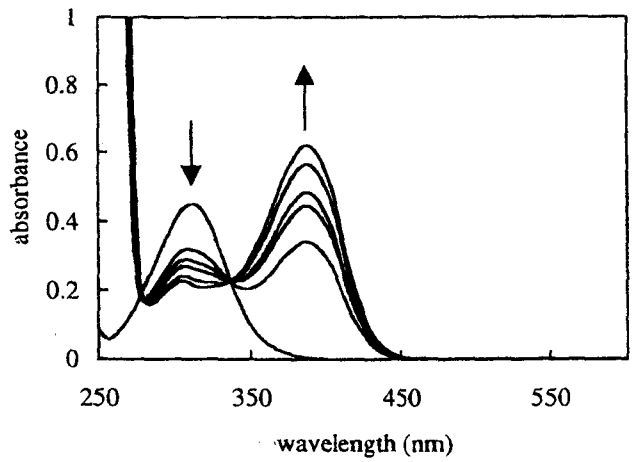

Figure 3.38 UV-vis spectral change of **12** upon addition of (*R*)-**53** in $CHCl_3$.

Table 3.36 Tabulated UV-vis titration data of **12** with (*S*)-**54** in $CHCl_3$ at 15 °C, and calculated association constant.

	$[H]_t$ (M) [a]	$[G]_t$ (M) [b]	$[G]_t$ / $[H]_t$	[C] / $[H]_t$ [c]	abs. [d]
1	0.00003600	0	0	0	0.0037
2	0.00003600	0.00199	55	0.39	0.315
3	0.00003600	0.00498	138	0.60	0.484
4	0.00003600	0.00796	221	0.71	0.569
5	0.00003600	0.01393	387	0.82	0.658
6	0.00003600	0.01990	553	0.87	0.694
					K =310±15

[a] Total concentration of **12**.

[b] Total concentration of (*S*)-**54**.

Suitable range of $[G]_t$ for titration was calculated from dissociation constant (K_d) according to the reference 2. ($K_d/10 < [G]_t < 10K_d$)

K_d = 0.00323 0.00032 < $[G]_t$ < 0.03226

K = 310

[c] The complexation ratio for the complex of **12** with (*S*)-**54**.

[d] Observed at absorption maxima (387 nm) for the complex of **12** with (*S*)-**54** .

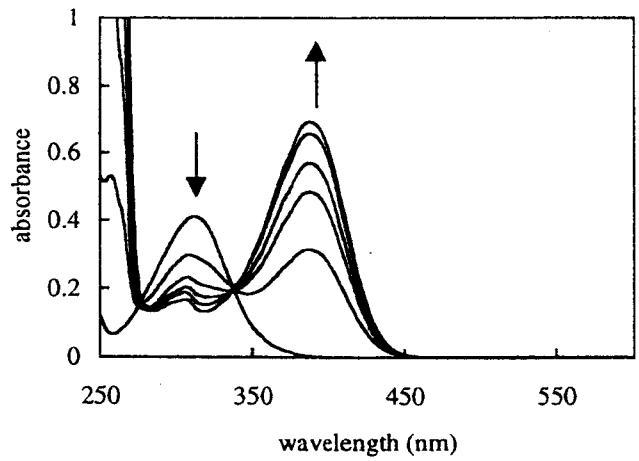

Figure 3.39 UV-vis spectral change of **12** upon addition of (*S*)-**54** in $CHCl_3$.

Table 3.37 Tabulated UV-vis titration data of **12** with (*R*)-**54** in $CHCl_3$ at 15 °C, and calculated association constant.

	$[H]_t$ (M) [a]	$[G]_t$ (M) [b]	$[G]_t$ / $[H]_t$	[C] / $[H]_t$ [c]	abs. [d]
1	0.00003600	0	0	0	0.0032
2	0.00003600	0.00200	56	0.27	0.221
3	0.00003600	0.00500	139	0.48	0.389
4	0.00003600	0.00800	222	0.60	0.484
5	0.00003600	0.01400	389	0.72	0.583
6	0.00003600	0.02000	556	0.78	0.639
					K =180±2.9

[a] Total concentration of **12**.

[b] Total concentration of (*R*)-**54**.

Suitable range of $[G]_t$ for titration was calculated from dissociation constant (K_d) according to the reference 2. ($K_d/10 < [G]_t < 10K_d$)

K_d = 0.00556 0.00056 < $[G]_t$ < 0.05556

K = 180

[c] The complexation ratio for the complex of **12** with (*R*)-**54**.

[d] Observed at absorption maxima (388 nm) for the complex of **12** with (*R*)-**54** .

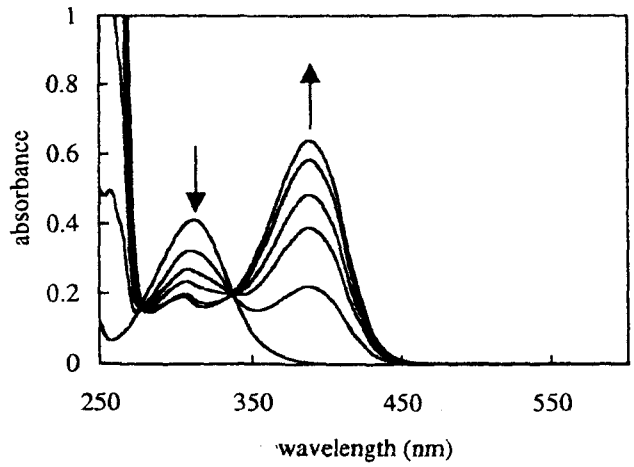

Figure 3.40 UV-vis spectral change of **12** upon addition of (*R*)-**54** in $CHCl_3$.

Table 3.38 Tabulated UV-vis titration data of **12** with (*S*)-**55** in $CHCl_3$ at 15 °C, and calculated association constant.

	$[H]_t$ (M) [a]	$[G]_t$ (M) [b]	$[G]_t$ / $[H]_t$	[C] / $[H]_t$ [c]	abs. [d]
1	0.00003310	0	0	0	0.0072
2	0.00003310	0.00209	63	0.27	0.103
3	0.00003310	0.01047	316	0.48	0.314
4	0.00003310	0.01675	506	0.60	0.402
5	0.00003310	0.02093	632	0.72	0.444
6	0.00003310	0.03140	949	0.79	0.507
					K =230±8.6

[a] Total concentration of **12**.

[b] Total concentration of (*S*)-**55**.

Suitable range of $[G]_t$ for titration was calculated from dissociation constant (K_d) according to the reference 2. ($K_d/10 < [G]_t < 10K_d$)

$K_d = 0.00435$ $\quad 0.00043 < [G]_t < 0.04348$

$K = 230$

[c] The complexation ratio for the complex of **12** with (*S*)-**55**.

[d] Observed at absorption maxima (386 nm) for the complex of **12** with (*S*)-**55** .

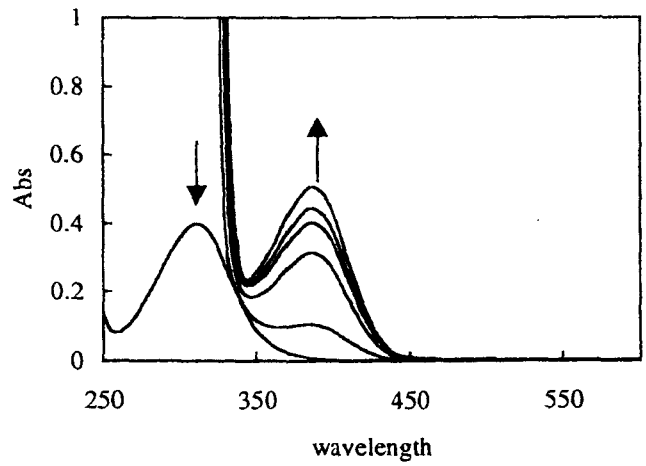

Figure 3.41 UV-vis spectral change of **12** upon addition of (*S*)-**55** in $CHCl_3$.

Table 3.39 Tabulated UV-vis titration data of **12** with (*R*)-**55** in $CHCl_3$ at 15 °C, and calculated association constant.

	$[H]_t$ (M) [a]	$[G]_t$ (M) [b]	$[G]_t$ / $[H]_t$	[C] / $[H]_t$ [c]	abs. [d]
1	0.00003841	0	0	0	0.0064
2	0.00003841	0.00131	34	0.32	0.256
3	0.00003841	0.00210	55	0.43	0.341
4	0.00003841	0.00262	68	0.49	0.382
5	0.00003841	0.00393	102	0.59	0.460
6	0.00003841	0.00524	137	0.66	0.517
					K =370± 14

[a] Total concentration of **12**.

[b] Total concentration of (*R*)-**55**.

Suitable range of $[G]_t$ for titration was calculated from dissociation constant (K_d) according to the reference 2. (K_d /10 < $[G]_t$ < 10K_d)

K_d = 0.00270 0.00027 < $[G]_t$ < 0.02703

K = 370

[c] The complexation ratio for the complex of **12** with (*R*)-**55**.

[d] Observed at absorption maxima (386 nm) for the complex of **12** with (*R*)-**55** .

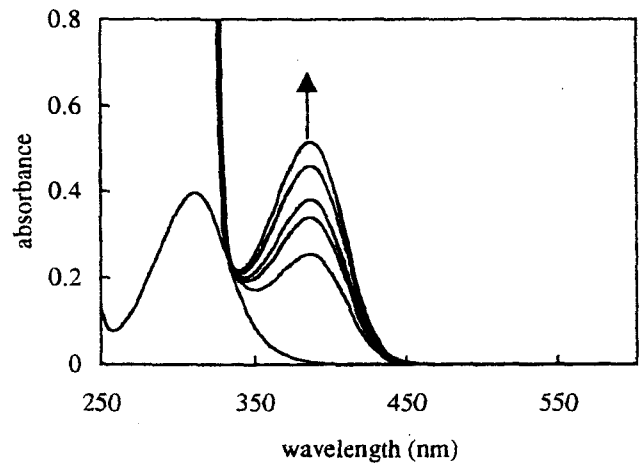

Figure 3.42 UV-vis spectral change of **12** upon addition of (*R*)-**55** in $CHCl_3$.

3.7 References and notes

1. (a) Rose, N. J.; Drago, R. S. *J. Am. Chem. Soc.* **1959**, *81*, 6138–6141; (b) Hirose, K. *J. Incl. Phenom. Macrocyclic Chem.* **2001**, *39*, 193–209.
2. Wilcox, C. J. in "*Frontiers in Supramolecular Organic Chemistry and Photochemistry*", Schneider, H. J.; Durr, H.; Lehn, J. M. VCH: Weinheim, New York, 1991; pp 123–144.
3. (a) Naemura, K.; Ueno, K.; Takeuchi, S.; Hirose, K.; Tobe, Y.; Kaneda, T.; Sakata, Y. *J. Chem. Soc., Perkin Trans.1* **1995**, 383–388; (b) Naemura, K.; Ueno, K.; Takauchi, S.; Tobe, Y.; Kaneda, T.; Sakata, Y. *J. Am. Chem. Soc.* **1993**, *115*, 8475–8476.
4. Bowman, W. C.; Rand, M. J. in "*Textbook of Pharmacology*", 2nd Eds. Blackwell Scientific Publications: London, 1980.
5. (a) Naemura, K.; Ogasahara, K.; Hirose, K.; Tobe, Y. *Tetrahedron: Asymmetry* **1997**, *8*, 19–22; (b) Naemura, K.; Matsunaga, K.; Fuji, J.; Ogasahara, K.; Nishikawa, Y.; Hirose, K.; Tobe, Y. *Anal. Science* **1998**, *14*, 175–182; (c) Ogasahara, K.; Hirose, K.; Tobe, Y.; Naemura, K.; *J. Chem. Soc., Perkin Trans. 1* **1997**, 3227–3236.
6. Hirose, K.; Ogasahara, K.; Nishioka, K.; Tobe, Y.; Naemura, K. *J. Chem. Soc., Perkin Trans. 2* **2000**, 1984–1993.
7. Saavendra, J. E. *J. Org. Chem.* **1985**, *50*, 2271–2273.
8. Habata, Y.; Bradshaw, J. S.; Young, J. J.; Castle, S. L.; Huszthy, P.; Pyo, T.; Lee, M. L.; Izatt, R. M. *J. Org. Chem.* **1996**, *61*, 8391–8396.

Appendix

List of host and guest compounds

Crown ethers, podands, amines, and their precursors are summarized for convenience of making reference to compounds.

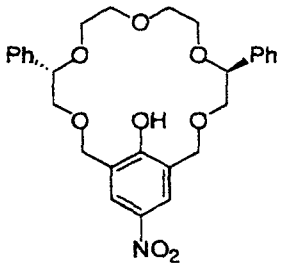

(*S*,*S*)-**9**

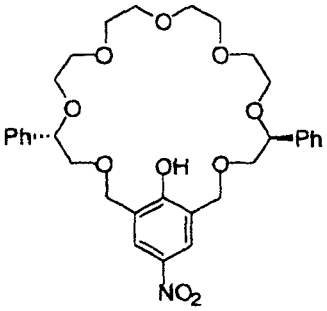

(*S*,*S*)-**10**

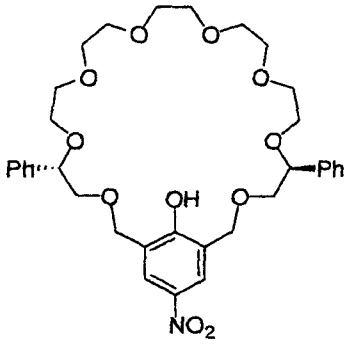

(*S*,*S*)-**11**

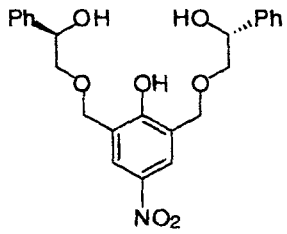

(*R*,*R*)-**12**

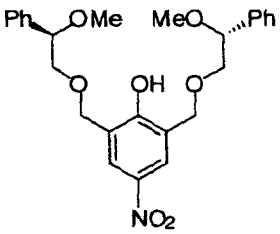

(*R*,*R*)-**13**

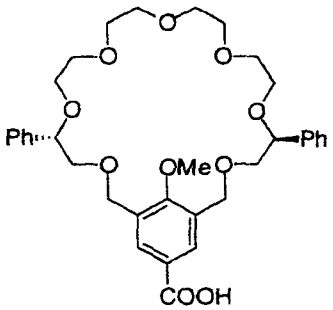

(*S*,*S*)-**14**

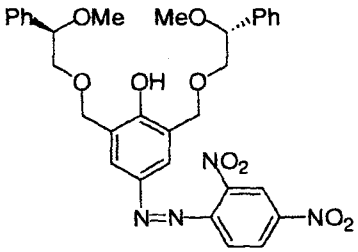

(*R*,*R*)-**15**

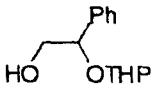

(*S*)- and (*R*)-**16**

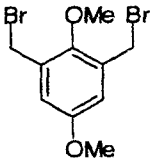

17

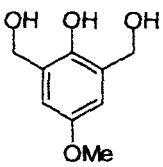

18

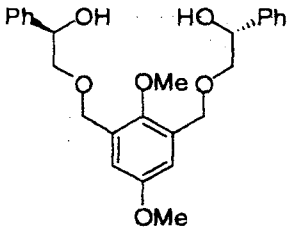

(*R*,*R*)-19

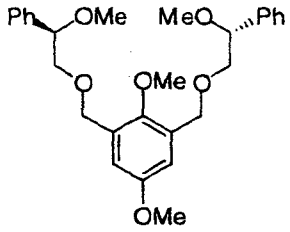

(*R*,*R*)-20

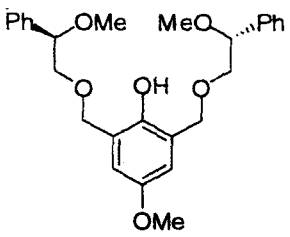

(*R*,*R*)-21

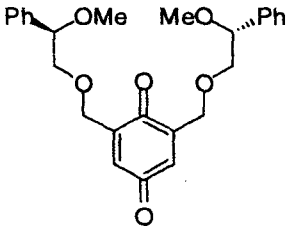

(*R*,*R*)-22

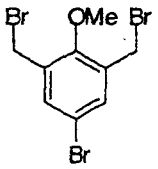

24

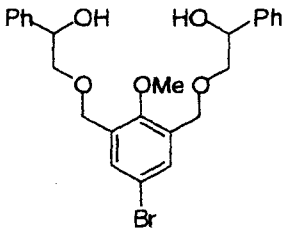

25

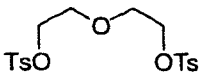

26

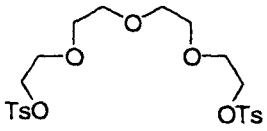

27

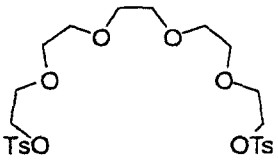

28

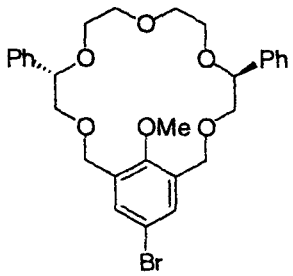

(*S*,*S*)-29

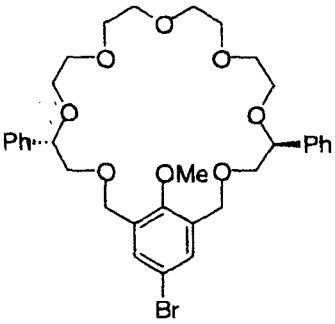

(*S*,*S*)-30

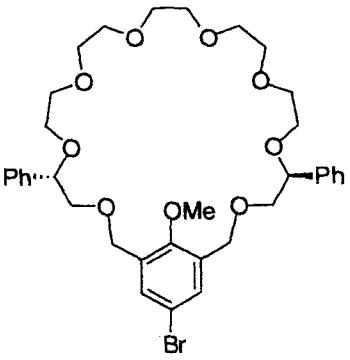

(*S*,*S*)-31

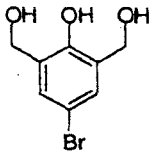

32

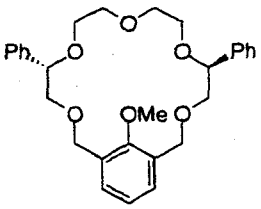

(*S*,*S*)-**33**

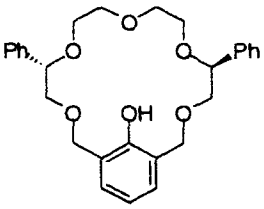

(*S*,*S*)-**34**

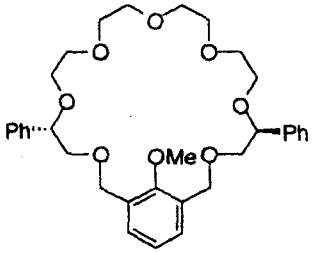

(*S*,*S*)-**35**

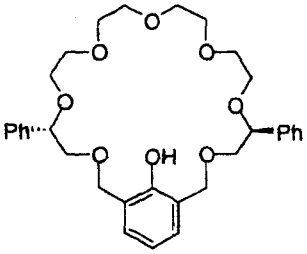

(*S*,*S*)-**36**

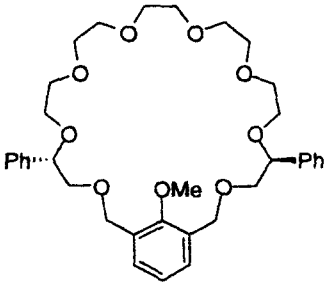

(*S*,*S*)-**37**

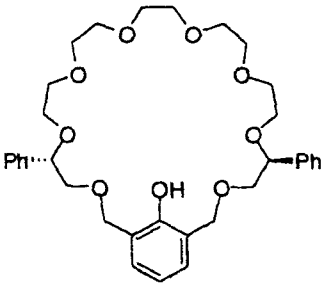

(*S*,*S*)-**38**

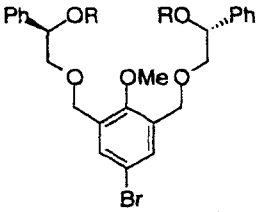

(*R*,*R*)-**39**
R=MOM

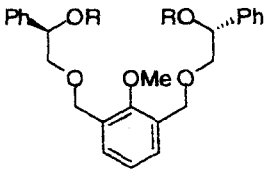

(*R*,*R*)-**40**
R=MOM

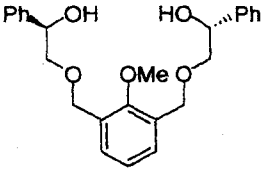

(*R*,*R*)-**41**

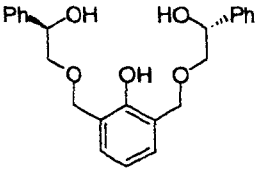

(*R*,*R*)-**42**

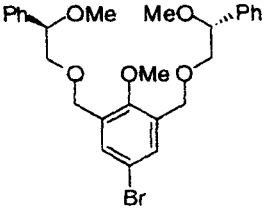

(*R*,*R*)-**43**

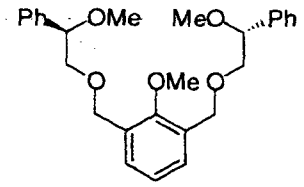

(*R*,*R*)-**44**

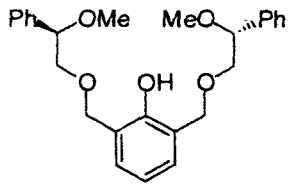

(*R*,*R*)-**45**

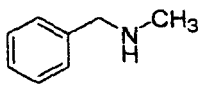

46

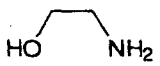

47

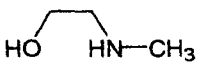

48

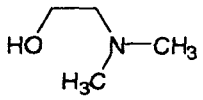

49

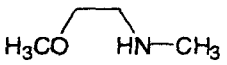

50

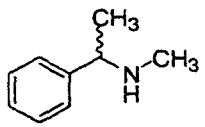

51

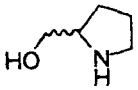

52

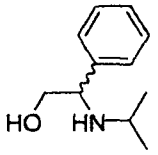

53

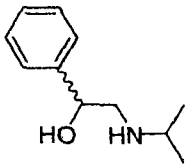

54

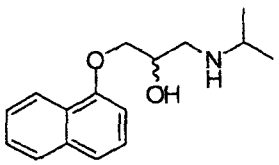

55

Publication List

1. "Chiral recognition of secondary amines by using chiral crown ether and podand," Hirose, K; Fujiwara, A.; Matsunaga, K.; Aoki, N.; Tobe, Y. *Tetrahedron Lett.* **2002**, *43*, 8539–8542.

2. "Preparation of phenolic crown ethers and podands and their enantiomer recognition ability toward secondary amines," Hirose, K; Fujiwara, A.; Matsunaga, K.; Aoki, N.; Tobe, Y. *Tetrahedron : Asymmetry* in press.

Acknowledgment

The present studies have been carried out at the Department of Chemistry, Graduate School of Engineering Science, Osaka University during 2000–2003 under the direction of Professor Yoshito Tobe.

The author wishes to express his sincere gratitude to Professor Yoshito Tobe for the instructive guidance and encouragement throughout the present work. The author wishes to thank Dr. Keiji Hirose for helpful advice and discussion. He would like thank to Dr. Motohiro Sonoda for helpful suggestions.

The author also thanks and feels very fortunate to have the opportunity to collaborate Mr. Kazuhisa Matsunaga and Nobuaki Aoki. Also, it is his pleasure to express his thanks to the fellows of Tobe laboratory for their pleasant atmosphere. The author also would like thank to Mr. Kazuo Fukuda of Faculty of Engineering Science, Osaka University for the measurement of mass spectra, and Mr. Yoshio Terawaki and Mr. Hiroshi Okuda for their help in obtaining NMR spectra.

The author wish to express his gratitude to Ni-hon Ikuei Kai for the scholarship support during 2000–2003.

Finally, the author wishes to express his sincere thanks to his parents Chikato and Sawako Fujiwara, his brother Masahito Fujiwara, and also his friends for their understanding and encouragement.

Akihito FUJIWARA
Division of Chemistry
Department of Chemical Science and Engineering